Linköping Studies in Science and Technology
Dissertation No. 1253

Design and Synthesis of Inhibitors Targeting the Hepatitis C Virus NS3 Serine Protease and the Aspartic Protease BACE-1

Marcus Bäck

Linköping University
INSTITUTE OF TECHNOLOGY

Division of Chemistry
Department of Physics, Chemistry and Biology
Linköping University, SE-58183 Linköping, Sweden

Linköping 2009

Cover Art: (top) compound 20 (Paper II) modeled in the active site of the HCV NS3 serine protease, (middle) model of compound 18 (Paper II) in the same protease (not used in the article), (below) X-ray crystal structure of compound 27 (Paper III) and the aspartic protease BACE-1.

Copyright © 2009 Marcus Bäck, unless otherwise noted

Marcus Bäck
Design and Synthesis of Inhibitors Targeting the Hepatitis C Virus NS3 Serine Protease and the Aspartic Protease BACE-1
ISBN 978-91-7393-642-2
ISSN 0345-7524
Published online at www.ep.liu.se
Linköping Studies in Science and Technology
Dissertation No. 1253

Printed in Sweden by LiU-tryck, Linköping 2009

”Bryt upp, bryt upp! Den nya dagen gryr.
Oändligt är vårt stora äventyr.”

From the poem *I rörelse*[1] by Karin Boye (1900-1941).

[1] Curiosity: The poem was read to the Swedish soccer squad by the national team manager (at the time) Tommy Svensson before their last 16 game against Saudi Arabia during the 1994 FIFAWorld Cup. (Source: Dokument-94, hela berättelsen…, *Offside, 1,* 2004.)

Abstract

This thesis describes the synthesis of molecules designed to inhibit the hepatitis C virus (HCV) NS3 serine protease and the human aspartic protease BACE-1, and it also reports the structure-activity relationships between potential inhibitors and the targeted enzymes. In addition, consideration is given to the class of enzymes known as proteases, as well as the question of why such enzymes can be regarded as suitable targets for developing drugs to combat diseases in general. Some strategies used to design protease inhibitors and the desired properties of such potential drug candidates are also briefly examined.

Infection with HCV gives rise to a predominantly chronic disease that causes severe liver damage and ultimately leads to cirrhosis and liver cancer, and hence it represents the main factor underlying most of the liver transplants in the developed world. The HCV NS3 serine protease is essential for replication of the virus, and it has become one of the most widely exploited targets for developing anti-HCV inhibitors. The results presented here concern the design and synthesis of linear and macrocyclic NS3 protease inhibitors containing a novel trisubstituted cyclopentane moiety as an *N*-acyl-(4*R*)-hydroxyproline bioisostere. Several highly potent compounds were evaluated, including inhibitors with K_i and replicon EC_{50} values in the subnanomolar and the low nanomolar range, respectively.

Alzheimer's disease is a fatal neurodegenerative disorder of the brain. It is characterized by loss of memory and cognition, and is associated with accumulation of plaques and tangles that cause serious impairment and functional decline of brain tissues. The plaques consist mainly of amyloid-β fragments that are generated through two cleavages of amyloid precursor protein (APP). The enzyme responsible for the initial cleavage is the aspartic protease BACE-1 (beta-site APP-cleaving enzyme), which was explored in the current studies as a pharmaceutical target. The synthetic work comprised development of two series of BACE-1 inhibitors with different central core isosteres; a statine-based and a hydroxyethylene-based series. Highly potent inhibitors were produced by varying the substituents coupled to the statine-based central core. X-ray crystallography and molecular modeling enabled analysis of the binding properties of these compounds. In the second series a hydroxyethylene central core was decorated with more advanced P1 substituents with the aim of increasing the binding interactions with the S1 site. This resulted in inhibitors with more drug-like properties and activities in the low micromolar range.

Populärvetenskaplig sammanfattning

Proteaser tillhör en klass av enzymer som katalyserar klyvningen av andra proteiner. Genom denna egenskap styr proteaserna livsviktiga processer i alla organismer; såsom matsmältning, reproduktion, sårläkning, åldrande m.m. Att reglera aktiviteten för mänskliga, bakteriella, virala och parasitiska proteaser har därför kommit att bli ett attraktivt sätt för forskare att angripa sjukdomar.

I denna avhandling beskrivs hur aktiviteten för två olika proteaser kunnat sänkas avsevärt med hjälp av så kallade proteasinhibitorer. Dessa inhibitorer är vanligtvis peptidlika organiska molekyler som designats och framställts på organisk-kemisk väg för att efterlikna enzymernas naturliga substrat. Man studerar sedan samband mellan strukturen på molekylerna och deras förmåga att hämma/inhibera aktiviteten hos proteaset. Målet är att optimera inhibitorns struktur så att den binder starkare till den aktiva ytan på det proteas som man vill inhibera, jämfört med det substrat som normalt binder in och klyvs där. Om detta lyckas kan man bromsa upp och i bästa fall förhindra ett fortsatt sjukdomförlopp.

Den inledande delen behandlar framtagandet (syntesen) av inhibitorer mot ett, för hepatit C viruset (HCV), livsviktigt proteas. Viruset angriper levern och infektionen, som ofta blir kronisk, leder i det långa loppet till skrumplever och levercancer med levertransplantation som enda utväg. Det proteas som inhiberats kallas HCV NS3 och är nödvändigt för virusets replikation.

Genom att systematisk variera den kemiska strukturen på våra potentiella HCV NS3 proteasinhibitorer producerades flera mycket intressanta molekyler. Den första inhibitorserien som syntetiserades var raka/linjära molekyler. Fortsatt arbete ledde till en serie med cyklisk struktur. Den mest aktiva av dessa cykliska strukturer ligger till grund för en läkemedelskandidat som för närvarande befinner sig i kliniska fas II studier.

I den senare delen syntetiserades inhibitorer mot det mänskliga proteaset BACE-1 som tros vara involverat i det cellnedbrytande förlopp i hjärnan som slutligen leder till Alzheimers sjukdom. BACE-1 utför den första av två klyvningar som resulterar i frigörandet av en olöslig peptid som veckar ihop sig på ett felaktigt sätt. Ansamlandet av sådana felveckade peptider ger upphov till plackbildning och med tiden utbredd celldöd i hjärnan.

I vårt arbete framställdes BACE-1-inhibitorer som baserades på två olika centrala s.k. transition state isosterer. Ett flertal aktiva inhibitorer producerades, och med hjälp av röntgenkristallografi kunde interaktionerna mellan en av de mest aktiva inhibitorerna och den aktiva ytan på BACE-1 beskrivas i detalj.

List of Papers

This thesis is based on the following papers, which are referred to in the text by their Roman numerals:

I. Johansson, P. O.; Bäck, M.; Kvarnström, I.; Jansson, K.; Vrang, L.; Hamelink, E.; Hallberg, A.; Rosenquist, Å.; Samuelsson, B.

Potent Inhibitors of the Hepatitis C Virus NS3 Protease. Use of a Novel P2 Cyclopentane-derived Template.

Bioorg. Med. Chem. **2006**, *14*, 5136-5151.

II. Bäck, M.; Johansson, P. O.; Wångsell, F.; Thorstensson, F.; Kvarnström, I.; Ayesa, S.; Wähling, H.; Pelcman, M.; Jansson, K.; Lindström, S.; Wallberg, H.; Classon, B.; Rydergård, C.; Vrang, L.; Hamelink, E.; Hallberg, A.; Rosenquist, Å.; Samuelsson, B.

Novel Potent Macrocyclic Inhibitors of the Hepatitis C Virus NS3 Protease: Use of Cyclopentane and Cyclopentene P2-Motifs

Bioorg. Med. Chem. **2007**, *15*, 7184-7202.

III. Bäck, M.; Nyhlen, J.; Kvarnström, I.; Appelgren, S.; Borkakoti, N.; Jansson, K.; Lindberg, J.; Nyström, S.; Hallberg, A.; Rosenquist, Å.; Samuelsson, B.

Design, Synthesis and SAR of Potent Statine-Based BACE-1 Inhibitors: Exploration of P1 Phenoxy and Benzyloxy Residues

Bioorg. Med. Chem. **2008**, *16*, 9471-9486.

IV. Bäck, M.; Kvarnström, I.; Rosenquist, Å.; Samuelsson, B.

Design and Synthesis of Hydroxyethylene-Based BACE-1 Inhibitors Incorporating Extended P1 Substituents

In manuscript

Abbreviations

Aβ	amyloid-beta
Abu	L-α-aminobutyric acid
AD	Alzheimer's disease
APP	amyloid precursor protein
BACE	beta-site APP-cleaving enzyme
Boc	*tert*-butyloxycarbonyl
Cat D	cathepsin D
Chg	L-cyclohexylglycine
DBU	1,8-diazabicyclo[5.4.0]undec-7-ene
DCM	dichloromethane
DIAD	diisopropyl azodicarboxylate
DIPEA	*N*,*N*-diisopropylethylamine
DMAP	4-dimethylaminopyridine
DMF	*N*,*N*-dimethylformamide
DPPA	diphenylphosphoryl azide
EC_{50}	inhibitor concentration causing 50% inhibition of replication in a cell culture system
EDC	1-(3-dimethylaminopropyl)-3-ethylcarbodiimide
Fmoc	9-fluorenylmethoxycarbonyl
HATU	*O*-(7-azabenzotriazol-1-yl)-*N*,*N*,*N'*,*N'*-tetramethyluroniumhexafluorophosphate
HCV	hepatitis C virus
HIV	human immunodeficiency virus
IC_{50}	inhibitor concentration causing a 50% decrease in the enzyme activity
K_i	dissociation constant of an enzyme (E) - inhibitor (I) complex; K_i = [E][I]/[EI]
NMR	nuclear magnetic resonance
NS3	nonstructural protein 3
Nva	L-norvaline
RCM	ring-closing metathesis
RNA	ribonucleic acid
SAR	structure-activity relationship
TFA	trifluoroacetic acid
THF	tetrahydrofuran
TPAP	tetrapropylammonium perruthenate

Table of Contents

Preface 1

1. Introduction 3

1.1 Proteases—Proteins that Cleave Proteins 3

1.1.1 Serine Proteases 3
1.1.2 Aspartic Proteases 4
1.1.3 Potential Drug Targets 5

1.2 Enzyme-Substrate Interactions 5

1.3 Protease Inhibitors 6

1.3.1 Inhibitor Design Strategies 6
1.3.2 Desirable Inhibitor Properties 6

2. Design, Synthesis, and Analysis of Structure-Activity Relationships (SARs) of Potential HCV NS3 Protease Inhibitors (Papers I and II) 9

2.1 The Hepatitis C Virus 9

2.1.1 The Viral Genome and Life Cycle 10

2.2 Potential Drug Targets 12

2.2.1 The NS5B RNA Polymerase 12
2.2.2 The NS3 Protease 13

2.3 Inhibitors of the HCV NS3 Protease 14

2.4 Design, Synthesis, and SAR Analysis of Linear HCV NS3 Protease Inhibitors (Paper I) 17

2.4.1 Design 17
2.4.2 Synthesis 17
2.4.3 SAR Analysis 21

2.5 Design, Synthesis, and SAR Analysis of Macrocyclic HCV NS3 Protease Inhibitors (Paper II) 28

2.5.1 Design 28
2.5.2 Synthesis 29
2.5.3 SAR Analysis 33

3. Targeting the Aspartic Protease BACE-1 to Identify Potential Drugs for Alzheimer's Disease—Design, Synthesis, and Analysis of SARs (Papers III and IV) 41

3.1 Alzheimer's Disease 41

3.2 APP and Aβ 42

3.3 The Amyloid Cascade Hypothesis 43

3.4 BACE-1 44

3.5 BACE-1 Inhibitors 45

3.6 Design, Synthesis, and SAR Analysis of BACE-1 Inhibitors Encompassing P1 Phenoxy and Benzyloxy Residues (Paper III) 47
3.6.1 Design 47
3.6.2 Synthesis 48
3.6.3 SAR Analysis 52
3.7 Design and Synthesis of Hydroxyethylene-Based BACE-1 Inhibitors Incorporating Extended P1 residues (Paper IV) 58
3.7.1 Design 58
3.7.2 Synthesis 59
3.7.3 Results 62
4. Concluding Remarks 65
5. Acknowledgments 67
6.References 69

Preface

First some perspective. The active site of an enzyme is very dynamic and complex in nature, and thus it is almost impossible to predict in advance how it will interact with a particular molecule. The smallest change in the structure of a compound that is already active can result in total loss of affinity for the enzyme. The human body is a masterpiece that has evolved over a very long period of time, but its slow evolution has also rendered it sensitive to sudden changes in both its outer and inner environment. Due to the inner sensitivity, the selectivity and distribution of a potential drug must be given careful consideration. Consequently, it is an extremely difficult, time-consuming, and expensive task to come up with a molecule that possesses all the properties required to fulfill every criteria of being a suitable drug. Numerous scientists in many different fields are engaged in such work, and hence it is not surprising that most research in medicinal chemistry is conducted by large teams that are often established and overseen by pharmaceutical companies.

Accordingly, the work presented in this thesis was done in collaboration with the pharmaceutical company Medivir AB in Huddinge, Sweden, over a period of approximately five years. Although my doctoral research was initially focused primarily on the organic synthesis of potential drug molecules, during that work I was also introduced to the area of medicinal chemistry, mainly considering the structure-activity relationships between the mentioned molecules and the active site of the targeted enzymes. In addition to the knowledge of organic chemists, such studies require the help of experienced protein chemists (to express and purify the enzymes), biologists (to set up and perform the activity measurements), analytical chemists, molecular modelers, x-ray crystallographers, NMR spectroscopists, and experts in many other fields. I guess what I am trying to say is that science in general is teamwork, and drug development is definitely no exception.

1. Introduction

This thesis deals with the design and synthesis of inhibitors targeting either the hepatitis C virus (HCV) NS3 serine protease or the human aspartic protease called β-secretase or BACE-1, which is assumed to be involved in the neurodegenerative cascade that leads to Alzheimer's disease. However, before considering any reaction schemes or structure-activity relationship (SAR) analyses, let us begin with the basics. What are proteases, what are their functions, and how can medicinal chemists take advantage of the properties of these enzymes when developing drugs to combat various diseases? These fundamental questions are addressed in this chapter.

1.1 Proteases—Proteins that Cleave Proteins

Proteins are macromolecules that are the building blocks of living organisms, but they can also be very dynamic and have specific catalytic properties. Such proteins are known as enzymes, and they are responsible for speeding up chemical reactions within cells and are thus essential for sustaining life. Enzymes are divided into different classes depending on the kind of catalytic activity they have. One such class comprises the proteases, which are characterized by their ability to hydrolyze polypeptide bonds, that is, the bonds that link together proteins. This property allows proteases to control the synthesis, turnover, and function of proteins, and thereby direct vital physiological processes.[1]

Based on their catalytic mechanisms, these important enzymes can be further divided into four major subclasses designated the serine proteases, aspartic proteases, cysteine proteases, and metalloproteases.[2] The focus will be on the first two subclasses, since they represent the classes of proteases for which synthesis of potential drug candidates will be discussed later in this thesis.

1.1.1 Serine Proteases

Nearly one-third of all proteases are serine proteases, a name they have been given because they possess a nucleophilic serine residue at the active site.[3] Based on their

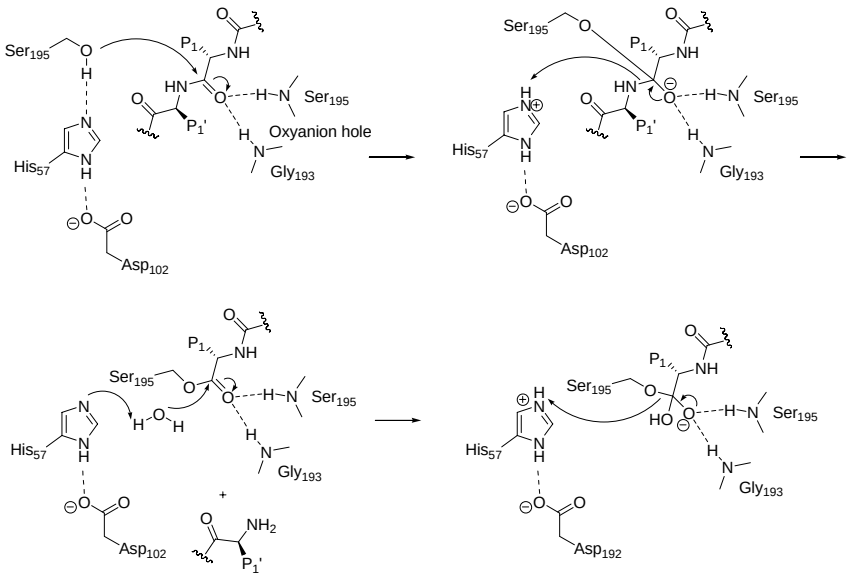

Figure 1. *General mechanism of peptide bond hydrolysis catalyzed by serine proteases.*

substrate specificity, particularly the type of residue found at position P1, they are divided into at least the following three categories: the trypsin-like proteases, which show preference for the positively charged Lys/Arg residues at P1; the chymotrypsin-like proteases, which favor large hydrophobic P1 residues (e.g., Phe/Tyr/Leu); the elastase-like proteases, which prefer small hydrophobic residues (e.g., Ala/Val) in the P1 position.[2]

The active site of serine proteases possesses a catalytic triad consisting of the amino acids Ser195, His57, and Asp102 (chymotrypsin numbering system), and it also contains an oxyanion hole that stabilizes the tetrahedral intermediate formed during the catalytic cleavage of the substrate.[3,4] Figure 1 illustrates the general mechanism by which serine proteases hydrolyze amide bonds.

1.1.2 Aspartic Proteases

Aspartic proteases are a well-characterized class of enzymes on which an extensive amount of structural information has now been accumulated. They tend to bind 6–10-amino-acid portions of the substrate to be cleaved,[2] sequence information that can be utilized in inhibitor drug design. A special feature of aspartic proteases is a hairpin turn, or flap, covering the active site. This region of the enzyme opens up to allow substrates to enter the active site, and then it closes during catalysis. The most widely accepted mechanism of action is the general acid-base catalysis that is performed by a water molecule and two catalytically active Asp residues. The water molecule is

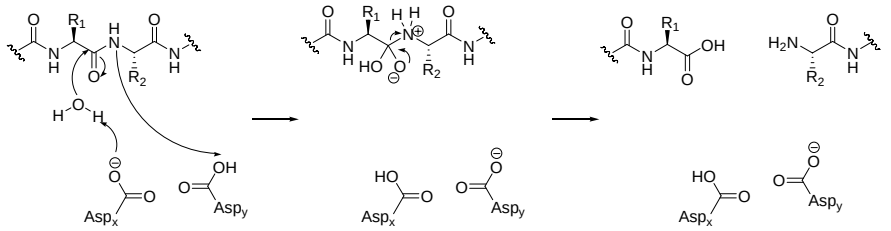

Figure 2. *General mechanism of peptide bond hydrolysis catalyzed by aspartic proteases.*

activated by an Asp residue and then attacks the scissile amide bond. Subsequent protonation of the amide nitrogen gives a zwitterionic tetrahedral intermediate that collapses to provide the cleaved products (Figure 2).[5]

1.1.3 Potential Drug Targets

As mentioned above, proteases regulate many essential physiological functions, such as digestion, growth, aging, fertilization, immune defense, and wound healing, and they can do so by virtue of their capacity to control the folding, turnover, and functions of proteins. Accordingly, being able to control the mammalian, viral, bacterial, or parasitic proteases that are associated with the mentioned qualities is of great interest when trying to devise new methods for treating various diseases.[1,2,4] There are many examples of proteases that have been targeted for drug development, including the following:[2] renin (regulates blood pressure in humans), HIV-1 protease, thrombin (facilitates blood clotting in humans), plasmepsins I and II (found in the most dangerous malarial parasite), DPP IV protease (anti-diabetic target)[6] HCV NS3 protease, and β-secretase.

1.2 Enzyme-Substrate Interactions

Most proteases have an active site that is sequence specific, which means that the size, depth, and hydrophobicity/hydrophilicity of the location allow interaction of certain parts of the active site with certain residues in the substrate but not others.[1,2] Schecter and Berger[7] introduced the nomenclature that is now standard for describing interactions between the enzyme and the substrate or inhibitor (peptide). The amide bond in the peptide, which is normally cleaved by a protease, is referred to as the scissile bond. The part of the substrate to the right of the scissile bond is called the prime side, and the part to the left is the non-prime side. The amino acids are designated P (or P´) indicating peptidyl residue, and the corresponding sites in the enzyme with which they interact are denoted S (or S´) denoting subsite. The positions are numbered according to their relative number of positions away from the scissile bond (Figure 3).

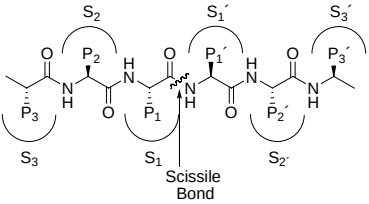

Figure 3. *The standard nomenclature for substrate/inhibitor residues (P and P´) and the corresponding sites of the enzyme (S and S´) with which the residues interact.*

1.3 Protease Inhibitors

The goal of medicinal chemists when targeting a protease involved in a particular disease is to prevent or inhibit the enzyme from catalyzing the reactions of its natural substrate. Therefore, drugs or inhibitors that have properties that permit them to efficiently interact with a particular protease can potentially impede, or even halt, the progression of the selected disease.

1.3.1 Inhibitor Design Strategies

Traditionally, developing protease inhibitors has involved screening of natural products or large libraries of compounds, followed by refining of any compounds that seem promising to hopefully arrive at a drug candidate. A more modern approach is to optimize the part of the natural substrate that interacts with the active site in the protease to obtain what are known as substrate analogs. Many proteases are also prone to inhibition by products of the cleavage of their natural substrates, and those fragments can be optimized to yield what are called product analogs. The optimization strategy often starts from a rather defined part (less than 10 amino acids) of a substrate or cleavage product, sometimes with the aim of replacing the scissile amide bond with a non-cleavable isostere (see discussion of aspartic protease inhibitors below). Optimization was previously mainly achieved by random structural modifications, basically through trial and error. However, this procedure has been substantially improved in recent years, and information on three-dimensional structure is now provided by X-ray studies, NMR experiments, and computer models of inhibitors docked in the active sites of proteases, which enables much more efficient and rational drug design.[2,8]

1.3.2 Desirable Inhibitor Properties

When designing a protease inhibitor, some desirable properties (regarding pharmacodynamics[9] and pharmacokinetics[10]) have to be taken into consideration. Besides being active against the protease of interest, a drug candidate should show

high selectivity over other proteases to avoid unwanted side effects. Low toxicity, a relatively long half-life, and a high therapeutic index[11] are also important qualities. Moreover, good bioavailability is necessary if a protease inhibitor is to be administered orally, and the following guidelines[12] have been outlined to facilitate the prediction of whether a compound will meet that criterion: molecular weight < 500, < 5 hydrogen bond donors, < 10 hydrogen bond acceptors, and Log P < 5 (as a measure of the hydrophobicity of a drug). An additional guideline was recently published,[13] which indicates that if a potential protease inhibitor is to have acceptable oral bioavailability, it should not have more than 10 rotatable bonds or a polar surface area that is more than 140 $Å^2$. Another feature that is related to the mentioned criteria is that an inhibitor should not be too peptide-like in nature, because peptides tend to be unstable and have poor pharmacokinetic qualities.[2]

2. Design, Synthesis, and Analysis of Structure-Activity Relationships (SARs) of Potential HCV NS3 Protease Inhibitors (Papers I and II)

2.1 The Hepatitis C Virus

For many years, a serious form of chronic hepatitis was unknowingly spread all over the world, mainly through blood transfusions.[14] Development of new tests for hepatitis A virus (HAV) and hepatitis B virus (HBV) in the mid 1970s led to the discovery that neither of these two viruses was responsible for the known cases of the chronic disease.[15] After becoming aware of the existence of a new pathogen, scientists assumed that it would soon be identified. However, 15 years were to pass before Houghton and coworkers[16] were able to clone and identify the genome of the virus isolated from chimpanzee serum.[15]

The new form of the pathogen, previously referred to as non-A, non-B hepatitis, was named hepatitis C virus (HCV).[17] The main reason HCV remained so obscure for decades is that infection with this virus has a silent onset and evolves asymptomatically into a chronic form of hepatitis.[18] Moreover, it proved difficult to achieve reliable growth of HCV in cell culture, and it seems that only chimpanzees and humans can be consistently infected.[19] Accordingly, investigation of HCV is associated with both high costs and ethical issues.

Today, hepatitis C afflicts approximately 200 million people or 3% of the global population,[20] thus representing a human epidemic that is over four times more widespread than infections with the human immunodeficiency virus (HIV).[21] The primary cause of the large number of global HCV infections can be assigned to the uncontrolled spreading that began in the early 1960s and lasted until the early 1990s.[14] Even though blood screening has been implemented since then, the number of infections continues to grow, mainly as the result of inadequate detection and intravenous drug abuse.[18] HCV differs from most other viruses in that it causes a

chronic disease. Infection with HAV usually lasts for only a few weeks, whereas HCV infection can last for decades.[15]

The hepatocytes (liver cells) are the main targets of HCV. Similar to other viruses, HCV itself does not kill the cells it infects, but instead triggers a mechanism in the host immune system that causes the cells to self-destruct.[22] The disease is associated with slow, progressive inflammation and fibrosis of the liver, which in time results in cirrhosis and eventually hepatic failure or hepatocellular carcinoma.[23] HCV infection is now the leading reason for liver transplantation in Western countries.[14] Furthermore, inasmuch as infected individuals can be carriers of the virus for a decade or more before symptoms appear, the population requiring medical treatment and possibly also liver transplants may increase dramatically over the next 10–20 years.[24]

At least six genotypes of HCV (designated 1–6) have been identified, of which genotype 1 is predominant.[25] The many genotypes have arisen due to the high mutation rate of the virus,[14] and they have made development of efficient drugs against HCV a very challenging task. At present, there is no vaccine against HCV. Furthermore, the current treatment regimen given to infected patients, which includes PEGylated interferon-α in combination with the nucleoside analog ribavirin (Figure 4),[26] is poorly tolerated and effective in less than 50% of cases with HCV genotype 1.[27] Consequently, there is an urgent need to develop new and improved drugs to treat HCV infection.

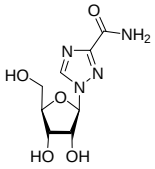

Ribavirin

Figure 4. *The structure of the nucleoside analog ribavirin.*

2.1.1 The Viral Genome and Life Cycle

HCV is a relatively small positive single-stranded RNA virus that belongs to the *Flaviviridae* family. The viral genome comprises an open reading frame (ORF) that consists of approximately 9,600 nucleotides and expresses a large polyprotein (Figure 5) once the virus is inside a host cell. This polyprotein undergoes proteolytic cleavage into three structural and six non-structural (NS) proteins.[28] The structural proteins include the core protein (C) and two envelope glycoproteins (E1 and E2). The core protein forms the nucleocapsid that encases the viral RNA, and the heavily glycosylated E1 and E2 proteins help the virus to interact with membranes of hepatocytes and other cells.[14] The structural proteins are separated from the NS proteins by a small membrane peptide designated p7, which has been suggested to act

as an ion channel. The NS proteins are designated NS2, NS3, NS4A, NS4B, NS5A, and NS5B, and they are essential for processing of the polyprotein and for directing translation and replication of the viral RNA. The NS2-NS3 zinc-dependent cysteine protease is autocatalytically cleaved to produce NS2 and NS3. The NS3 protein has an *N*-terminal serine protease domain and a *C*-terminal RNA helicase/NTPase domain, and those two parts form a complex with the cofactor NS4A, and the complexed protease is responsible for cleavage of the remaining NS proteins. The function of the small hydrophobic protein NS4B is not clear, whereas NS5A and NS5B represent the replication machinery (Figure 5).[29]

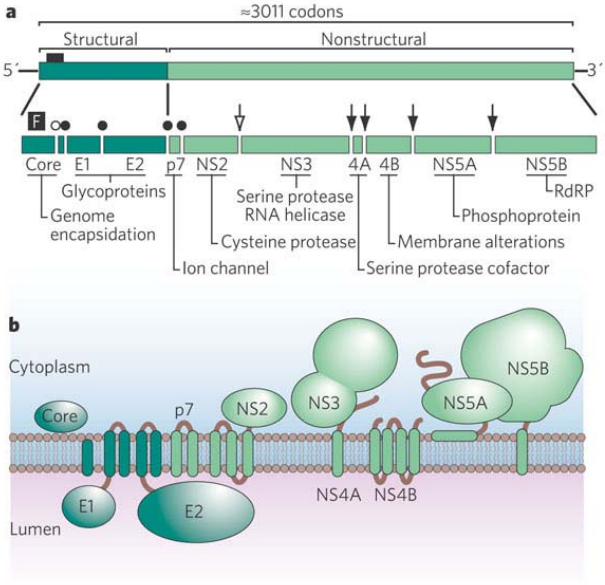

Figure 5. *(a) The genome of the hepatitis C virus, the polyprotein it encodes, and potential cleavage sites in the polyprotein. (b) Potential interactions between HCV proteins and the membrane of a host cell.*[30]

Due to a very high rate of replication and the lack of proofreading by the NS5B polymerase, the HCV RNA genome exhibits a large degree of variability. As mentioned above, this has resulted in six main genotypes, and there are also several subtypes of HCV. The predominant genotype 1 is divided into two subtypes designated 1a and 1b; both subtypes are common in the United States and Europe, whereas 1b is predominant in Asia.[14]

A rather simplified diagram of the HCV life cycle is presented in Figure 6. In short, attachment and endocytosis (cell entry) of the viral particle is promoted by interaction of the viral envelope proteins with specific surface receptors on the host

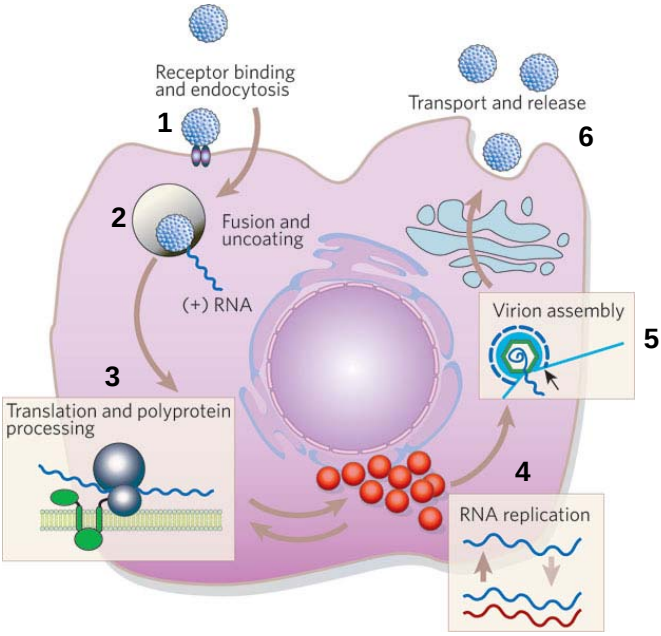

Figure 6. *Schematic diagram of the HCV life cycle: (1) cell receptor-mediated endocytosis (cell entry); (2) release of the viral genome via fusion of the viral cellular membranes; (3) translation and polyprotein processing; (4) RNA replication; (5) encapsulation of new virions; (6) virion release.*[30]

cell. Within the cell, low pH mediates release of the single-stranded RNA, which then has three main roles: to participate in translation of the polyprotein; to act as a template for replication; and to serve as the genome to be packaged into new virus particles (virions).[29]

2.2 Potential Drug Targets

Theoretically, all of the NS proteins that are encoded by HCV might be suitable targets for anti-HCV therapy. However, in general, somewhat greater interest has been directed toward two enzymes in particular: NS3 protease, which was the HCV target in the work underlying the first part of this thesis, and NS5B RNA polymerase, which is discussed only briefly here.

2.2.1 The NS5B RNA Polymerase

The enzyme HCV NS5B is an RNA-dependent RNA polymerase (RdRp) that is essential for replication of the virus, because it facilitates synthesis of positive- and negative-stranded viral RNA. There are no known human enzymes that show similar biochemical activity, which makes it possible to identify very selective inhibitors of HCV NS5B.[19] The crystal structure of this polymerase has been solved,[31-33] and

several nucleoside-based and non-nucleoside-based RNA replicase inhibitors (designated NRRIs and NNRRIs, respectively) have been identified. NRRIs interact with the active site and terminate the RNA chain by interfering with the subsequent nucleoside propagation step through steric hindrance, whereas NNRRIs inhibit the polymerase in an allosteric manner.[21] Active RdRp inhibitors have also been shown to reduce the viral load *in vivo*.[21,34-36] On the whole, HCV NS5B polymerase constitutes a very promising anti-HCV target and several compound are currently evaluated in clinical trials (Figure 7).[37]

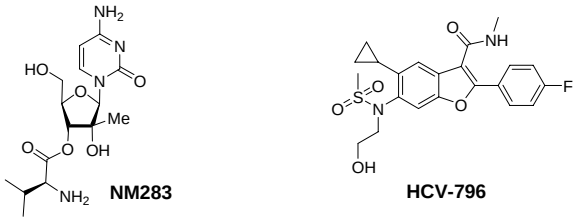

Figure 7. *Two NS5B RNA replicase inhibitors: the nucleoside-based prodrug* ***NM283*** *(phase II) and the non-nucleoside-based* ***HCV-796*** *(phase II). Both are currently on hold due to non-beneficial side effects observed in clinical trials.*[35]

2.2.2 The NS3 Protease

NS3 emerged at an early stage as the most popular anti-HCV target, and it is the most intensively studied and best characterized of the NS proteins. NS3 is a 631-amino-acid bifunctional enzyme; the first 180 amino acids are defined by a serine protease, and the remainder of the protein encompasses a domain with both RNA helicase and nucleoside triphosphatase (NTPase) activity.[21] Structurally, the protease is a member of the chymotrypsin serine protease family,[38] but is nevertheless unique in that it requires a noncatalytic structural zinc atom and the small peptide cofactor NS4A to be catalytically active.[26] In addition, it was recently shown that the serine protease activity is enhanced by the helicase domain and *vice versa*.[39] The NS3-NS4A complex is responsible for cleavages of the entire downstream region of the polyprotein,[40] which renders it essential for viral replication and thereby also a potential pharmaceutical target.[41] Moreover, successful use of protease inhibitors in the treatment of HIV[40] has verified the idea of blocking key proteases to fight viral diseases, and the efficacy of inhibiting the HCV NS3 protease was also validated in recent proof of concept studies.[42]

HCV NS3 protease has a shallow, solvent-exposed active site, and it requires a long peptide substrate with many weak interactions distributed along an extended surface area. Furthermore, it has been established that this enzyme shows preference for a cysteine in the P1 position,[43] which was initially a considerable problem for

medicinal chemists (see below). These findings, along with the high mutation rate of the virus, to some extent illustrate the difficulties involved in designing HCV NS3 protease inhibitors. Nonetheless, great efforts made by many research groups around the world have led to identification of several potent inhibitors in a relatively short period of time.

2.3 Inhibitors of the HCV NS3 Protease

Among the first inhibitors to be developed were decamer substrate analogs spanning from the P6 to the P4´ position of the active site of NS3 protease. The activity of these peptides was gained by incorporating cyclic residues such as proline or pipecolinic acid in the P1´ position, which made the peptides non-cleavable and thereby gave them the potential to inhibit the enzyme in a competitive manner.[43,44]

Substrate specificity studies have shown that NS3 protease is prone to feedback inhibition by hexapeptide products of substrate cleavage,[45,46] and, based on that observation, two research groups set out to optimize the hexapeptides. Examples of such product analog inhibitors that were synthesized at an early stage are compounds **A**[47] and **B**[48] (with P designations) in Figure 8, which required both a two-acid "anchor" in the P5–P6 position and a cysteine P1 residue with a terminal carboxylic acid in order to reach optimum activity. Since cysteine is not preferred as a building block in drug synthesis, major efforts were made to come up with acceptable P1 replacements. This resulted in the (*S*)-4,4-difluoro-2-aminobutyric acid inhibitor **C**[43] and the 1-aminocyclopropyl carboxylic acid inhibitor **D**,[48] which were equipotent to the corresponding cysteine inhibitors.

However, it is well known that combining polypeptides and multiple carboxylate functionalities does not have favorable effects on the stability and bioavailability of a potential drug. Therefore, refining of inhibitor **D** comprising truncation of the P5–P6 positions, optimization of a P2 aromatic moiety, and insertion of an exceptionally good P1 residue led to the extremely potent tetrapeptide inhibitor **E**.[49] Synthesis of that compound was the result of years of systematic research and optimization carried out primarily by Llinàs-Brunet and coworkers[45,49-53] at Boehringer Ingelheim, Canada. The use of (1*R*,2*S*)-1-amino-2-vinylcyclopropane carboxylic acid as an excellent cysteine mimic, along with large aromatic systems extending from the P2 position, constituted a major breakthrough that enabled production of small peptide inhibitors without substantial loss of activity. Although very potent, compound **E** had poor biopharmaceutical properties, mainly due to its highly peptidic nature. Nevertheless, analysis of crystallographic and NMR data had revealed that the P1 and P3 side chains of bound inhibitors were positioned close to each other and pointing toward each other.[54] Consequently, further refinements of inhibitor **E**, including capping the

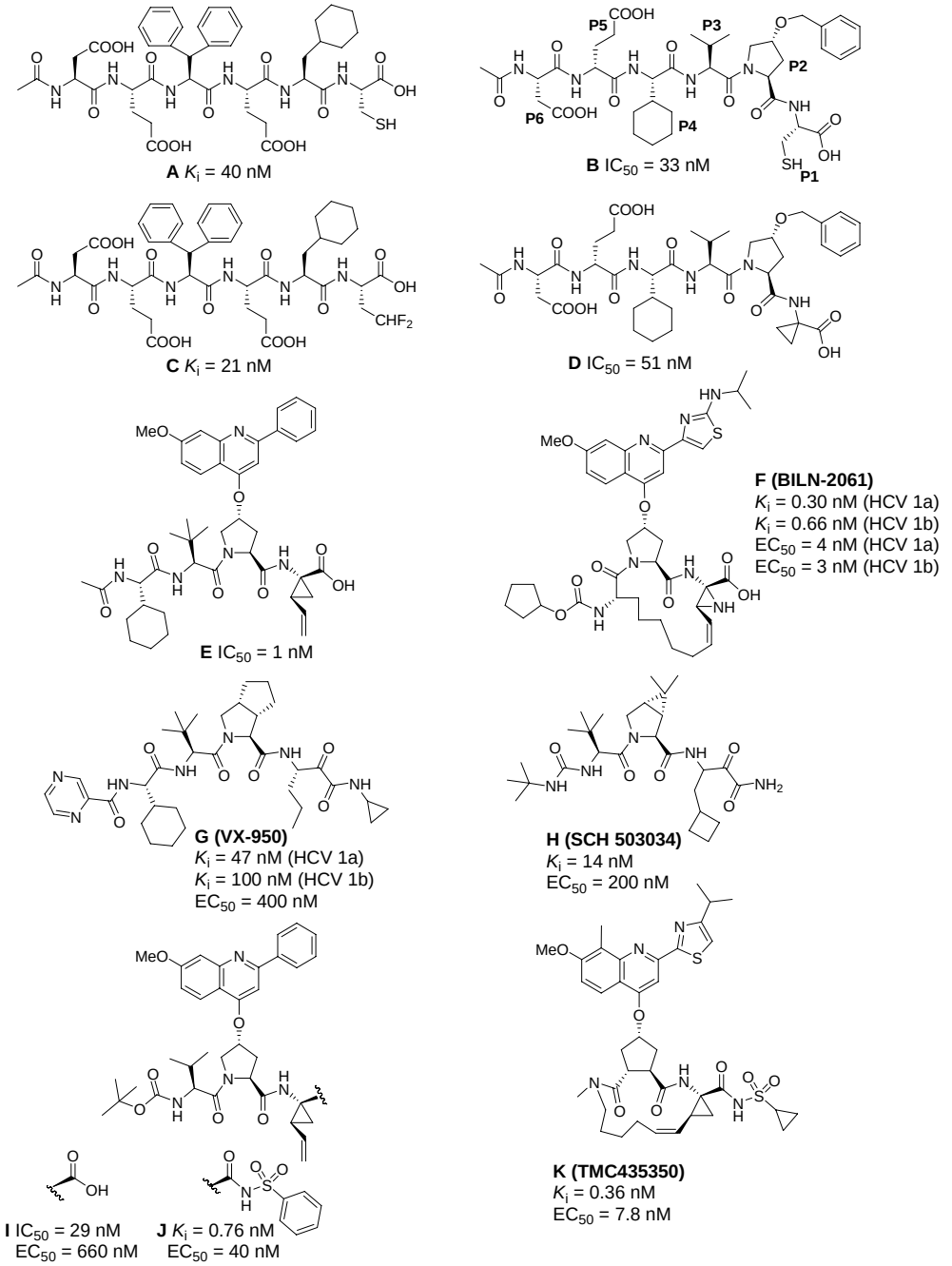

Figure 8. *HCV NS3 protease inhibitors.*

P3 position with a cyclopentyl moiety,[49] rigidification of the inhibitor into its bound conformation, and replacement of the phenyl moiety of the quinolinol with an

aminothiazole derivative, resulted in the less peptidic macrocyclic inhibitor **F** (**BILN 2061**).[42,55-58] **BILN 2061** was the first HCV protease inhibitor to enter clinical trials, and the early testing proved it to be very effective, causing a rapid decline in virus levels in all treated patients who were infected with HCV genotype 1.[42] Unfortunately, cardiac toxicity was observed in laboratory animals given high doses for four weeks, and the clinical trials were therefore suspended.[59]

Two other very promising compounds are the α-ketoamides **G** (**VX-950**)[60-62] and **H** (**SCH 503034**).[63-65] In addition, the research team behind compound **H** has published results regarding a similar, very promising α-ketoamide inhibitor further indicating that the ketoamide motif is highly effective.[66] Compared to all the other compounds in Figure 8, which are noncovalent product analogs, **G** and **H** represent another class of inhibitors known as transition state analogs or serine trap inhibitors. In these analogs, the scissile amide bond has been replaced with an electrophilic group that forms a covalent adduct with the catalytic serine of the protease, and, in the case of **G** and **H**, the covalent bond is slowly reversible.[61,67] The results of the first phase clinical trials were promising, and additional evaluation from phase III trials is currently underway.[68,69] Notably, in vitro studies have shown that mutants resistant to **BILN 2061** are still sensitive to **VX-950** and vice versa,[24,70] which indicates that combination therapy might be a plausible strategy for treating HCV patients. In fact it will probably be necessary to use combination therapy in order to avoid viral resistance to future inhibitors.[21]

As mentioned, a *C*-terminal carboxylic acid was found to be required for optimum activity of noncovalent, product-based inhibitors, and that rather unique feature led to the search for bioisosteric replacements of this critical group. Work in this area resulted in identification of an array of P1 cysteine replacements, and it was noted that acylsulfonamide derivatives reaching into the S1´ and S2´ sites were particularly effective in increasing the potency in both enzymatic and cell-based assays.[27,71-73] Compound **J**[74] exemplifies the benefits of incorporating sulfonamide carboxylic acid bioisosteres, and it should be compared with compound **I**.[49] Inhibitor **K (TMC435350)**[75] has the advantage of combining in a single compound all the benefits of macrocyclization, use of an acylsulfonamide as a carboxylic acid bioisostere, and incorporation of a particularly optimized quinoline moiety. Another significant feature of this compound is the insertion of a trisubstituted cyclopentane in the P2 position. **TMC435350** represents further development of the inhibitors that emerged in the present research (Papers I and II), and it is currently undergoing phase II clinical trials (Figure 8).

2.4 Design, Synthesis, and SAR Analysis of Linear HCV NS3 Protease Inhibitors (Paper I)

2.4.1 Design

The amino acid L-proline is frequently employed as a building block when designing inhibitor drugs, and it has been incorporated into numerous molecules that target various key proteases and diseases.[51,76-78] Therefore, much work has been devoted to mimicking this motif (Figure 9). Previous studies in our laboratories revealed that *N*-acylproline **I** can be replaced with five-membered carbocyclic ring isosteres such as **II**[79] and **III**,[80] the latter of which gave rise to moderately potent thrombin inhibitors. Furthermore, pioneering work at Boehringer Ingelheim resulted in the discovery of novel and very potent HCV NS3 protease inhibitors incorporating *N*-acyl-(4*R*)-hydroxyproline **IV** in the P2 position (compounds **E** and **F** in Figure 8). Inspired by those inhibitors and based on modeling, we chose to synthesize the trisubstituted cyclopentane structure **V** and incorporate it into HCV NS3 inhibitors.

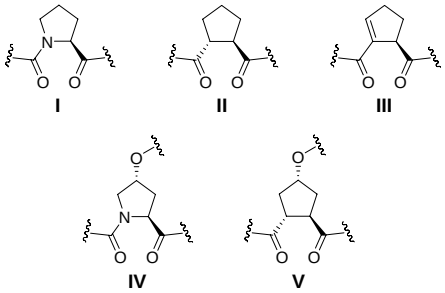

Figure 9. *N-Acylproline (**I**), previously reported N-acylproline isosteres (**II** and **III**), N-acyl-(4R)-hydroxyproline (**IV**), and the cyclopentane-based N-acyl-(4R)-hydroxyproline isostere (**V**) we used to synthesize novel HCV NS3 protease inhibitors.*

2.4.2 Synthesis

Figure 10 depicts the generic structure of the linear HCV NS3 inhibitors we synthesized (Paper I), all of which encompass the trisubstituted cyclopentane scaffold **V**. Also shown are the different R^1, R^2, and R^3 substituents used to optimize these inhibitors. A majority of the substituents in Figure 10 were commercially available or were readily synthesized from commercially available amino acids or precursors. Therefore, it is not necessary to describe in detail the chemistry that was employed, although, for the sake of clarity, some comments should be made. R^1 amino acid derivatives **A1**, **A2**, and **A4** were purchased or easily synthesized from suitably protected and commercially available precursors. The vinylcyclopropane amino acid derivative **A3** was synthesized according to the protocol published by Llinàs-Brunet et

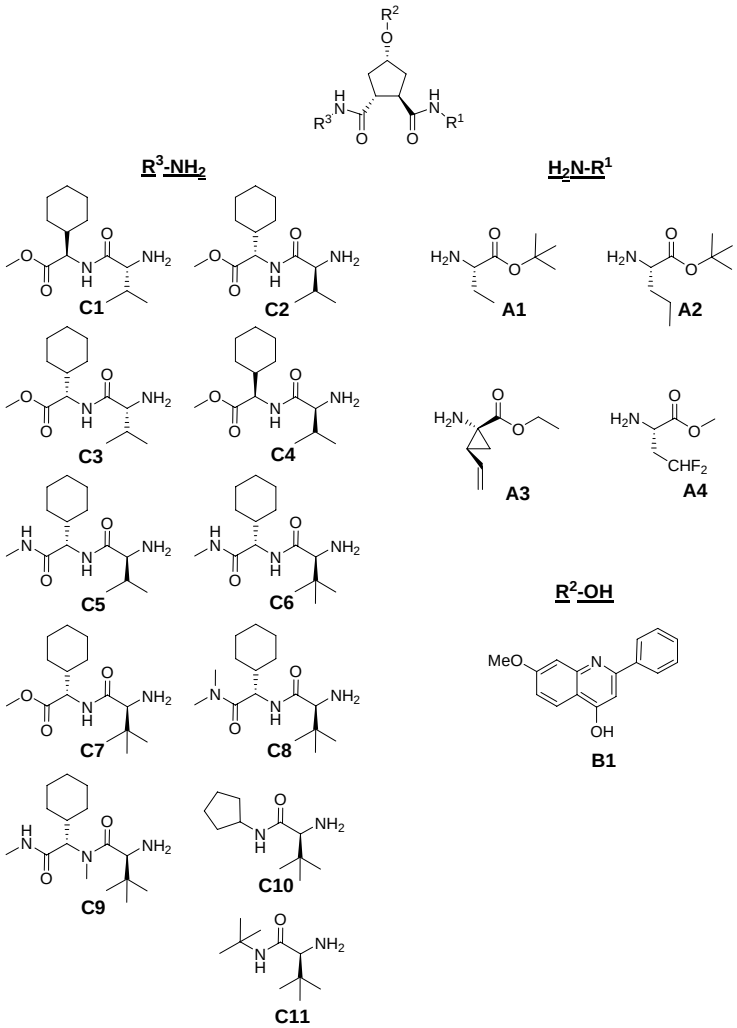

Figure 10. *A general picture of the central cyclopentane scaffold and the different R_1, R_2, and R_3 substituents that were used in the present research.*

al.,[56,81] and the R^2 2-phenyl-7-methoxy-4-quinolinol **B1** moiety was also produced as reported in the literature.[49,82] R^3 dipeptide or capped amino acid substituents **C1–C8** and **C10–C11** were generated by standard coupling, protection, and deprotection procedures (see general synthetic procedures in Paper I) using commercially available amino acids and amines. To obtain the *N*-methylated dipeptide **C9**, Fmoc-protected cyclohexylglycine was treated first with paraformaldehyde and *p*-toluenesulfonic acid in refluxing toluene, and then with triethylsilane (Et_3SiH) and trifluoroacetic acid (TFA) in chloroform[83] (see general synthetic procedures in Paper I). The resulting *N*-methylated amino acid was coupled by standard peptide synthesis to afford dipeptide

C9 (Scheme 1). The same procedure was used to obtain the corresponding dipeptide, in which the nitrogen on *tert*-butyl glycine had been methylated instead of the nitrogen on cyclohexylglycine. However, despite several attempts using a vast number of coupling reagents and conditions, the dipeptide could not be coupled to the scaffold. Consequently, this dipeptide, which we had intended to use together with **C8** and **C9** in an *N*-methylation study of the P3 and P4 substituents, was never evaluated as an R^3 substituent. The low coupling reactivity was probably due to steric hindrance during coupling between this particularly bulky amine and the scaffold.

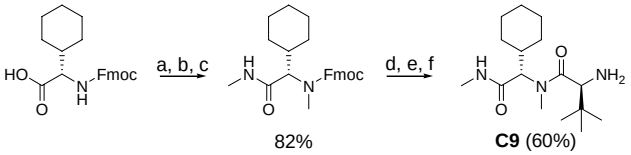

Scheme 1. *Reagents and conditions: (a) paraformaldehyde, p-TsOH, toluene; (b) TFA, triethylsilane, $CHCl_3$; (c) methylamine, DIPEA, HATU, DMF; (d) piperidine, DMF; (e) Boc-tert-butylglycine, DIPEA, HATU, DMF; (f) TFA, triethylsilane, DCM.*

The bicyclic lactone **3** (Scheme 2) served as a template from which eighteen P2-trisubstituted cyclopentane HCV NS3 inhibitors were synthesized. Using sodium borohydride in MeOH, alcohol **2**[84] was prepared (76% yield) by starting from enantiomerically pure *trans*-(3*R*,4*R*)-bis(methoxycarbonyl)cyclopentanone (**(-)-1**),[85] produced as described by Rosenquist et al.[86] Thereafter, both methyl esters of **2** were hydrolyzed with NaOH in MeOH and subsequently treated with acetic anhydride in pyridine,[87] which effected lactonization to give **3**[84] in a total yield of 88%. We then needed to protect lactone **3** in two different ways in order to have orthogonal protecting groups when coupling to differently protected R^1 substituents. Using methyl iodide and silver (I) oxide in acetone delivered methyl ester-protected scaffold **4** in 81% yield, whereas reaction with di-*tert*-butyl dicarbonate (Boc_2O) and 4-dimethylaminopyridine (DMAP) in dichloromethane (DCM) provided the corresponding *tert*-butyl-ester-protected scaffold **5** in 52% yield. An initial approach

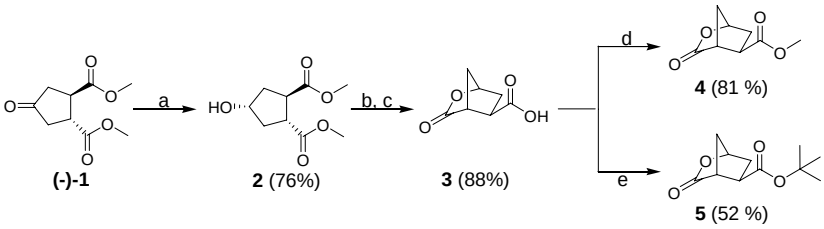

Scheme 2. *Reagents and conditions: (a) $NaBH_4$, MeOH, 0 °C; (b) NaOH (1M), MeOH; (c) Ac_2O, pyridine; (d) MeI, Ag_2O, acetone; (e) Boc_2O, DMAP, CH_2Cl_2.*

to promote *tert*-butyl ester protection involved the use of *tert*-butanol, EDC, and DMAP in DCM,[88] but that strategy consistently furnished less product and more byproducts compared to the Boc_2O protocol.

Depending on which of the two scaffolds was used and which R^1 substituent was chosen, two slightly different methods were employed to synthesize the target compounds.

Scheme 3 illustrates synthesis of target molecule **9** according to Method I, which was also used to generate target molecules **14–20** (Table 1). Methyl-ester-protected lactone **4** was initially opened using H-Nva-O*t*Bu, diisopropylethylamine (DIPEA) and 2-hydroxypyridine in refluxing THF to give amide **6** in 96% yield. The bifunctional catalyst 2-hydroxypyridine is known to promote the amide formation between amines and different kinds of esters.[89] That accelerating effect proved to be very important, because it shortened the reaction time and resulted in higher yields when opening lactone **4**.

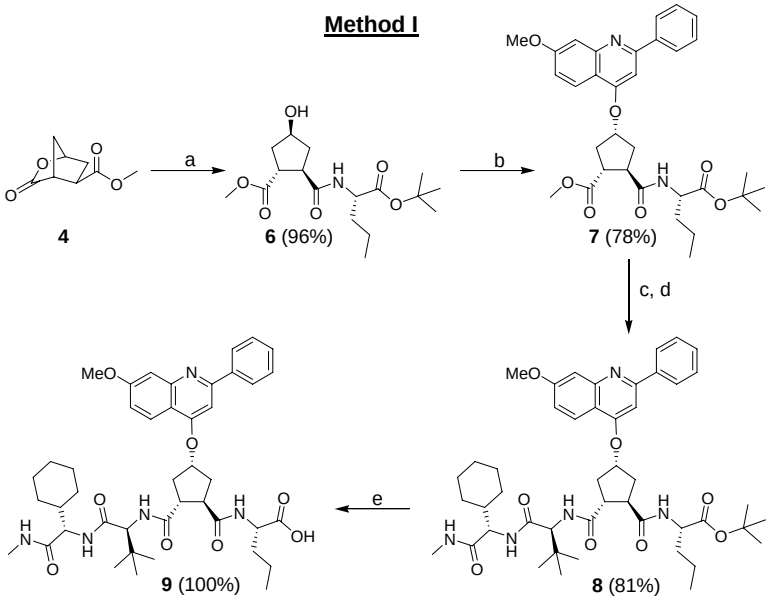

Scheme 3. *Reagents and conditions: (a) H-Nva-OtBu, DIPEA, 2-hydroxypyridine, THF, reflux; (b) 2-phenyl-7-methoxy-4-quinolinol (**B1**), PPh_3, DIAD, THF; (c) LiOH, dioxane/H_2O 1:1; (d) **C6**, HATU, DIPEA, DMF; (e) TFA, Et_3SiH, CH_2Cl_2.*

Next, Mitsunobu[90]-like conditions using R^2 substituent 2-methyl-7-methoxy-4-quinolinol (**B1**), triphenylphosphine (PPh_3), and diisopropyl azodicarboxylate (DIAD) in dry THF[56] gave the methyl ester **7** in 78% yield. Treating **7** with LiOH in dioxane/H_2O 1:1 afforded the corresponding acid, which was subsequently coupled to amine **C6** using the coupling reagent HATU and DIPEA in DMF to provide **8** in 81%

yield. Final treatment with TFA and Et_3SiH in DCM removed the *tert*-butyl ester and produced target compound **9** in quantitative yield.

Synthesis of target molecule **13** was done by Method II as outlined in Scheme 4, and the same technique was used to prepare target compounds **21–25**. Our initial attempts to use vinylcyclopropyl amino acid **A3** to open lactone **5** according to Method I were unsuccessful. Accordingly, a different strategy was applied in which lactone **5** was first opened by careful treatment with LiOH in dioxane/H_2O 1:1, and the resulting acid was subsequently coupled to amine **A3** by use of HATU and DIPEA in DMF to afford compound **10** in 89% yield. The Mitsunobu-like procedure was performed according to Method I (Scheme 3) to attach quinoline moiety **B1** with inversion of configuration, providing **11** in 68% yield. Removal of *tert*-butyl ester by use of TFA and Et_3SiH in DCM and coupling to amine **C6** with the aid of HATU and DIPEA in DMF gave compound **12** in 74% yield. Finally, ethyl ester hydrolysis was achieved with LiOH in THF/MeOH/H_2O 2:1:1, which delivered the desired target compound **13** in 67% yield.

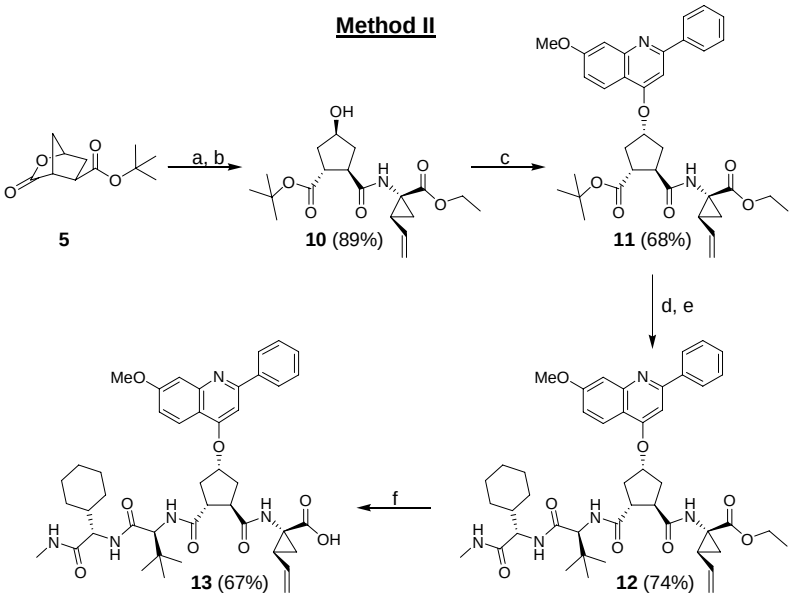

Scheme 4. *Reagents and conditions: (a) LiOH, dioxane/ H_2O 1:1, 0 °C; (b)* ***A3****, HATU, DIPEA, DMF; (c) 2-phenyl-7-methoxy-4-quinolinol (****B1****), PPh_3, DIAD, THF; (d) TFA, Et_3SiH, CH_2Cl_2; (e)* ***C6****, HATU, DIPEA, DMF; (f) LiOH, THF/MeOH/H_2O 2:1:1.*

2.4.3 SAR Analysis

The structures of all target compounds are presented in Table 1, along with methods of synthesis, total yields over the last five or six steps, and biological data. The

inhibitors were screened against HCV NS3 1a protease, and the percent inhibition was determined at three different concentrations: 10, 1, and 0.1 μM. K_i values were also determined for the most promising inhibitors in the initial screenings. For the inhibitors in Table 1 whose K_i values were not determined, comparison of potency was instead based solely on data on percent inhibition at 10 μM.

All inhibitors included in Table 1 contain a P2 2-phenyl-7-methoxy-4-quinolinol substituent that has frequently been included in potent HCV NS3 protease inhibitors,[27,54] like compounds **E**[49] and **J**[74] (Figure 8). Such aromatic P2 elongations have been reported to play an important role in stabilizing the catalytic machinery in a desired geometry by shielding that part of the protease from exposure to solvent.[50,91] Furthermore, it has been suggested that the P2 aryl substituent interacts in a favorable manner with the helicase domain of the NS3 protein.[92-94] The approach involving incorporation of such P2 substituents in combination with optimizations of the critical P1 position has significantly revolutionized the synthesis of HCV NS3 protease inhibitors, and it is in fact the main reason that medicinal chemists have been able to produce a new generation of small, less peptidic and more drug-like inhibitors that are equally or even more potent than the previous generation of hexapeptide inhibitors.

Let us now examine the properties of the inhibitors presented in Table 1 in greater detail. When using the cyclopentane central core, we were initially concerned about which stereochemistry to select for the P3 and P4 positions in our novel inhibitors. Comparison of compounds incorporating our cyclopentane-derived template and those based on the 4-hydroxyproline (e.g., **E** in Figure 8) reveals some striking differences. First of all, our scaffold protrudes one atom farther than the 4-hydroxyproline scaffold, and the P3–P4 substituents have to be turned away from the *N-C* direction (used in 4-hydroxyproline compounds) to face the *C-N* direction when coupling to the carboxylic acid functionality of our template. In addition, position 1 in our P2 template is sp^3 hybridized, whereas proline, which has nitrogen in this corresponding ring position, is planar. In light of these differing P2 template properties, it was apparent that the L-L stereochemistry of the P3–P4 substituents that produced the most potent 4-hydroxyproline-based inhibitors would not necessarily yield the most potent inhibitors when using our scaffold. To predict the stereochemical requirements of the substituents at P3–P4, a modeling study was initiated using the X-ray crystal structure of a bound product of the NS3-mediated cleavage[94] (i.e., the C terminus of the full-length, single-strand NS3 construct) as a starting point (Figure 11). The next step was to align compound **14** (Table 1), which exhibits D-configuration at the P3 and P4 positions, with the NS3 product. This strategy did not result in good alignment between the P3–P4 side chains in compound **14** and the side chains of the product (Figure 12). In contrast, alignment was very

Table 1. *Target molecules, methods of synthesis, total yields, and inhibition constants*

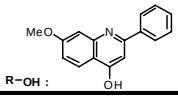

Cpd.	Structure	Method	Yield[a] (5 or 6 steps)	K_i (μM)[b] HCV NS3 1a	% Inh[c] at 10 μM
14	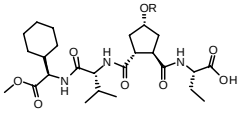	**I**	30%	ND	21
15	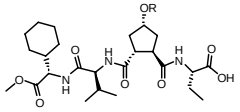	**I**	21%	ND	65
16	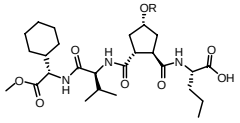	**I**	66%	2.3	100
17	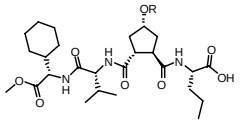	**I**	42%	ND	35
18	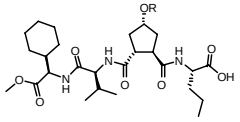	**I**	32%	ND	37
19	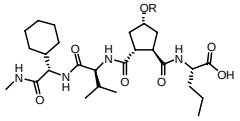	**I**	40%	6.6	
9	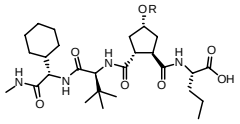	**I**	61%	1.7	
20	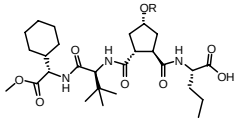	**I**	61%	1.2	

Table 1. *(Continued)*

Cpd.	Structure	Method	Yield[a] (5 or 6 steps)	K_i (μM)[b] HCV NS3 1a	% Inh[c] at 10 μM
13	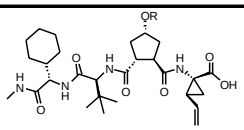	**II**	30%	0.022	
21	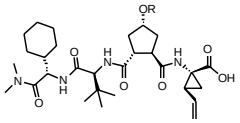	**II**	37%	0.016	
22	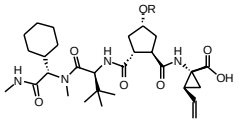	**II**	23%	>10	
23	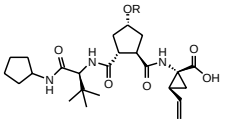	**II**	23%	2.7	
24	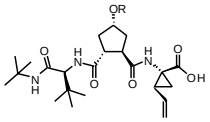	**II**	40%	6.9	
25	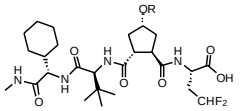	**II**	16%	0.56	

[a] Total yield over five steps for Method I and over six steps for Method II. [b] ND = not determined. [c] Inh at 10 μM for compounds where K_i was not measured or where it is important for discussion of the SAR.

good when using compound **15** (Table 1), which possesses L-amino acids at P3 and P4, together with the bound cleavage product (Figure 13). Taking a closer look at Figure 13, the following is apparent: the acyl cyclopentyl moiety of compound **15** adopts the same position as the P3-carbonyl of the product; the P3-NH of **15** shows the same interaction as the P2-NH of the product; and the P3 side chains of the two compounds are equally positioned in space. The same spatial pattern of binding and positioning is valid for the side chain and the amide of the P4 substituent. The results of this modeling study indicated that the L-configuration would be preferred for the P3 and P4 amino acids.

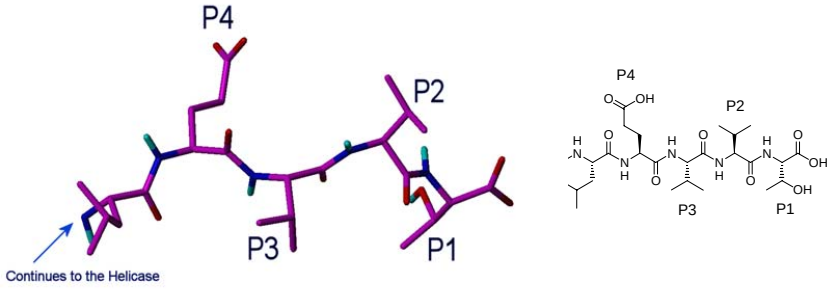

Figure 11. *The C terminus of the helicase domain (a product of the NS3-mediated cleavage of the NS3-NS4A junction of the HCV polyprotein) in its conformation bound to the NS3 active site, based on the published x-ray crystal structure (PDB entry 1CU1). A simple illustration of the chemical structure of the amino acid sequence in question is also given.*

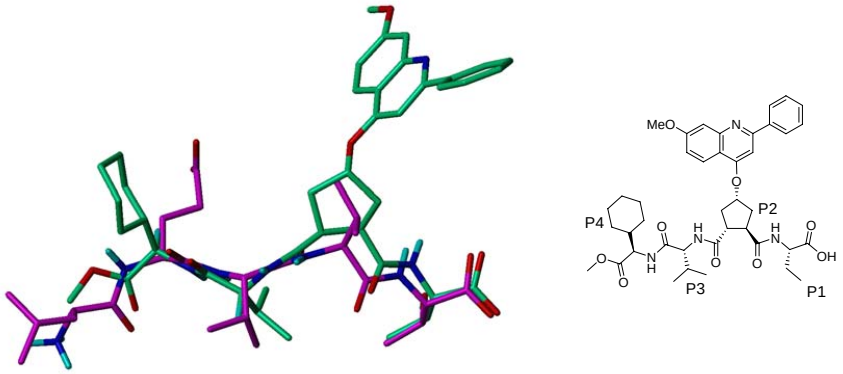

Figure 12. *Modeled structure of compound* ***14*** *containing* D*-amino acids at the P3 and P4 positions (green) superimposed on the bound C-terminal helicase residue (magenta). The P3 and P4 side chains do not overlay with the side chains of the product and will not fit in the S3 and S4 sub-pockets of the NS3 protease.*

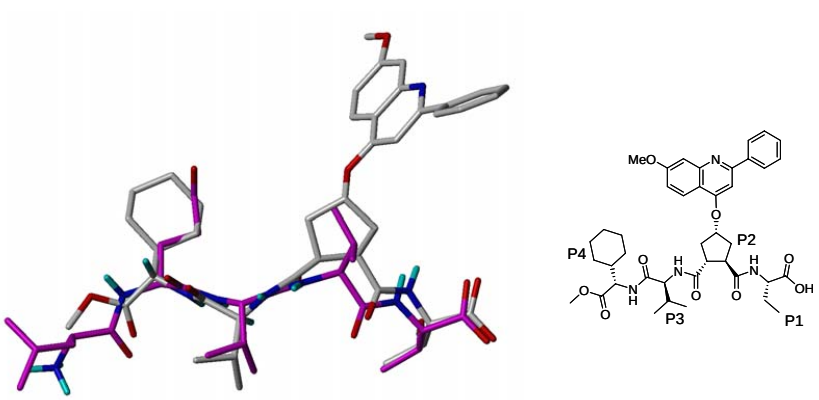

Figure 13. *Compound* ***15*** *(gray) containing the natural* L*-amino acids in P3 and P4 superimposed on the bound C-terminal helicase residue (magenta). The diagram clearly shows that* L*-configuration of P3 and P4 is required to achieve good overlay with the conformation of the bound product.*

Although molecular modeling can be helpful when trying to explain similarities and differences in the adopted positions and directions of substituents in an active site, it is still rather hypothetical. Consequently, to verify the modeling experimentally, we synthesized compounds **14** and **15**, both of which incorporate 2-aminobutyric acid (Abu) as a cysteine mimic in the P1 position. Neither of these compounds is very active, although **15**, which has the L-configured P3 valine and P4 cyclohexylglycine moieties, exhibits a stronger inhibition of 65% at a concentration of 10 μM compared to 21% for compound **14** with the corresponding D-configured moieties. These results suggest that, as seen with the 4-hydroxyproline-based inhibitors, L-configuration of the P3 and P4 residues in our novel inhibitors incorporating the cyclopentane-based template gave the best fit in the active site, which also agrees with the modeling predictions. The somewhat weak potencies of these compounds can be explained by the use of the rather poor Abu cysteine mimic in the P1 position. Introduction of the reportedly better norvaline cysteine mimic gave compound **16**, with a measurable K_i value of 2.3 μM and 100% inhibition at a concentration of 10 μM, as compared to values of > 10 μM and 65% inhibition for the corresponding Abu compound **15** (Table 1). To ascertain whether combinations of D-L or L-D configurations of the P3-P4 substituents could provide inhibitors with a better fit, compounds **17** (D-L) and **18** (L-D) were prepared and were found to display 35% and 37% inhibition, respectively, at a concentration of 10 μM. These results confirm the importance of L-configuration of both the P3 and the P4 residue.

All of the compounds discussed thus far incorporate a P4 amino acid substituent capped with a methyl ester. It is assumed that the methyl amide has greater metabolic stability than the more easily hydrolyzed methyl ester, thus we prepared compound **19**. Regretfully, introduction of the methyl amide resulted in a slight decrease in potency to a K_i value of 6.6 μM for this compound, whereas a K_i of 2.3 μM was observed for the corresponding methyl ester compound **16**. It has previously been shown that replacement of valine with *tert*-butyl glycine in the P3 position can produce more potent NS3 inhibitors.[49] Accordingly, this modification yielded compound **9** with a K_i of 1.7 μM, which makes it almost four times more potent than the corresponding valine compound **19**. The corresponding methyl-ester-capped compound **20**, with a K_i of 1.2 μM, is essentially equipotent to compound **19**. Thus it appears that the methyl amide can be used as a methyl ester isostere in more optimized compounds.

Llinàs-Brunet and coworkers[53,56] have shown that (1*R*,2*S*)-1-amino-2-vinylcyclopropane carboxylic acid is an excellent cysteine replacement and P1 substituent with exceptional fit in the hydrophobic S1 pocket, and it has been incorporated into several highly potent inhibitors, such as compounds **E**[49] and **J**[74]

(Figure 8). Considering that the S1 site interaction has proven to be of the utmost importance for optimum activity, it seemed natural to incorporate this P1 substituent into our cyclopentane series. Hence, introduction of the vinyl cyclopropane P1 residue yielded compound **13** with a very promising K_i of 0.022 μM, making it almost 80 times more potent than the corresponding norvaline-substituted compound **9**.

At this point, we conducted a methylation study to further examine the binding modes, in particular the hydrogen bond interactions of the P3–P4 portion of these inhibitors. The compound in which the amide nitrogen closest to the cyclopentane ring had been methylated was never produced and thus could never be evaluated. Compound **21**, which has an added methyl group on the nitrogen of the capping group, exhibits a K_i value of 0.016 μM, which makes it almost equipotent to compound **13**. This observation suggests that the hydrogen of the capping methyl amide does not take part in any hydrogen bond interactions. In contrast to **21** with the methylated amide capping group, compound **22** contains the methylated amide nitrogen of the cyclohexylglycine moiety and has a K_i of >10 μM, which implies that there is a very important hydrogen bond interaction in this area of the active site. However, the dramatic loss of activity might also suggest that the P3-P4 portion is distorted due to the crowdedness caused by replacement of the amide hydrogen with a methyl group, which forces the residues out of their positions.

In attempts to truncate the P3–P4 portion of inhibitor **13**, we synthesized compounds **23** and **24** in which the P4 substituent was replaced by a simple amine, cyclopentylamine in the former and *tert*-butyl amine in the latter. Notably this caused significant loss of activity, as indicated by the K_i values of 2.7 μM for **23** and 6.9 μM for **24**. This observation implies that inhibitors based on the cyclopentane scaffold are, although optimized, highly sensitive to modifications in the P3–P4 region.

Another very good cysteine mimic in the P1 position is the (*S*)-2-amino-4,4-difluorobutyric acid (compound **C** in Figure 8) previously reported by Narjes and coworkers.[95] Introduction of this P1 substituent results in a greater gain in activity than is displayed by the corresponding molecules comprising Abu or norvaline. Nonetheless, the level of activity exhibited by compound **25** (K_i 0.56 μM) still makes it significantly (about 25 times) less potent than the corresponding inhibitor **13** with incorporated (1*R*,2*S*)-1-amino-2-vinylcyclopropane carboxylic acid.

Finally, it should be mentioned that the enantiomeric scaffold (**VI**) and the scaffold with the acyl substituents in *cis* configuration (**VII**) were also synthesized and incorporated into target molecules to allow proper evaluation (Figure 14). The compounds that were produced turned out to be totally inactive against NS3 protease. This observation shows that the scaffold (**V**) on which the inhibitors in Table 1 are based did indeed give the best fit in the active site of NS3.

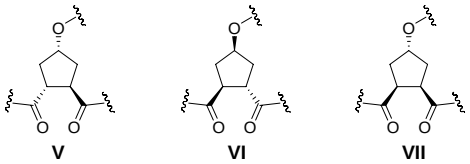

Figure 14. *The cyclopentane-based scaffold used in the present research (**V**), the enantiomeric scaffold (**VI**), and the cis-acyl cyclopentane scaffold (**VII**).*

Summarizing the results in Table 1, it can be seen that incorporation of systematically optimized and evaluated P1 and P3–P4 substituents into our novel trisubstituted cyclopentane-based template provided several very promising inhibitors (e.g., compounds **13**, **21**, and **25**) with K_i values in the nanomolar range (22, 16, and 560 nM, respectively). The substituents that gave the best fit were (1*R*,2*S*)-1-amino-2-vinylcyclopropane carboxylic acid in the P1 position, L-*tert*-butyl glycine in the P3 position, and L-cyclohexylglycine in the P4 position. Notably, comparison of the inhibitors in our cyclopentane-based series with inhibitors utilizing the 4-hydroxyproline central core reveals that our compounds seem to be very sensitive to modifications in the P3–P4 portion, such as *N*-methylation in a certain position or truncation of the P4 substituent, which result in dramatic loss of activity. Furthermore, it became apparent that use of the right P1 substituent was crucial for obtaining potent compounds.

Notwithstanding, we were able to show that a trisubstituted cyclopentane dicarboxylic acid can be readily synthesized and successfully used as a 4-hydroxyproline mimic to produce potent HCV NS3 protease inhibitors. Also, further refinements of these compounds have provided even more potent and drug-like compounds, as discussed below.

2.5 Design, Synthesis, and SAR Analysis of Macrocyclic HCV NS3 Protease Inhibitors (Paper II)

2.5.1 Design

In the study reported in Paper I, we were able to show that incorporation of a novel trisubstituted cyclopentane dicarboxylic acid in the P2 position, instead of the much more frequently used *N*-acyl-(4*R*)-hydroxyproline, produced very promising linear HCV NS3 protease inhibitors. Encouraged by that observation and inspired by the findings of other investigators, especially those concerning **BILN 2061**[42,55-58] (Figure 8; Llinàs-Brunet et al. at Boehringer Ingelheim, Canada), we wanted to determine whether macrocyclization could give our inhibitors more desirable properties. Previous analyses have revealed that the P1 and P3 substituents of bound 4-

hydroxyproline-based inhibitors are situated close to each other.[54] Thus, by connecting these positions in an appropriate manner, it may be possible to rigidify the structure, which might reduce the entropic penalty of binding and deliver a less peptidic and more drug-like inhibitor.[58] Moreover, it has been reported that introduction of carboxylic acid bioisosteres, like acyl sulfonamides, improves the inhibitory activities in both enzyme- and cell-based assays.[27,71,73,74] Considering that our aim was to synthesize compounds with better biopharmaceutical properties, we also wanted to investigate the effects of replacing the *C*-terminal carboxylic acid in our inhibitors with such activity-enhancing isosteres. In addition, our research group has recently found that a trisubstituted cyclopentene dicarboxylic acid is an effective *N*-acyl-(4*R*)-hydroxyproline mimic in the synthesis of novel linear NS3 inhibitors.[96] With that in mind, we applied olefin ring-closing metathesis (RCM) to synthesize P2 cyclopentane- and cyclopentene-incorporating macrocyclic HCV NS3 protease inhibitors with different ring sizes (Figure 15).

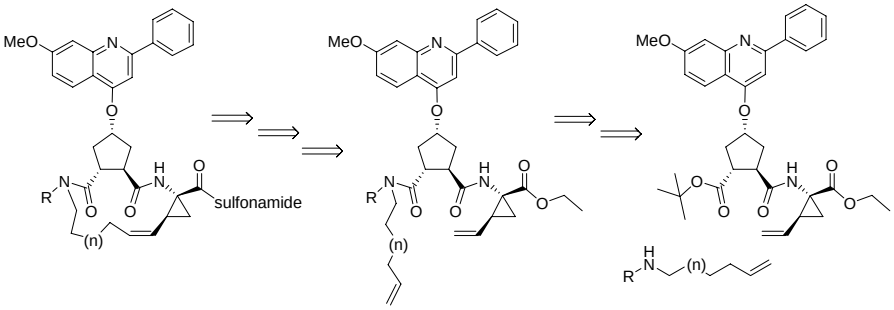

Figure 15. *A simplified retrosynthetic scheme for our macrocyclic inhibitors.*

2.5.2 Synthesis

Ring-closing metathesis (RCM) is a modern and very convenient approach to intramolecular creation of rings from molecules incorporating two olefin functionalities. Scheme 5 illustrates the synthesis of six P3 olefin linkers used in the coupling steps applied to generate diolefins **36a–f** (Scheme 6).

Four hydrazine linkers were obtained according to two different protocols. One of the strategies comprised direct alkylation of commercially available *tert*-butyl carbazate with 5-bromo-1-pentene (**26a**) and 6-bromo-1-hexene (**26b**) at 100 °C in DMF[97], which produced the hydrazine olefin linkers **27a** and **27b** in 72% and 75% yields, respectively. The other approach employed a two-step reductive amination protocol in which the commercially available alcohols 6-heptenol (**28a**) and 7-octenol (**28b**) were initially oxidized using a catalytic amount of tetrapropylammonium perruthenate (TPAP) and 4 Å molecular sieves in DCM with *N*-methylmorpholine *N*-

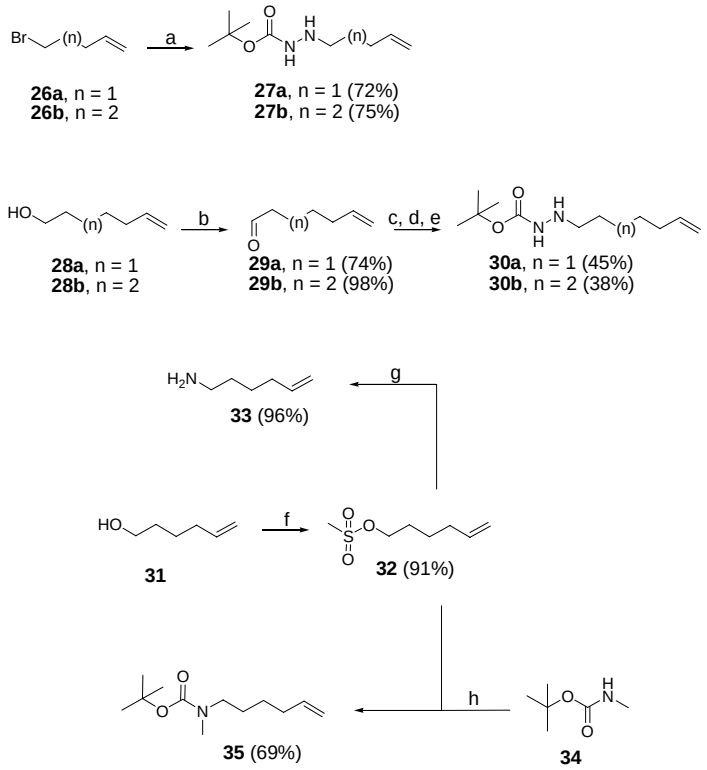

***Scheme 5**. Reagents and conditions: (a) tert-butyl carbazate, DMF, 100 °C; (b) N-methylmorpholine N-oxide, TPAP, molecular sieves (4 Å), CH_2Cl_2; (c) tert-butyl carbazate, molecular sieves (3 Å), MeOH; (d) $NaBH_3CN$, AcOH/THF, 1:1; (e) NaOH (2M), MeOH; (f) MsCl, pyridine, DCM; (g) NH_3 (aq), MeOH; (h) NaH, DMF.*

oxide as reoxidizing agent.[98] That strategy gave the crude aldehydes **29a** and **29b** in 74% and 98% yields, respectively. These two products were extremely volatile, thus concentration of the reaction mixture and evaporation of the solvent after purification were performed without heating, and no further drying was done under reduced pressure. Treatment of aldehydes **29a** and **29b** with *tert*-butyl carbazate in MeOH containing 3 Å molecular sieves gave the hydrazones, which were subsequently reduced to their corresponding hydrazine cyanoborane adducts using sodium cyanoborohydride in acetic acid/THF 1:1. Final hydrolysis of the borane adducts with NaOH in MeOH[99] rendered the desired hydrazines **30a** and **30b** in 45% and 38% total yields, respectively, over three steps.

The direct alkylation using a large excess of *tert*-butyl carbazate was found to work surprisingly well in our hands, producing the monoalkylated hydrazine linkers **27a** and **27b** in good yields. Initially, we were concerned about possible dialkylation, and hence we employed the reductive amination protocol to synthesize analogs **30a** and **30b**. However, synthesis of aldehydes shorter than **29a** was inconvenient due to

the extreme volatility of the compounds. In addition, the longer reaction sequence and the poor total yields provided by the protocol forced us to switch to the direct alkylation approach when synthesizing analogs **27a** and **27b**.

Treating commercial 5-hexenol (**31**) with pyridine and methanesulfonyl chloride in DCM gave mesylate **32** (91%), which was subjected to two different reaction conditions. Stirring **32** in a solution of aqueous ammonia and MeOH gave amine **33** in 96% yield,[100] whereas adding the mesylate to a solution of *N*-Boc-methylamine (**34**) and sodium hydride in DMF gave compound **35** in 69% yield (Scheme 5).

Scheme 6 describes synthesis of the macrocyclic target compounds containing a P2 cyclopentane proline mimic. Building block **11** was synthesized as previously described (Scheme 2 and 4) and was employed as a starting template to obtain the cyclopentane-based inhibitors listed in Tables 2 and 3. Initial *tert*-butyl ester hydrolysis using TFA and Et_3SiH in DCM produced the corresponding carboxylic acid, which was subsequently coupled to a linker (i.e., **27a**, **27b**, **30a**, **30b**, or **33**, or **35** deprotected with HCl in dioxane prior to coupling) using HATU and DIPEA in DMF to give dienes **36a–f** in yields of 64–85%. The pivotal macrocyclization step was effected by letting dienes **36a–f** react with a catalytic amount of 2nd generation Hoveyda-Grubbs ruthenium catalyst in refluxing DCM,[56] which gave macrocyclic compounds **37a–f** in 10–79% yield. The poor yield of the 13-membered ring **37a** can probably be explained by generation of more byproducts due to unfavorable ring strain and the increasing difficulty for olefins to interact during the metathesis step when using the short olefin linker. Ethyl esters **37a–f** were hydrolyzed with lithium hydroxide in refluxing THF/MeOH/H_2O 2:1:1 to deliver the first target compounds **38a–f** (Table 2) in 32–100% yields. We also chose to treat compounds **37b–d** with TFA and Et_3SiH in DCM to afford hydrazines **39b–d** in yields ranging from 63% to 74%. Subsequent hydrolysis of the ethyl esters according to the synthesis of **38a–f** provided target molecules **40b–d** in 46–71% yields.

A slightly different coupling procedure was applied to introduce an acyl sulfonamide as a *C*-terminal carboxylic acid bioisostere. Since sulfonamides are fairly deactivated compared to ordinary amines, compounds **38b**, **38e**, and **38f** were first subjected to preactivation with EDC in DCM. The oxazolones (Figure 16) that were obtained were subsequently reacted with cyclopropanesulfonic acid amide and 1,8-diazabicyclo[5.4.0]undec-7-ene (DBU) in DCM to give target compounds **41**, **43**, and **44** in 23–80% yields. Boc-removal of **41** according to the previous procedure furnished target compound **42** in 95% yield (Scheme 6).

We also employed a cyclopentene moiety as a proline mimic to prepare two target compounds. Diastereomeric building block **45** (Scheme 7) was synthesized as previously described[86,96,101,102] and used as a precursor. Coupling of carboxylic acid

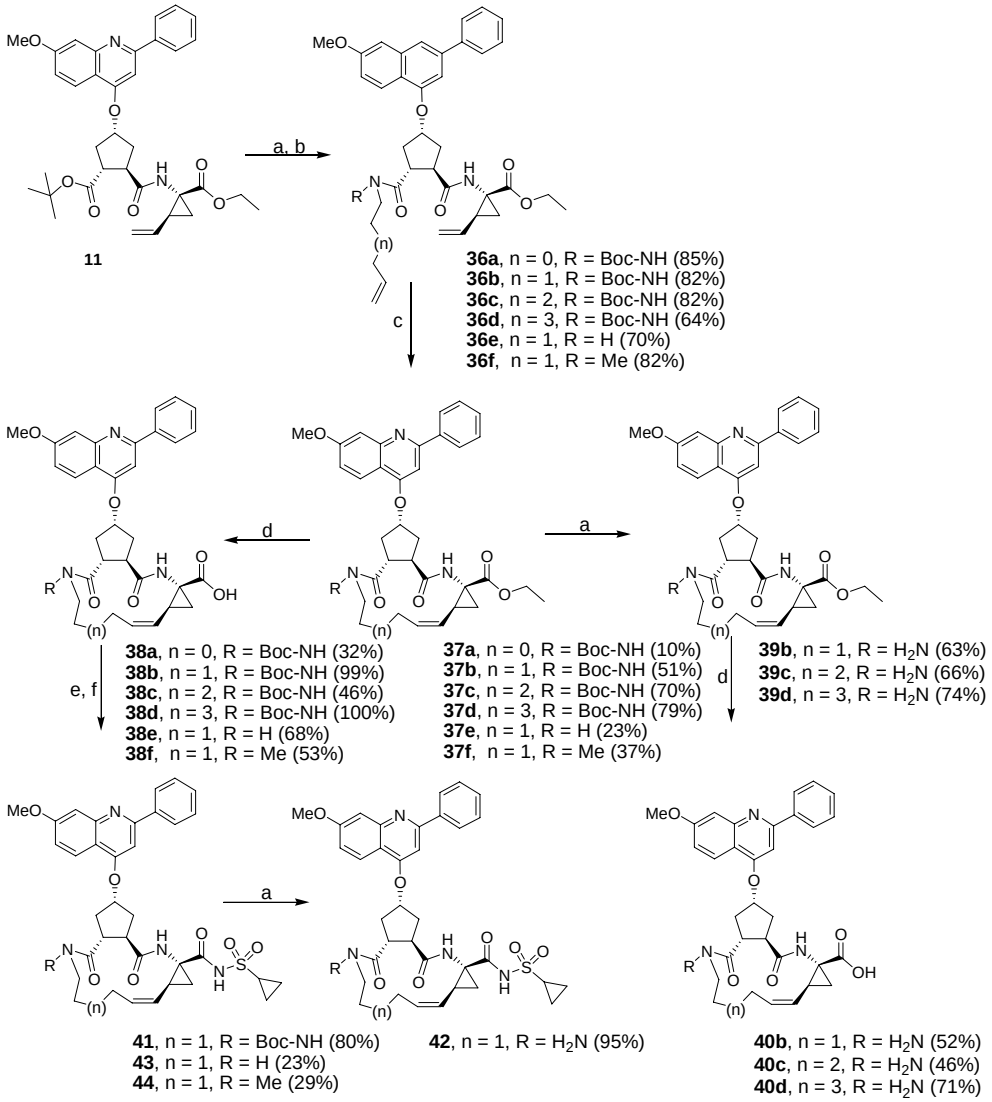

***Scheme 6**. Reagents and conditions: (a) TFA, Et_3SiH, CH_2Cl_2; (b) **27a**, **27b**, **30a**, **30b**, **33**, or **35** (**35** subjected to HCl in dioxane prior to coupling), HATU, DIPEA, DMF; (c) Hoveyda-Grubbs Catalyst 2nd Gen. CH_2Cl_2, reflux; (d) LiOH (1M), THF/MeOH/H_2O 2:1:1, reflux; (e) EDC, DCM; (f) cyclopropanesulfonic acid amide, DBU, DCM.*

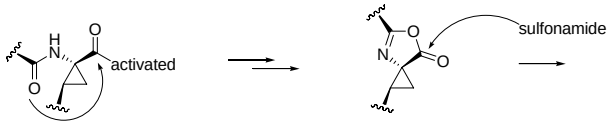

***Figure 16.** The oxazolone derivative that was obtained in the preactivation step using EDC and was opened with cyclopropanesulfonic acid amide in the presence of DBU.*

45 to linker **27b** or **30a** according to the previously used coupling procedure furnished dienes **46a** and **46b** in 81% and 79% yields, respectively. Ring-closing metathesis using 2nd generation Hoveyda-Grubbs catalyst produced macrocycles **47a** and **47b** in 81% and 53% yields, respectively. Final hydrolysis of the *tert*-butyl ester and the Boc group of **47a** and **47b** with TFA and Et_3SiH in DCM generated target compounds **48a** and **48b** (diastereomeric mixtures) in 38% and 47% yields, respectively (Scheme 7).

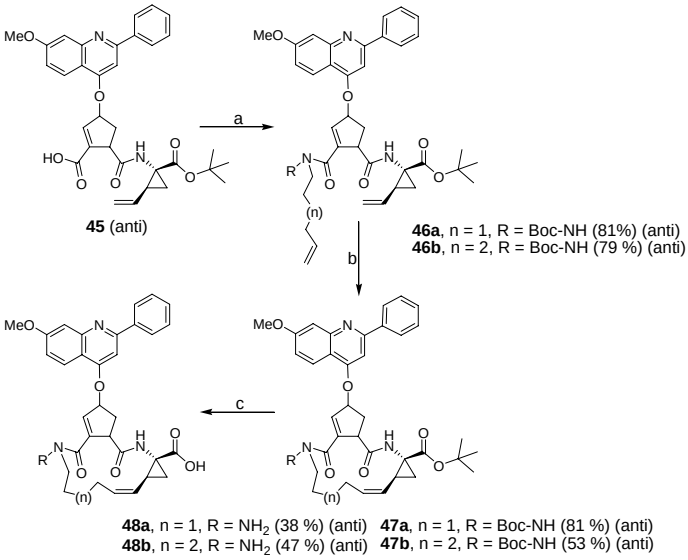

Scheme 7. *Reagents and conditions: (a)* ***27b*** *or* ***30a****, DIPEA, HATU, DMF; (b) Hoveyda-Grubbs Catalyst 2nd Gen.,* CH_2Cl_2*, reflux; (c) TFA,* Et_3SiH*,* CH_2Cl_2*.*

2.5.3 SAR Analysis

All target compounds were screened against the HCV NS3 1a protease to determine Ki values, and they were also subjected to the cellular genotype 1b replicon assay to obtain EC50 values. Those values are given in Tables 2–4, along with NS3 inhibition constants. NMR analyses indicated that all of the inhibitors discussed below have Z-configured double bonds. The compounds also contain the P2 2-phenyl-7-methoxy-4-quinoline substituent, which, as mentioned above in the discussion of linear inhibitors, is essential not only for shielding the catalytic machinery from exposure to solvent,50,91 but probably also to allow favorable interaction with the both the protease and helicase domain of the NS3 protein.92-94 We anticipated that connecting the P1 and P3 positions in our inhibitors would provide several advantages. It has been suggested that if an inhibitor can be fixed in a conformation in which it is more likely to be when binding to the active site, it will reduce the entropy penalty of binding and increase the overall binding energy of the compound. Furthermore,

transformation of a linear inhibitor such as **13** (Table 1) into a macrocycle decreases the peptidic nature of the compound and is thus likely to improve its pharmacokinetic properties.[58]

We were initially interested in establishing the ring size that would provide our cyclopentane-based inhibitors with the best fit in the S1–S3 pocket of the active site. Scrutinization of the structure of **BILN 2061** reveals that it is a 15-membered macrocycle with a planar bond protruding from the proline nitrogen, and it is also apparent that the "linker" protrudes from the sp^3-configured P3 α-carbon. In contrast, our inhibitors possess an sp^3-hybridized carbon in the corresponding P2 ring position, and the linker protrudes from a planar nitrogen bond (Figure 17). Considering these differences, it was not certain that the 15-membered ring used in **BILN 2061** would be the optimal ring size when employing our cyclopentane-based template. Consequently, we decided to synthesize and evaluate each of the 13–16-membered rings and continue from there.

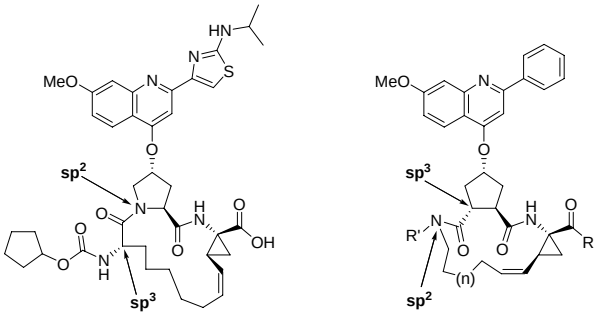

Figure 17. *Comparison of* ***BILN 2061*** *(left) with the general structure of our cyclopentane-derived macrocyclic inhibitors (right).*

The first compound in Table 2 is the 13-membered macrocycle **38a**, which has a K_i value of 130 nM. Although very promising, the activity of **38a** still indicates that the S1–S3 pocket may accommodate larger rings. Compound **38b** contains a 14-membered ring, and it is over four times more active than the corresponding 13-membered ring, with an even more promising K_i value of 31 nM. The 15-membered macrocyclic compound in our series is **38c**, which has a K_i of 710 nM, indicating that 14-membered rings give our cyclopentane-derived inhibitors better fit into the S1-S3 pocket of NS3. A further increase in ring size led to total loss of activity, as shown by the K_i value of >10 μM for the 16-membered macrocycle **38d**.

At this point, we decided to explore the effect of removing the P4 Boc groups from compounds **38b–d**. This modification increased the potency more than fivefold, with K_i values of 6 and 120 nM for **40b** and **40c**, respectively, compared to the corresponding Boc-protected derivatives. Boc removal had no effect on the 16-

Table 2. *Macrocyclic P2 cyclopentane P1 carboxylic acid inhibitors: effect of ring size and P3 capping groups on inhibition of NS3/4A and EC_{50} in the replicon assay*

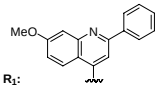

Cpd.	Structure	R_2 P3 capping group	Ring size	K_i (nM) HCV NS3 1a	EC_{50} (µM) HCV NS3 1b
38a	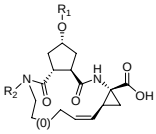	Boc-NH	13	130	> 10
38b	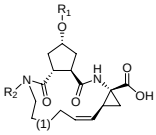	Boc-NH	14	31	> 10
38c	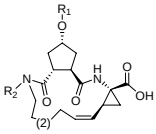	Boc-NH	15	710	>10
38d	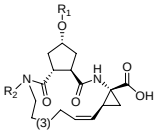	Boc-NH	16	> 10000	> 10
40b	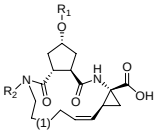	H_2N	14	6	7.6
40c	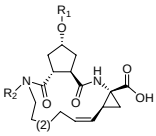	H_2N	15	120	> 10
40d	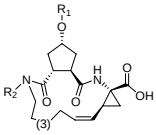	H_2N	16	> 10000	> 10

Table 2. *(Continued)*

Cpd.	Structure	R_2 P3 capping group	Ring size	K_i (nM) HCV NS3 1a	EC_{50} (μM) HCV NS3 1b
38e	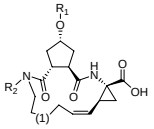	H	14	260	> 10
38f	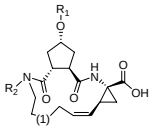	Me	14	44	2.2

membered ring **40d** (K_i >10 μM), which further implies that this large ring is not tolerated by the S1–S3 pocket. Nevertheless, this gave us the indication that it might be possible to prepare highly active inhibitors from compounds that do not interact with the S4 sub-pocket.

Even though the small polar P3-NH_2 cap increased the enzyme potency compared to the NH-Boc, it was necessary to improve the activity in the cell-based assay. Consequently, in order to reduce the zwitter-ionic character of inhibitor **40b** and to further explore the effect of excluding the P4 substituent, amide **38e** and methyl amide **38f** were produced, resulting in K_i values of 260 and 44 nM, respectively. Perhaps of greatest interest, **38f** also showed activity, albeit still poor, in the cell-based assay.

Previous studies have shown that replacing the carboxylic acid of product-based inhibitors with bioisosteres such as acyl sulfonamides not only improves the pharmacokinetic properties, but also substantially increases the potency of HCV NS3 inhibitors in both enzyme and cell-based assays.[27,71,73,74] Hence, in order to improve the poor activities displayed by our inhibitors in the cell-based assay, we initially introduced a cyclopropyl acyl sulfonamide into compounds **38b** and **40b**. This modification gave inhibitors **41** and **42** (Table 3) with substantially better enzyme and cell activities indicated by K_i values of 0.07 and 0.19 nM and EC_{50} values of 530 and 33 nM, respectively. Modifying compounds **38e** and **38f** in the same way delivered inhibitors **43** and **44** with K_i values of 2.2 and 0.41 nM and EC_{50} values of 4400 and 9.1 nM, respectively. In addition, an excellent selectivity profile was obtained for the 14-membered rings when they were screened against the human serine proteases cathepsin B, chymotrypsin, and elastase. Selectivity data on compound **44** are included in Table 3.

Table 3. *Macrocyclic P2 cyclopentane P1 cyclopropyl acyl sulfonamide inhibitors: effect of ring size and P3 capping groups on inhibition of NS3/4A and EC_{50} in the replicon assay*

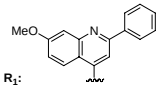

Cpd.	Structure	R_2 P3 capping group	Ring size	K_i (nM) HCV NS3 1a	EC_{50} (µM) HCV NS3 1b
41	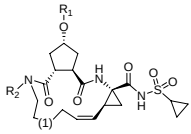	Boc-NH	14	0.07	0.53
42	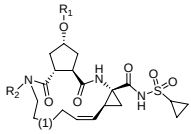	H_2N	14	0.19	0.033
43	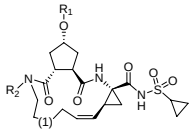	H	14	2.2	4.4
44*	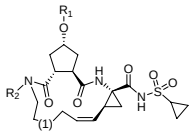	Me	14	0.41	0.0091

* *Selectivity data: K_i 2200, > 5000, and > 5000 nM for the human serine proteases cathepsin B, chymotrypsin, and elastase, respectively.*

The diastereomeric cyclopentene derivatives **48a** and **48b** have the same planar configuration at the P2 ring position as the compounds that have 4-hydroxyproline in this position (see **BILN 2061** in Figure 17), but, as also seen for the cyclopentane derivatives, they differ in that their linkers protrude from a planar nitrogen bond. Nevertheless, the 14-membered macrocyclic inhibitor **48a** is more active than the 15-membered macrocycle **48b** (Table 4), which agrees with the character of their corresponding cyclopentane derivatives **40b** and **40c**. Inhibitor **48a** is slightly less potent than **40b** (K_i values 15 vs. 6 nM), whereas **48b** and **35c** are almost equipotent (K_i values 110 vs. 120 nM). Accordingly, cyclopentane compounds **40b** and **40c** are equipotent to, or more active than, cyclopentene compounds **48a** and **48b**. These findings, along with the fact that the synthesis route was less convenient (i.e., provided diastereomers) for the cyclopentene target compounds, and the knowledge that these inhibitors are potential Michael acceptors, rendered the cyclopentene

derivatives less suitable as drug candidates and thus they were not investigated further.[96]

Table 4. *Macrocyclic P2 cyclopentene P1 carboxylic acid inhibitors: effect of ring size on inhibition of NS3/4A and EC_{50} in the replicon assay*

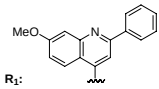

Cpd.	Structure	R_2 P3 capping group	Ring size	K_i (nM) HCV NS3 1a	EC_{50} (μM) HCV NS3 1b
48a	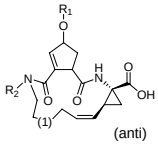	H_2N	14	15	5.4
48b	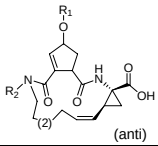	H_2N	15	110	4.5

Modeling was used to explain the SARs seen for inhibitors with and without the P4 substituent, and for those that contained only small P3 capping groups. Conformational studies of the P3-H compounds **38e** and **43** suggest that there might be an internal hydrogen bond interaction between the P3-H and the P2 carbonyl. The breaking of this interaction is unfavorable but is probably necessary if proper binding is to be achieved between the inhibitor and the active site of NS3. Conformational analyses were also performed to rationalize the difference in potency observed between **40b** containing only the small P3-NH_2 extension and **38b** comprising the larger P4-NHBoc. The results indicate that two possible rotations around the reversed amide of these inhibitors may give rise to different conformations that may differ in terms of stability and energy. Thus it appears that **40b** can be docked into the active site in any of the two rotations around the reversed amide bond, whereas **38b** only fits in the higher energy rotamer state.

Modeling of compound 44. Compound **44** was docked and minimized in the active site using a previously published crystal structure of full-length NS3.[94] Figure 18 shows how compound **44** interacts with both the protease and the helicase of NS3. The protease interactions are the most important, and the inhibitor forms hydrogen bonds with five residues in the active site of the protease. The cyclopropyl acyl sulfonamide adds potency to the inhibitors, which can be explained by the interactions

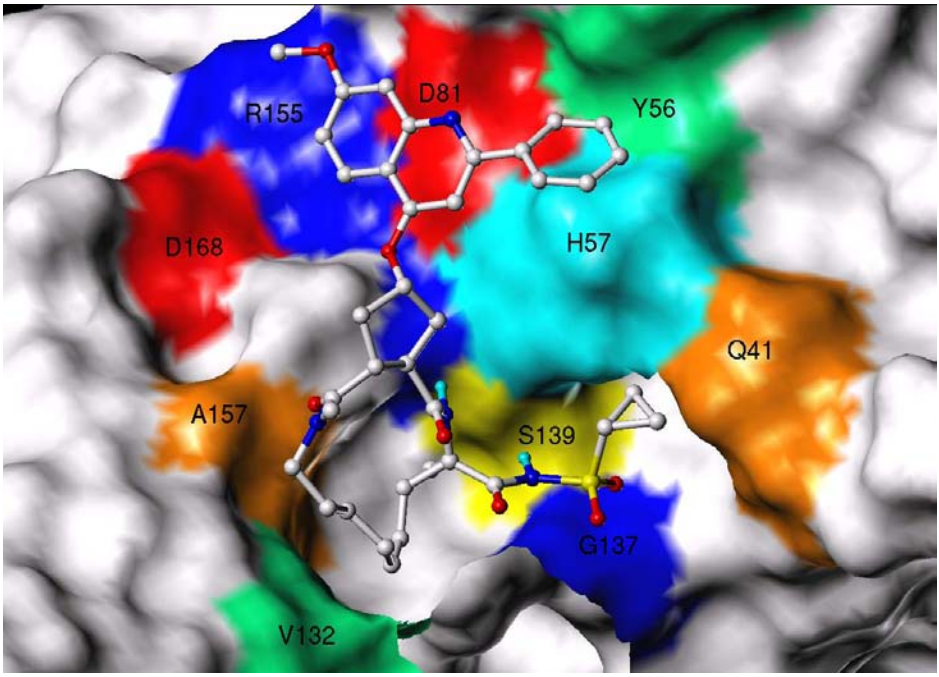

Figure 18. *Model of compound* ***44*** *in the active site of the NS3 protease. The NS3 crystal structure 1cu1 from PDB was used in modeling, and Arg 155 was rotated to accommodate the P2 quinoline substituent.*

of this group with the NS3 protease. In this model, the sulfone oxygens of the acyl sulfonamide bind to the oxyanion hole, i.e. the NH of both Gly137 and Ser139. The flexible side chain of Lys136 has the possibility to interact with both one of the sulfone oxygens and the amide carbonyl of the acyl sulfonamide. The cyclopropyl group has close-contact interactions with Gln41 and the catalytic His57 in the S1´ sub-pocket. The amides flanking the P2 cyclopentyl have main chain hydrogen bonds with Arg155 and Ala157. Also, the aliphatic P1-P3 linker of the macrocycle displays close-contact interactions with the side chain of Val132. The introduction of an extending P2 substituent seems to be accompanied by an inhibitor-induced conformational change in the Arg155 and Asp168 side chains, leading to the formation of a salt bridge.[16] This change enables the methoxyquinoline to achieve a favorable interaction with the guanidine of Arg155. The quinoline also shields the catalytic interaction between His57 and Asp81, whereas the extending phenyl seems to add interactions and stabilize the position of the P2 substituent through aromatic stacking with Tyr56. The P2 substituent also interacts with some residues from the NS3 helicase, mainly the side chains of Pro482, Met485, Val524, and Gln526.

Summarizing the results regarding the series of macrocyclic compounds, it is evident that very promising HCV NS3 protease inhibitors were produced by

macrocyclization of P2 cyclopentane linear inhibitors. The 14-membered macrocycles provided the best fit, and very potent inhibitors were produced, for example, compounds **41**, **42**, and **44** with K_i values of 0.07, 0.19, and 0.41 nM, and EC_{50} values of 530, 33, and 9.1 nM, respectively. Interestingly, even though they lack the P4 substituent, compounds **42** and **44** showed excellent potencies in both the enzyme and the cell-based replicon assay.

3. Targeting the Aspartic Protease BACE-1 to Identify Potential Drugs for Alzheimer's Disease—Design, Synthesis, and Analysis of SARs (Papers III and IV)

3.1 Alzheimer's Disease

Alzheimer's disease (AD) is a fatal degenerative disorder of the brain that was first described by Alois Alzheimer in 1906. It is characterized by loss of memory and cognition, and represents the most common form of dementia among the elderly. Age is the major risk factor for AD, and since the average age of the world population is increasing, the number of AD patients is expected to grow exponentially. It has been estimated that the damage to neurons starts 20–30 years before appearance of the first clinical symptoms, which makes development of preventive strategies a crucial issue.[103] Patients are diagnosed with probable AD based on established dementia and global decline of cognitive function.[104] The progress is slow but eventually leaves patients bedridden and dependent on continuous supervision and care, with death occurring on average nine years after diagnosis.[105] The only way to confirm a diagnosis of AD is to examine the patient's brain after death. Evidence of AD is based on several neuropathologies, including extracellular plaques, intracellular tangles, and neurodegeneration. Plaques and tangles are also found in cognitively normal adults, although to a lesser extent, thus making dementia an important criterion for diagnosis of the disease.[104] The current standard of care comprises two types of compounds that are often used in combination: (1) cholinesterase inhibitors and (2) the *N*-methyl-D-aspartate (NMDA) antagonist memantine. The cholinesterase inhibitors are given to combat the destruction of cholinergic neurons by slowing the degradation of acetylcholine that is released at synapses. Memantine is administered to prevent overstimulation of NMDA, which is a glutamate receptor subtype that may participate in the progress of AD and other neurodegenerative conditions by damaging and killing nerve cells (excitotoxicity). Unfortunately, the beneficial effect of this

treatment regimen is marginal, and many patients do not respond at all. Other drugs are given to ease mood disorder, agitation, and psychosis in the latter stages of the disease.[106] Consequently, there is an enormous need to develop new therapies that can modify the progression of AD.

3.2 APP and Aβ

Amyloid precursor protein (APP) is a large transmembrane protein of unknown function[103] that can be processed by different proteases along either of two major routes (Figure 19): the α-secretase pathway and the amyloid forming β-secretase (BACE-1) pathway. In the former, APP is cleaved by α-secretase to release a large soluble extracellular amino-terminal portion of APP (α-APPs); the carboxy-terminal portion of APP can then be further metabolized by γ-secretase to liberate a small P3 peptide, which is considered to be non-amyloidogenic. The amyloid-forming pathway is dependent on two proteolytic cleavages: initially, β-secretase cleaves APP to free a large soluble amino-terminus portion designated β-APPs;[107,108] thereafter, the remaining carboxy-terminal peptide C99 is cleaved by γ-secretase at several positions to form amyloid-β fragments ranging from 37 to 43 residues,[104] with amyloid-β40 (Aβ40) and amyloid-β42 (Aβ42) being the major species. Aβ42 has two additional hydrophobic amino acids and is considered to be the more amyloidogenic and toxic of the two.[103]

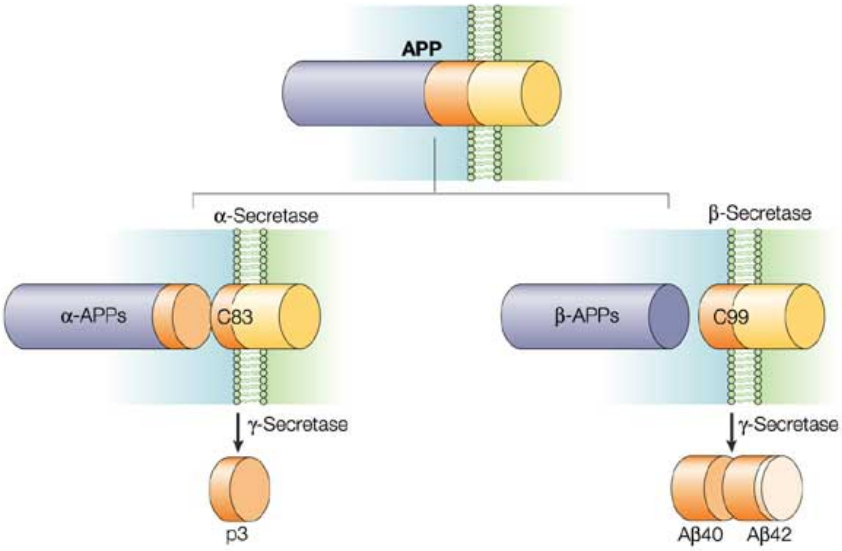

Figure 19. *The two routes by which the amyloid precursor protein is processed: the α-secretase pathway and the amyloid-forming β-secretase pathway.*[109]

Studies of the genetics associated with familial AD have shown that mutations in three different genes (encoding presenilin 1, presenilin 2, and APP) all serve to increase the abundance of Aβ42. Familial AD is characterized by much earlier onset of symptoms, and it accounts for less than 1% of all cases. The remaining 99% belong to the category referred to as sporadic AD, for which inheritance of the ε4 allele of the apolipoprotein E constitutes the only well-established risk factor for early development of the disease.[110]

3.3 The Amyloid Cascade Hypothesis

Genetic and pathological studies support the amyloid cascade hypothesis,[111] which states that the extracellular accumulation and aggregation of mainly amyloid-β42 (Aβ42) in the brain triggers a neurotoxic cascade that stimulates the hyperphosphorylation of tau proteins. The amyloids and the tau proteins are deposited in the brain as plaques and tangles, respectively, resulting in neuronal cell death and dementia (Figure 20).[107,112] Amyloid plaques are assumed to be relatively specific for AD, whereas tangles are associated with other diseases as well. The hyperphosphorylation of the tau protein is believed to be required for toxicity, and is probably stimulated by the increase of Aβ42 in the brain.[103] Consequently, it is assumed that the overproduction of amyloid-β42 (Aβ42) within the neurons is the starting point for a cascade that ultimately gives rise to dementia and AD.

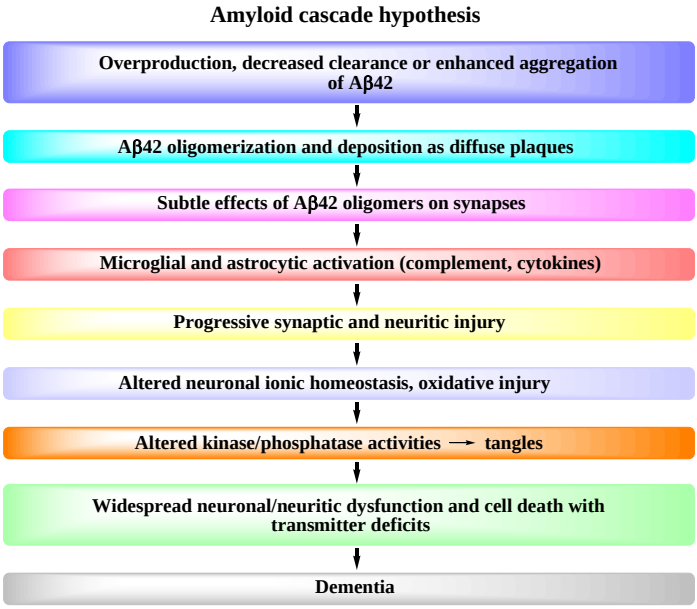

Figure 20. *The sequence of pathogenic events believed to result in Alzheimer's disease.*

3.4 BACE-1

BACE-1 (beta-site APP-cleaving enzyme), also known as memapsin 2 or β-secretase, is a transmembrane protein in which the active catalytic area reaches out into the lumen,[108,113,114] and, in accordance with other aspartic proteases it comprises two characteristic aspartic acids (Asp32 and Asp228) at the active site. BACE-1 belong to a group of aspartic proteases that show similarities with human pepsin family members like renin, memapsin 1 (BACE-2), and cathepsin D.[115] Compared to its most closely related family member memapsin 1, BACE-1 is expressed more extensively in the brain.[116] Early crystal structure analyses of peptidic inhibitors (e.g., OM99-2 in Figure 21) in complex with BACE-1 have provided substantial amounts of important information about this protease. The active site consists of a long cleft comprising eight main subsites spanning from S4 to S4´, with the catalytic Asp residues positioned at the location of peptide bond hydrolysis.[117] Comparable to other aspartic proteases, the substrate specificity of BACE-1 is altered by the presence of a flap that closes down on top of the inhibitor.[118] For inhibitor OM99-2, it was shown that six residues (P4 to P2´) were bound to their corresponding subsites, whereas subsites S3´ and S4´ had little preference for amino acids. However, other crystal structures of BACE-1 have indicated the existence of additional subsites (S5-S7) beyond S4.[119]

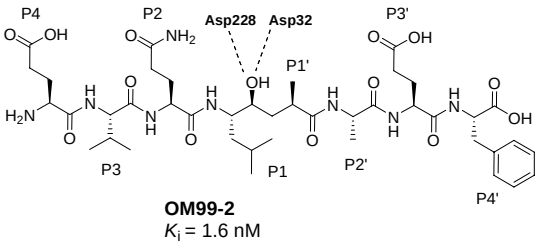

Figure 21. *One of the earliest BACE-1 inhibitors reported. P designations are illustrated, and interactions with the catalytic aspartic acids are also shown.*

So what makes BACE-1 a plausible target? First, and most importantly, BACE-1 performs the initial cleavage of APP resulting in the production of Aβ. Second, it has been observed that removal of the BACE-1 gene in mice (i.e., creation of BACE-1-knockout animals) greatly reduced the production of Aβ but generated only minor behavioral changes in the different phenotypes.[120-122] Third, extensive work focused on drugs that inhibit aspartic proteases has produced a vast knowledge base on the action of inhibition and the design of transition state analog isosteres (see below), and the successful development of inhibitors of the aspartic HIV protease was inspiring. Fourth, proof of concepts studies using a BACE-1 inhibitor in mice have validated the use of BACE-1 as a therapeutic target for AD. Moreover, it appears that BACE-1 has

a much smaller number of substrates compared to γ-secretase, which is responsible for a variety of transmembrane cleavages.[108,112] Taken together, these findings support the use of BACE-1 as a promising AD drug target.

3.5 BACE-1 Inhibitors

Orally administered β-secretase inhibitors should display selectivity over similar human aspartic proteases such as cathepsin D, and they should also be sufficiently small and drug-like to be able to penetrate the blood brain barrier.[105] These requirements make development of potential inhibitor drugs a challenging task.

An efficient strategy that emerged during the preparation of aspartic protease inhibitors is to replace the scissile amide bond with an non-cleavable transition-state isostere that mimics the tetrahedral intermediate formed during peptide cleavage that is catalyzed by aspartic proteases.[2,4,5,123] Figure 22 illustrates the tetrahedral intermediate formed during substrate cleavage mediated by aspartic proteases and the γ-amino acid statine, which constitutes a pivotal part of the hexapeptide inhibitor pepstatin A.[124] Pepstatin A was initially isolated from bacteria and was found to strongly inhibit pepsin, although it soon became clear that pepstatin A is an effective inhibitor of many aspartic proteases.[125] Therefore statine and similar transition-state motifs have become widely employed as central parts of inhibitors designed to target different aspartic proteases. In the case of BACE-1 some of the most commonly used are statine-based isosteres, hydroxyethylene (HE), hydroxymethylcarbonyl (HMC, norstatine), and hydroxyethylamine (HEA) (Figure 22). The isosteres share the feature of a secondary alcohol, and they differ from one another through the functionality alpha and beta to the hydroxyl group and in the way they engage the catalytic aspartate side chains.[126]

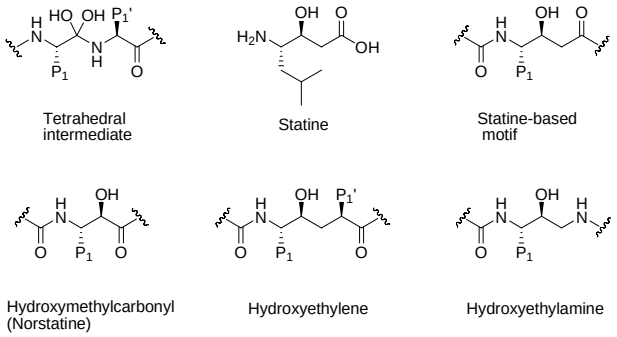

Figure 22. *The tetrahedral transition-state intermediate formed during substrate cleavage, the γ-amino acid statine, and four transition-state mimics used in BACE-1 inhibitors.*

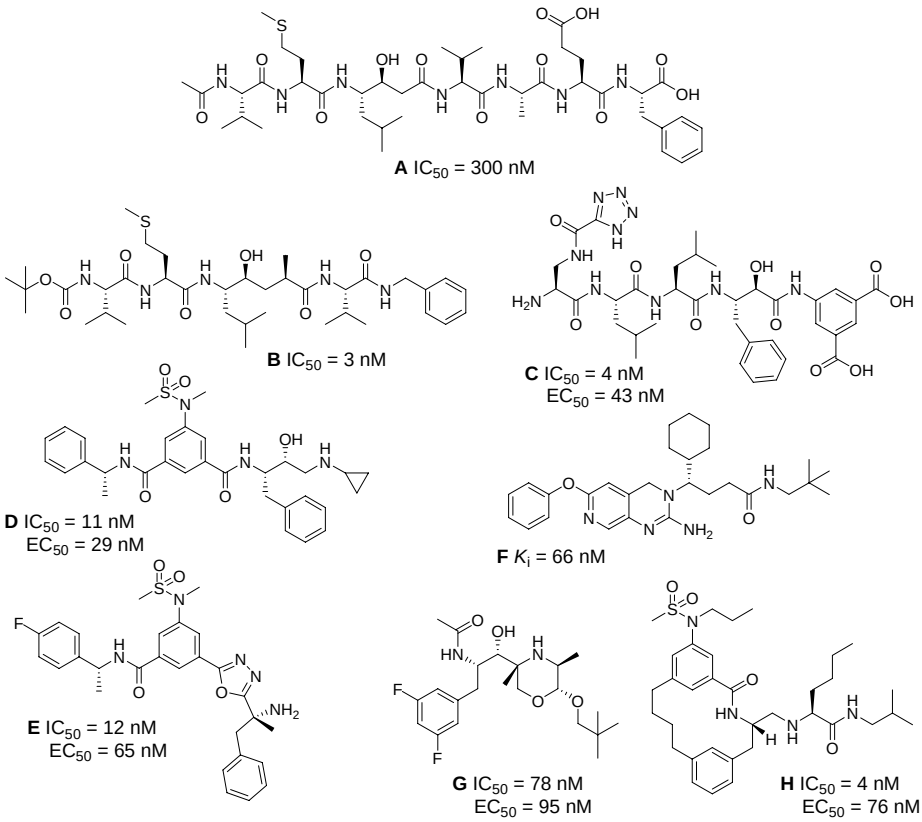

Figure 23. *BACE-1 inhibitors.*

Substrate analogs were among the earliest BACE inhibitors reported in the literature. Initial key results came from specificity and inhibition studies of a substrate spanning from position P13 to P5´, which were performed by the Elan team.[127] The aim was to define effective P1 and P1´ residues, and one of the first products of their work was heptapeptide **A** (Figure 23), which contains a valine residue in the P1´ position and has a non-cleavable statine core. Other important results were presented by Tang and colleagues at the University of Oklahoma, the group that synthesized OM99-2 (Figure 21) and later further developed that compound to give hydroxyethylene inhibitor **B**.[128] Research using other central cores has also yielded potent inhibitors such as hydroxymethylcarbonyl inhibitor **C**[129,130] from Kyoto Pharmaceutical University. In addition, an important step towards smaller sized compounds was hydroxyethylamine **D**,[131] which was produced by the Merck group and was reported to have substantial cell permeability; the drug-like properties achieved in **D** were further improved in the less peptidic inhibitor **E**[132] containing a

tertiary carbinamine, but it was anticipated that **E** would be too polar to penetrate the blood brain barrier.

There is a very broad range of highly diverse non-peptidic compounds, that have the potential to inhibit BACE-1 *in vitro*.[133] Examples of structural elements that have been incorporated into BACE inhibitors include piperazines, piperidines, aminothiazoles, aminopyridines, and guanidines (**F**).[134] A large number of the compounds that have been produced are effective *in vitro*, and there are also quite a few that show efficacy *in vivo*. Nonetheless, before a BACE candidate drug can be in question for clinical trials, it must fulfill requirements such as offering selectivity over other human aspartic proteases, metabolic stability, oral bioavailability, and brain penetrability. Hence, the necessary activity and further optimization of a compound in an AD animal model must be accomplished before administering the potential drug to humans.[133] Only very few inhibitors have shown positive results in animal models (i.e., have been able to reduce Aβ levels in laboratory animals), among those are compounds **C**,[129] **G**,[133,134] and **H**[135] shown in Figure 23.

3.6 Design, Synthesis, and SAR Analysis of BACE-1 Inhibitors Encompassing P1 Phenoxy and Benzyloxy Residues (Paper III)

3.6.1 Design

Central core **I** (Figure 24) has been used in inhibitors to target not only BACE,[136,137] but also the malaria aspartic proteases plasmepsins I and II.[125] The P1 methylphenyl residue that is incorporated into this central core is frequently utilized in BACE inhibitors.[134]

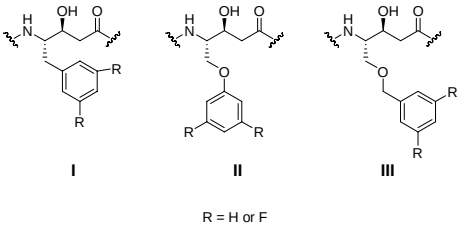

Figure 24. *Comparison of three statine-based central cores incorporating different P1 residues. Central core* ***I*** *was recently used in inhibitors to target BACE-1, and the modified central cores* ***II*** *and* ***III*** *are described in this thesis.*

Previous studies from our group have shown that insertion of oxygen in the appropriate position of peptidomimetic structures generates new centers that can facilitate diversification of compounds. Such an approach may also simplify synthesis

and provide increased potency against proteases of interest.[138-141] At the time the following research was performed, BACE-1 was a new and unexplored target for our team, and thus, to obtain early SAR information, we decided to prepare statine-based inhibitors containing somewhat elongated P1 ether residues. Our intention was to explore the possibility of stretching further into the BACE S1 site, and to achieve that goal we employed central cores **II** and **III**,[139] which include a P1 phenyloxymethyl and a P1 benzyloxymethyl residue, respectively.

3.6.2 Synthesis

Figure 25 depicts the general structure of the statine-based BACE inhibitors, along with the different R^1, R^2, and R^3 moieties that were used. Amines **C** and **D** were both

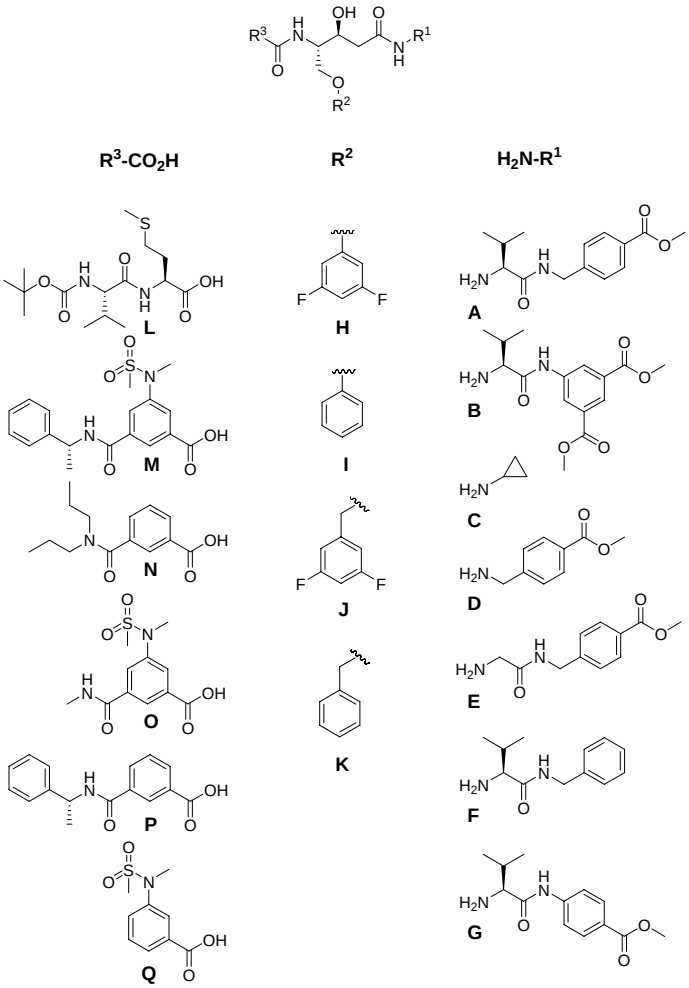

Figure 25. *A general picture of the different R-moieties connected or coupled to the central core.*

commercially available, and substituents **A**, **B**, **E–G**, **L**, **N**, and **P** were readily synthesized from suitably protected and commercially available precursors. Sulfonamides **M** and **O** were produced according to the procedure reported by Stachel et al.,[131] except that methyl amine was used instead of *R*-(+)-α-methylbenzylamine in the amide formation step for **O**. **Q** was obtained by starting from commercial methyl 3-aminobenzoate and performing mesylation, methylation, and deprotection as specified in the same protocol. A more detailed description of the synthesis procedures is given in the experimental section of Paper III.

The central core building blocks comprising the different phenyloxy and benzyloxy P1 residues were synthesized as outlined in Scheme 8. Starting from commercially available diacetone-D-glucose, 3-deoxy-1,2-*O*-isopropylidene-α-D-glucose (**49**) was synthesized over three steps in an overall yield of 60% according to literature procedures.[142-144] Two slightly different routes were subsequently employed to obtain the phenyloxymethyl templates **53** and **56** and the benzyloxymethyl templates **59** and **62**.[139]

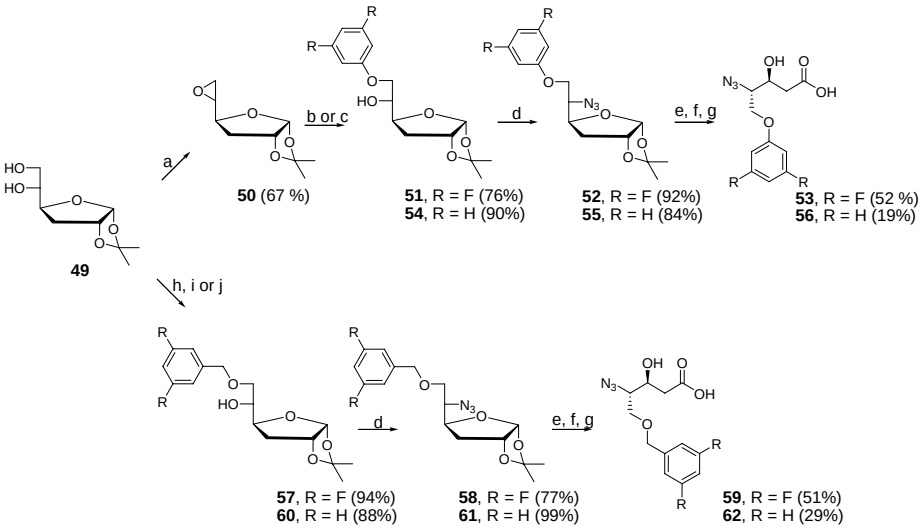

Scheme 8. *Reagents and conditions: (a) PPh_3, DIAD, $CHCl_3$; (b) 3,5-difluorophenol, K_2CO_3, DMF, 100 °C; (c) phenol, K_2CO_3, DMF, 100 °C; (d) PPh_3, DIAD, DPPA, THF; (e) HOAc/H_2O 1:1, 110 °C; (f) $NaIO_4$, $KMnO_4$, t-BuOH/H_2O 2:3; (g) 1 M NaOH; (h) Bu_2SnO, toluene, reflux; (i) tetrabutylammonium bromide (TBAB), 3,5-difluoroBnBr, toluene, 90 °C; (j) TBAB, BnBr, toluene, 90 °C.*

Synthesis of templates **53** and **56** began with the conversion of diol **49** into the corresponding epoxide[145,146] using triphenylphosphine (PPh_3) and diisopropyl azodicarboxylate (DIAD) in refluxing chloroform,[147] which gave **50** in 67% yield. The epoxide was opened regioselectively at the sterically least hindered position by heating it with 3,5-difluorophenol or phenol together with potassium carbonate in

DMF.[148] Phenoxy ethers **51** and **54** were obtained in 76% and 90% yields, respectively. Treatment of **51** and **54** (using Mitsunobu conditions) with PPh_3, DIAD, and diphenylphosphoryl azide (DPPA) in dry THF[148] produced azides **52** and **55** with inversion of configuration in 92% and 84% yields, respectively. Templates **53** and **56** were finally delivered in a three-step reaction sequence, starting with the hydrolysis of the isopropylidene groups of **52** and **55** using 50% acetic acid at 110 °C to produce the corresponding diols. Subsequent oxidation of the diols with sodium periodate and a catalytic amount of potassium permanganate generated a mixture of carboxylic acids **53** and **56** and their corresponding formic esters. These mixtures were finally treated with 1 M aqueous sodium hydroxide to give compounds **53** and **56** in 52% and 19% yields, respectively, over three steps.[139,146]

To synthesize the extended benzyloxy templates (**59** and **62**), diol **49** was first converted into its corresponding tin acetal by reacting it with dibutyltin oxide in refluxing toluene. Subsequent treatment with tetrabutylammonium bromide and 3,5-difluorobenzyl bromide or benzyl bromide furnished the primary alkylated[149] compounds **57** and **60** in 94% and 88% yields, respectively. Azides **58** and **61** were obtained in 77% and 99% yields, respectively, using the same Mitsunobu-like procedure as employed to synthesize compounds **52** and **55**, and templates **59** and **62** were delivered in 51% and 29% yields, respectively, according to the same three-step procedure applied to produce templates **53** and **56**.

Target compounds **64** and **65** (Table 5) were synthesized as shown in Scheme 9. Template **53** was coupled to amine **A** (Figure 25) by employing HATU and *N*,*N*-diisopropylethylamine (DIPEA) in DMF to give compound **63** in 76% yield. The azide functionality of **63** was reduced using PPh_3 and methanol containing a few drops of water. Subsequent coupling of the corresponding amine to carboxylic acid **M**

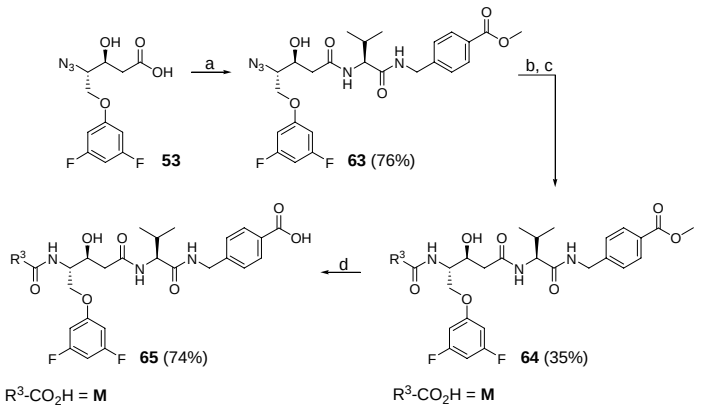

Scheme 9. *Reagents and conditions: (a)* ***A****, DIPEA, HATU, DMF; (b) PPh_3, MeOH, H_2O; (c)* ***M****, DIPEA, HATU, DMF; (d) 1 M LiOH, THF, MeOH, H_2O.*

(Figure 25) using HATU and DIPEA in DMF furnished target compound **64** in 35% yield over two steps. Final methyl ester hydrolysis using lithium hydroxide in THF/MeOH/H_2O 2:1:1 provided target compound **65** in 74% yield.

Studies of HIV protease inhibitors have shown that the (*R*)-hydroxyl stereochemistry is preferable for rather small HEA motif inhibitors,[150] whereas the opposite *S* stereochemistry is better for HE and statine-based isosteres. Furthermore, since the hydroxyl group is used to engage the catalytic dyad, we thought it would be important to evaluate both configurations of this alcohol. Scheme 10 outlines a protocol for compound **67** in which the hydroxyl of the central core partially is in inverted configuration. Compound **62** was treated with thionyl chloride in MeOH to afford methyl ester **66** in 85% yield. Thereafter, as a first attempt, we applied another Mitsunobu protocol to obtain **66**, in this case employing *p*-nitrobenzoic acid, PPh_3, and DIAD in THF. It was our intent to follow with benzoate cleavage using NaOMe in MeOH, but, unfortunately, the methylene protons were very prone to causing beta elimination during the Mitsunobu step. Consequently, as an alternative, we performed a four-step sequence, without purifications, which led to compound **67**. Initially, we exposed methyl-ester-protected central core **53** to the Dess-Martin[151] oxidation conditions in Scheme 10, but in this case the phenol was eliminated due to the acidic alpha hydrogens located beta to the phenol; this elimination problem was avoided by using substrate **66**. Oxidation by Dess-Martin periodinane gave the ketone, which, after workup, was subsequently reduced using $NaBH_4$ in MeOH. Successive workup followed by methyl ester hydrolysis with LiOH gave the corresponding acid, which was subsequently coupled to amine **A** (Figure 25) to provide diastereomeric compound **67** (*S* /*R* ~1:1) in 74% yield over four steps. Thus, to be exact, Scheme 10 illustrates the synthesis of a mixture of epimers of compound **67**. However, the diastereomers were successfully separated by HPLC, and the desired *R*-isomer was confirmed by HPLC retention time and NMR analysis, using a sample of the previously synthesized *S*-isomer as reference compound. Target compound **73** (Table 5) with *R*-configuration of the hydroxyl was finally synthesized from the *R*-isomer of compound **67** in three steps according to Scheme 9.

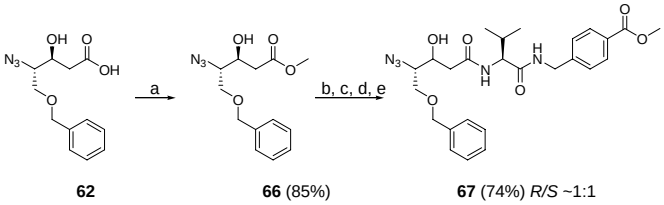

Scheme 10. *Reagents and conditions: (a) $SOCl_2$, MeOH; (b) Dess-Martin periodinane, DCM; (c) $NaBH_4$, MeOH, –15 °C; (d) LiOH, dioxane/H_2O 1:1; (e)* **A***, DIPEA, HATU, DMF.*

3.6.3 SAR Analysis

All target compounds were synthesized according to Scheme 9, starting from template **53**, **56**, **59,** or **62** and employing the appropriate amines and carboxylic acids among those shown in Figure 25. Tables 5–7 present the structures, the IC_{50} values, and the K_i values for inhibition of BACE-1 and human cathepsin D by the target compounds. P2 methionine and P3 valine inhibitors have been described in the literature,[128] and highly potent statine-based inhibitors carrying carboxylic acid moieties on the P´ side have also been reported.[136] Those observations encouraged us to prepare methyl ester **68** and carboxylic acid **69** (Table 5) with the 3,5-difluorophenyloxymethyl residue in the P1 position. Both turned out to be inactive, with IC_{50} values > 10 µM. Accordingly, we turned our attention to an approach published by Vacca and coworkers (Merck),

Table 5. *Target compounds and inhibition data*

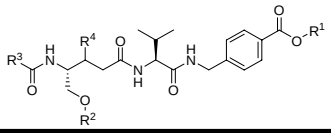

Cpd.	R^1	R^2	R^3	R^4	IC_{50} (µM) BACE-1	K_i (µM) Cat D
68	Me		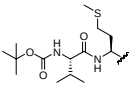	(*S*)-OH	> 10	0.015
69	H		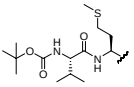	(*S*)-OH	> 10	0.024
64	Me		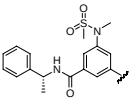	(*S*)-OH	0.20	0.73
65	H		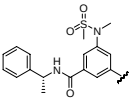	(*S*)-OH	0.013	0.51
70	H		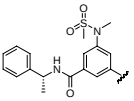	(*S*)-OH	0.014	0.36
71	H		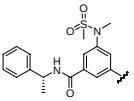	(*S*)-OH	0.12	0.43
72	H		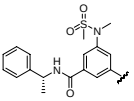	(*S*)-OH	0.024	0.18
73	H		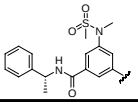	(*R*)-OH	1.2	> 5

which uses isophthalamide **M** in the P2-P3 position of potent hydroxyethylamine inhibitors (**D**, Figure 23).[131] Replacing the methionine-valine P2-P3 portion with isophthalamide **M** furnished ester **64** and acid **65** with promising IC_{50} values of 0.2 and 0.013 μM, respectively.

Exploration of the SAR of the P1 residue resulted in compounds **70–72**. Compound **70** (IC_{50} = 0.014 μM) incorporating a phenyloxymethyl P1 residue proved to be equipotent with the corresponding 3,5-difluorophenyloxymethyl analog **65**. Also compared to **65**, compound **71** containing a P1 3,5-difluorobenzyloxymethyl residue was found to be about nine times less active, whereas compound **72** incorporating a benzyloxymethyl residue was only slightly less active (IC_{50} values 0.12 and 0.024 μM, respectively). These findings indicate that the S1 pocket is limited in size; at least as it is accessed and utilized by the statine-based inhibitor cores.

To confirm that *S* configuration of the hydroxyl was the stereochemistry that gave the best fit to our statine cores, we prepared compound **73** having the *R* configuration. As anticipated the change in hydroxyl stereochemistry resulted in a large drop in activity to an IC_{50} value of 1.2 μM (Table 5).

Inhibitors **74–80** all carry an isophthalic diacid group[130] and they were the result of further exploration of interactions with the S3´ pocket (Table 6). In agreement with the activities seen for monoester **64** and monoacid **65**, the diester **74** was found to be less potent than the corresponding diacid **75**, with IC_{50} values of 0.22 and 0.037 μM, respectively, which also indicated that diacid **75** is slightly less active than the monoacid analogue **65** (IC_{50} 0.013 μM). When we extended the P1 moiety from 3,5-difluorophenoxymethyl to 3,5-difluorobenzyloxymethyl as in compound **76**, no change in activity was observed compared to **75**, whereas incorporation of the non-fluorinated extended P1 group led to enhanced activity, as exemplified by compound **77** (IC_{50} 0.012 μM). Notably, the trend towards less tolerance of the larger P1 residues compared to the smaller residues that was observed for the compounds in Table 5 did not hold true for these isophthalic-diacid compounds. It seems that, depending on how the P1 residue enters the S1 site, larger residues may be accommodated, and the angle at which it enters is most certainly influenced by the interactions of the other parts of the inhibitor.

Compounds **78–80** comprising smaller and more simplified P2-P3 groups and display considerably lower potency compared to the inhibitors that include the larger sulfonamide-containing isophthalamide (Table 6).

Table 6. *Target compounds and inhibition data*

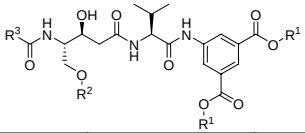

Cpd.	R^1	R^2	R^3	IC_{50} (μM) BACE-1	K_i (μM) Cat D
74	Me		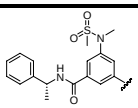	0.22	1.95
75	H		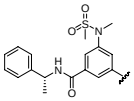	0.037	0.78
76	H		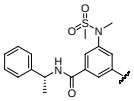	0.040	0.44
77	H		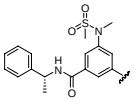	0.012	0.63
78	H		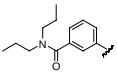	2.23	0.93
79	H		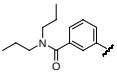	1.89	0.35
80	H		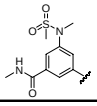	1.6	> 5

At this point in our work, compound **65** stood out as one of the most potent and promising inhibitors. Therefore, we decided to conduct a small SAR study, keeping the central core fixed to (core **53**) the one used in compound **65** (Table 7). Truncating the P2´-P3´ portion and replacing it with a small cyclopropyl residue or a p-carboxybenzyl residue generated inactive compounds (**81** and **82**). Removal of the P2´ side chain as in compound **83** also gave rise to a large drop in activity, indicating that S2´ site interactions are indeed essential for potency. Moving on, we found that compound **84**, which lacks the carboxylate functionality of **65**, has essentially the same level of activity as the methyl ester analog **64** (IC50 values of 0.21 and 0.20 μM for **84** and **64**, respectively), emphasizing the importance of the acidic function of this position in the S3´ pocket. Shortening the P3´ group as in compound **85** led to a 20-fold drop in activity compared to **65** (i.e., 0.26 versus 0.013 μM), suggesting that the favorable carboxylate interaction is reduced in **85**. Truncation of the P2-P3 M group

generated the inactive inhibitors **86** and **87**, which confirms the significance of both the S2 and S3 groups for the efficacy of these BACE-1 inhibitors (Table 7).

Table 7. *Target compounds and inhibition data*

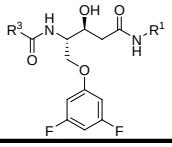

Cpd.	R^1	R^3	IC_{50} (μM) BACE-1	K_i (μM) Cat D
81		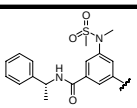	> 10	> 5
82	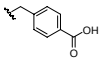	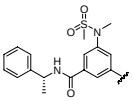	4.0	> 5
83	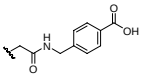	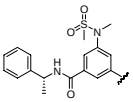	2.3	>5
84	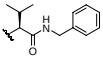	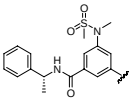	0.21	0.57
85	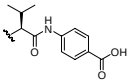	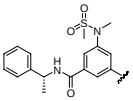	0.26	1.5
86	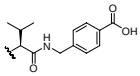	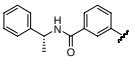	> 10	> 5
87	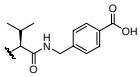		> 10	> 5

X-ray crystal structure results for inhibitor 75 (Figure 26). To further elucidate the binding mode of our inhibitors, we co-crystallized compound **75** with BACE-1. The key binding interactions obtained from the X-ray crystal structure (Figure 26; PDB code, 3dm6) are described below. The hydrogen bonds on the nonprime side of the inhibitor backbone are formed between the P3 NH and the carbonyl of Gly230, between the P3 carbonyl and the side chain of Thr232, between the P2 carbonyl and the back bone of the flap residue Gln73, and also between the P1 NH (like the P3 NH) and the carbonyl of Gly230. The hydrogen bond interactions of the backbone prime side occur between the followin: the P1´ carbonyl and the backbone NH of the flap residue Thr72; the P2´ NH and the carbonyl of Gly34; the P2´ carbonyl and the side chain hydroxyl of Tyr198; and the P3´ NH and the carbonyl

of Pro70. The hydroxyl group of the statine-based transition-state isostere is positioned between the two catalytic residues Asp32 and Asp228 to form a hydrogen bond network.The P3 capping phenyl interacts closely with several residues in the S3 sub-pocket, and it is stacked between Thr232 and Gly13 from top to bottom and has

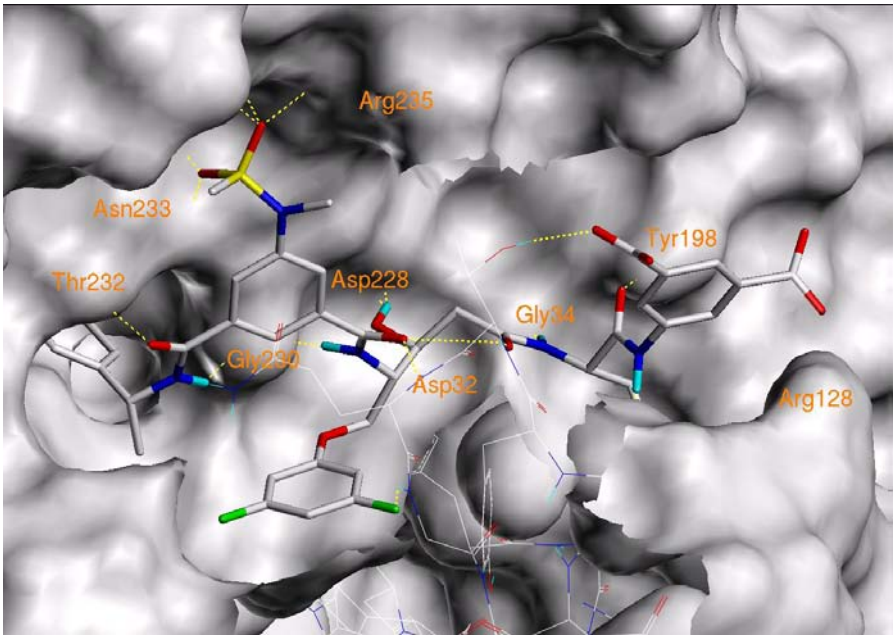

Figure 26. *X-ray crystal structure of inhibitor **75** and BACE-1 showing the key interactions between the inhibitor and the active site.*

edge on contact interactions with Gly11, Tyr14, Ser229, Gly230, and Arg307. The P3 methyl group participates in close interactions with Gln12, Gly13, Leu30, and Ile110 in the S3 pocket. The P2 aromatic ring is stacked between Thr231 and the side chain of the flap residue Gln73. The sulfonamide forms hydrogen bonds with the backbone NH of Thr232 and Asn233, and with the side chains of Ser325 and Arg235. The P1 side chain contributes to the activity of inhibitor **75** via aromatic stacking interactions with the side chains of Tyr71, Phe108, and Trp115, and close contact interactions with Gln73, Gly74, Lys107, and Ile110 in the S1-S3 pocket. The P2´ valine side chain interacts mainly with Ser35, Val69, Ile126, and Arg128 in the S2´ pocket. The P3´ isophthalic acid group interacts weakly with the solvent-exposed S3´ pocket and appears less hindered to rotate compared to the other side groups. However, in one out of three observations of the asymmetric unit, the isophthalic acid group was found to be locked in position by two hydrogen bonds formed between the carboxylates and the side-chains of Thr72 and Arg128. This increase in interactions with the S3´ pocket

may be related to the gain in efficacy that was achieved in this class of inhibitors by adding carboxylate functionalities in P3´.

Modeling of selected compounds in BACE and cathepsin D. A modeling study was conducted in an attempt to better understand the somewhat inconsistent BACE-1 activities of some of the compounds in this series. The information obtained from the crystal structure of **75** was used to rationalize the SARs of compounds **65**, **84**, and **85**. Notably, modeling of compound **65** showed that an additional strong interaction is possible between the P3´ *p*-carboxyl group and the side chain of Lys75, which explains the increased activity of compound **65** over compound **84** lacking the carboxyl. Moreover, none of the carboxylic acids of compound **75** can produce this interaction, and the acid functionality of compound **85** (the shorter analog of compound **65**) and the side chain of Lys75 are too far apart to interact strongly.

We also tested all the inhibitors in Tables 5–7 regarding their ability to inhibit human cathepsin D. The results show that the examined variations in the P1 and P2´-P3´ side chains in this series of inhibitors have little effect on the cathepsin D selectivity, as compared to the variations in P2-P3 side chains, which contribute more significantly to the activity against cathepsin D. The importance of the P2-P3 portion in this respect becomes evident when considering compounds **68**, **69**, **78**, and **79**, which have cathepsin D IC_{50} values of 0.015, 0.024, 0.93, and 0.35 μM, respectively. Compounds **68** and **69** are completely inactive towards BACE-1 but are highly active against cathepsin D, whereas compounds **78** and **79** are weak inhibitors of BACE-1 and moderately strong inhibitors of cathepsin D.

To explain the potency of compound **68** as an inhibitor of cathepsin D, a model was constructed using the crystal structure of the enzyme (1lyb).[152] This work revealed that **68** has an extensive hydrogen bonding network with the active site in cathepsin D, which includes four strong hydrogen bonds with the flap. The methionine side chain in the P2 position of the inhibitor interacts closely with the side chains of methionine 307 and 309 in the S2 pocket. The difluorophenoxy P1 group also fits well in the S1 pocket showing the possibility of favorable aromatic stacking interactions.

On the other hand, modeling of compound **68** in BACE-1 revealed that the large hydrophobic P2 methionine is not well accommodated in the polar environment of the S2 pocket of the protease. The lack of activity of compound **68** towards BACE-1 may also be the result of the bulky and inflexible *tert*-butoxycarbonyl group that does not fit well in the narrow space that exists between the flap of Gln73 and the S3 and S4 pockets of BACE-1.

Summarizing the results regarding the statine-based BACE-1 inhibitors, it is obvious that carboxylate functionalities in the P3´ position were required to obtain

highly potent inhibitors. All of the BACE inhibitors were also evaluated for their cellular activities by measuring the production of secreted soluble Aβ40 by cultured HEK-293 cells. However, although many of the compounds clearly inhibited BACE-1 in the enzyme assay, they lost all activity in the cell-based assay, resulting in IC_{50} values greater than 10 μM.

3.7 Design and Synthesis of Hydroxyethylene-Based BACE-1 Inhibitors Incorporating Extended P1 residues (Paper IV)

3.7.1 Design

In the work reported in Paper III, we explored the possibility of moving further into the S1 pocket by employing statine-based BACE-1 inhibitors containing somewhat prolonged P1 ether residues. Some of the inhibitors displayed substantial activity against BACE-1 in the enzyme assay, but they were still inactive in the cell-based assay. As a means of improving the drug-like properties of the compounds, we began attempts to reduce the size and polarity of the inhibitors. We also decided to abandon the statine-based isostere in favor of a hydroxyethylene (HE) central core (Figure 27)

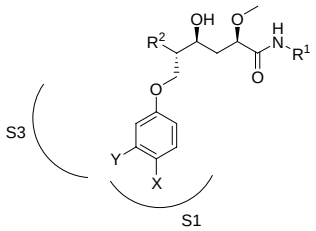

Figure 27. *A general illustration of the HE isostere with a methoxy residue in the P1´ position. The purpose of the X substituent is to protrude deeper into the S1 pocket, and the Y substituent is intended to extend into the S3 pocket.*

that has previously been employed in our laboratories to synthesize potent BACE-1 inhibitors.[153] The main reason for that change was that carboxylic acid functionalities had proven to be crucial for high activity in the statine series. In addition, the HE isostere contains one less amide linkage compared to the statine core, a feature that would further decrease the peptidic character of the potential inhibitors. Earlier studies of aspartic proteases such as the malaria plasmepsins[140] and human renin[154] have shown that the S1 pocket of these targets can accommodate large P1 residues, many of which that reach out into the S3 pocket. Modeling suggested that similar modifications may also be favorable when designing BACE-1 inhibitors. Therefore,

we initiated the synthesis of inhibitors with a hydroxyethylene central core containing a variety of P1 residues extending into the S1-S3 binding pocket (Figure 27).

3.7.2 Synthesis

Figure 28 illustrates the general structures of the inhibitors that were synthesized along with the various R substituents used. However, unlike what is shown in that figure, most of the target compounds were evaluated as free amines, i.e., without any P2 R^3 carboxylic acid substituent.

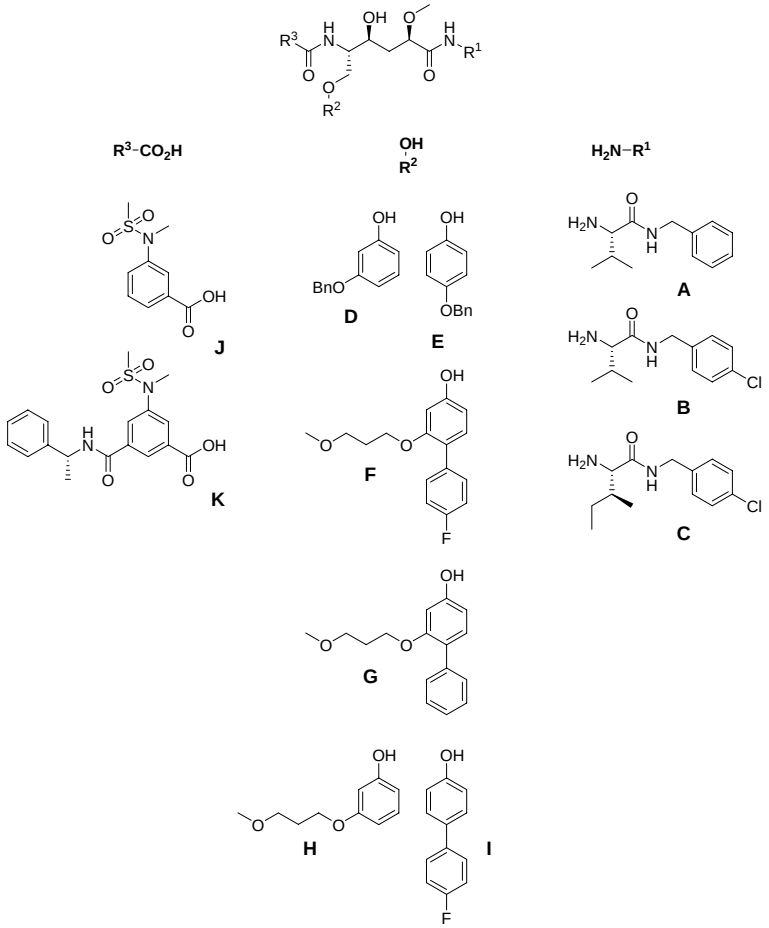

Figure 28. *A general illustration of the hydroxyethylene central core and the different R substituents that were used.*

R^1 amines **A–C** were synthesized from commercially available precursors using standard peptide coupling and deprotection procedures (see the experimental section of paper IV), and phenols **D** and **E** were purchased. The largest P1 R^2 residues, **F** and

G, were obtained as their corresponding benzyl ethers, as shown in Scheme 11. An electrophilic aromatic substitution was performed on 3-benzyloxy-phenol (**D**) utilizing *N*-bromosuccinimide (NBS) in DCM at –15 °C, which produced aryl halide **88** in 71% yield.[155] Compound **88** was subsequently subjected to Mitsunobu-like conditions using 3-methoxy-1-propanol, PPh_3, and DIAD in THF to give compound **89** in 90% yield. We then applied microwave-assisted palladium coupling conditions,

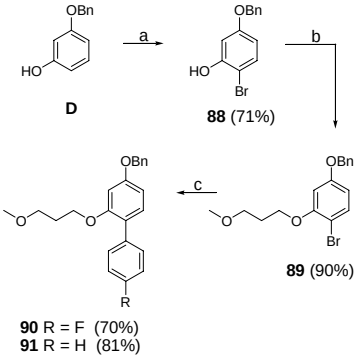

Scheme 11. *Reagents and conditions: (a) NBS, DCM, –15 °C; (b) 3-methoxy-1-propanol, PPh_3, DIAD, THF; (c) 4-fluorophenylboronic acid or phenylboronic acid, K_3PO_4, PEPPSI™-IPr catalyst, DMF, EtOH, H_2O.*

which in this case involved treatment of **89** with 4-fluorophenylboronic acid or phenylboronic acid, K_3PO_4, and PEPPSI™-IPr catalyst in EtOH, H_2O, and DMF. Microwave irradiation at 125 °C for 15 min produced biphenyl derivatives **90** and **91** in 70% and 81% yields, respectively. The corresponding benzyl ether of **H** was synthesized from **D** by applying the same conditions as utilized to prepare compound **89**, and compound **I** was obtained from commercially available 4-bromophenol using the same Suzuki protocol as employed to synthesize compound **90**. Sulfonamides **J** and **K**, which were also used in paper III, were synthesized accordingly.[131]

Scheme 12 depicts the synthesis of compound **99**, which served as a scaffold for

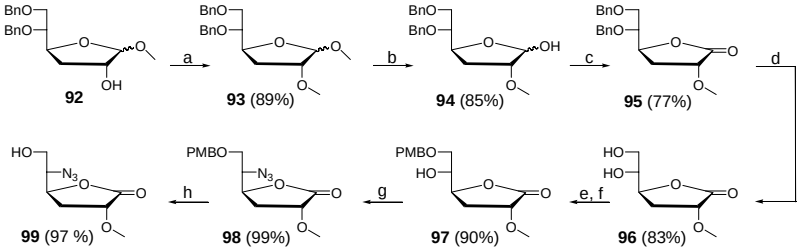

Scheme 12. Reagents and conditions: (a) MeI, Ag_2O, DMF; (b) H_2SO_4, dioxane; (c) PDC, 4 Å molecular sieves; (d) H_2, $Pd(OH)_2$-C, AcOH, EtOH; (e) Bu_2SnO, toluene, reflux; (f) tetrabutylammonium bromide, 4-OMeBnBr, toluene, 90 °C; (g) PPh_3, DIAD, DPPA, THF; (h) DDQ, H_2O,DCM.

making all the target compounds. Again, diacetone-D-glucose was used as a precursor from which compound **92** was synthesized in 49% yield over five steps as described in the literature.[142-144,156] Treatment of **92** with MeI and Ag_2O in DMF furnished methyl ether **93** in 89% yield. Hydrolysis of **93** using H_2SO_4 in dioxane gave hemiacetal **94** in 85% yield, and subsequent oxidation with PDC in DCM produced lactone **95** in 77% yield.[153] Next, **95** was exposed to catalytic hydrogenolysis effected by H_2 on $Pd(OH)_2$-C in AcOH and EtOH to prepare diol **96** in 83% yield. Selective primary alkylation was performed as described previously[149] (see compounds **57** and **60**) although this time using 4-methoxybenzyl bromide, which gave benzyl ether **97** in 90% yield. Employing the by-now-familiar Mitsunobu protocol, i.e., PPh_3, DIAD, and DPPA in dry THF, provided azide **98** (99%); and finally an oxidative removal accomplished using 2,3-dichloro-5,6-dicyano benzoquinone (DDQ) in H_2O and DCM delivered compound **99** in 97% yield.[157]

Scheme 13 depicts the synthesis of target compounds **102** and **103**. The first step involved a substitution reaction to prepare compound **100**. To obtain this compound, it was necessary to make some initial modifications to **90** and **99**. First, compound **90** was converted into the phenol by catalytic hydrogenolysis using H_2/Pd-C in EtOH. Then we once again applied Mitsunobu conditions to achieve the substitution reaction with alcohol **99**, but, like so many times before, we encountered elimination problems.

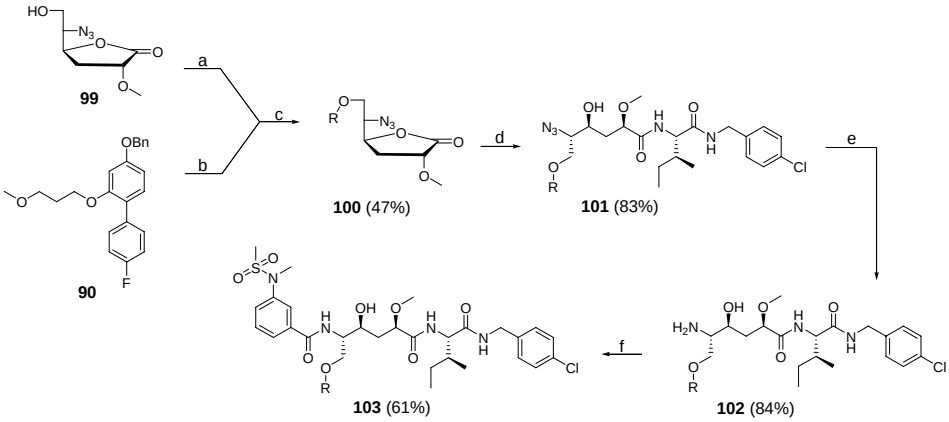

Scheme 13. *Reagents and conditions: (a) triflic anhydride, pyridine, DCM; (b), H_2, Pd-C, EtOH; (c) Cs_2CO_3, 4 Å molecular sieves, DCM, 40 °C; (d)* ***C****, 2-hydroxypyridine, DIPEA, DMF, 75 °C; (e) PPh_3, MeOH, H_2O; (f)* ***J****, DIPEA, HATU, DMF.*

Therefore, we instead chose to transform alcohol **99** into the corresponding triflate using triflic anhydride and pyridine in DCM. It was then possible to substitute the triflate with the phenol by using Cs_2CO_3 in DCM containing 4 Å molecular sieves.

This gave compound **100** in 47% yield. It should be mentioned that the elimination problems could not be fully avoided by the approach using triflate. However, we were able to minimize the difficulties in that context by letting the triflate and the phenol react with each other for a rather short amount of time in the presence of fresh Cs_2CO_3 in extra dry and heated solvent (40 °C) under N_2 atmosphere. The reason for heating the reaction was that longer reaction times gave rise to additional elimination and also to the regeneration of alcohol **99**.

Lactone **100** was opened using amine **C** and 2-hydroxypyridine in DIPEA and DMF, which gave **101** in 83% yield. Employing PPh_3 in MeOH and H_2O afforded target compound **102** in 84% yield from **101**. Amine **102** was coupled to acid **J** using HATU and DIPEA in DMF to provide target compound **103** in 61% yield.

3.7.3 Results

Table 8 summarizes all the target compounds, which were synthesized according to Scheme 13 using appropriate R substituents shown in Figure 28. Enzyme activities were measured against BACE-1, and the IC_{50} values are also presented in Table 8.

To begin with, *m*-benzyloxy modification in the P1 position gave the inactive amine **104** and the modestly active sulfonamide **105** (IC_{50} values > 10 and 2.2 μM, respectively). The P1 *p*-benzyloxy-modified sulfonamide **106** proved to be slightly less active (IC_{50} 4.6 μM) than the corresponding P1 *m*-benzyloxy compound **105**. Nonetheless, the results for **105** and **106** were promising and indicated that more advanced P1 substituents could provide these kinds of inhibitors with increased activity. Further development led to BACE-1 inhibitors **107** and **102** containing P1 R^2 substituent **F** and P2´-P3´ R^1 substituents **B** and **C** (Figure 28) with a *p*-chloro substituent in P3´. Compound **102** has an isoleucine in P2´ position and an IC_{50} value of 1.2 μM, making it more active than the corresponding P2´ valine inhibitor **107** (IC_{50} 2.7 μM). In addition, the fluorine substituent on the P1 moiety contributes significantly to the activity, as seen for compound **108** (IC_{50} 2.5 μM) lacking the fluorine. The activity of this class of inhibitors depends on interactions from both the *para* and the *meta* groups in the P1 position, as observed for **109** and **110** (IC_{50} values > 10 μM) lacking the *para* and the *meta* substituent, respectively. Notably, **102** is clearly a more potent inhibitor than **105**, even though it does not contain a P2 substituent. This can probably be explained by the increased number interactions provided by the more advanced P1 substituent. Unfortunately, introduction of the P2 sulfonamide substituent **J** into **102** and **108** rendered those compounds highly hydrophobic in character, which caused precipitation problems during the activity measurements and thus no inhibition data were obtained for **103** and **111**. Compound **112** contains the larger P2-P3 portion **K** and has an IC_{50} value of 0.069 μM, which is

Table 8. *Target compounds and inhibition data*

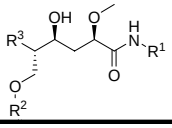

Cpd.	R^1	R^2	R^3	IC_{50} (μM)[a] BACE-1
104	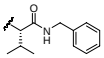		H_2N	> 10
105	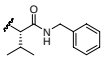			2.2
106	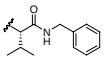			4.6
107	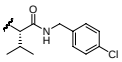	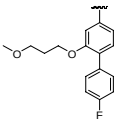	H_2N	2.7
102	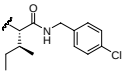	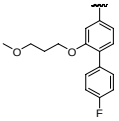	H_2N	1.2
108	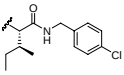	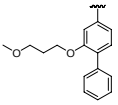	H_2N	2.5
109	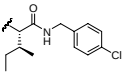	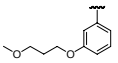	H_2N	> 10
110	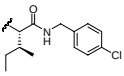	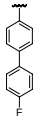	H_2N	> 10
103	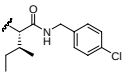	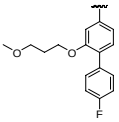		ND
111	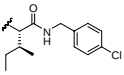	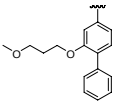		ND
112	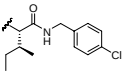	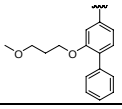	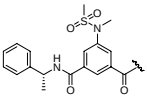	0.069

intriguing, since it indicates that the active site can tolerate such a large compound having both the P3 portion and the sizable P1.

Summarizing the results presented in Table 8, it is apparent that **102**, **107**, and **108** display promising activities even though they lack a P2 substituent. Moreover, these compounds possess only two amide bonds, which renders a more drug-like character. Further optimization of this class of inhibitors may produce additional interesting compounds, and possibly a few candidates that are even more promising for further development.

4. Concluding Remarks

The primary aim of the studies underlying this thesis was to explore the possibility of developing potential drug candidates (or at least compounds showing activity) against two different proteases. The target enzymes were the hepatitis C virus NS3 serine protease and the human aspartic protease BACE-1. The work gave rise to several novel and very promising compounds and has been reported in Papers I–IV, which are summarized below.

Paper I:

- A novel P2 cyclopentane-derived scaffold was synthesized to be used as an *N*-acyl-(4*R*)-hydroxyproline bioisostere in potential HCV NS3 protease inhibitors.
- Two synthetic routes were developed to provide orthogonal protecting groups during coupling to different substituents, and they readily gave several target compounds in good yields.
- Systematic variation of P1 and P3–P4 substituents produced promising inhibitors, some with activities in the nanomolar range: compounds **13**, **21**, and **25** with K_i values of 22, 16, and 560 nM, respectively.
- The most potent inhibitors were obtained by incorporating (1*R*,2*S*)-1-amino-2-vinylcyclopropane carboxylic acid at the P1 position, L-*tert*-butyl glycine at the P3 position, and L-cyclohexylglycine at the P4 position. All inhibitors contain 2-phenyl-7-methoxy-4-quinolinol as a P2 elongation.

Paper II:

- Very potent macrocyclic P2 cyclopentane- and cyclopentene-derived HCV NS3 protease inhibitors were synthesized from two previously developed series of linear inhibitors.
- Ring-closing metathesis gave 13-, 14-, 15- and 16-membered rings, and the best fit in the active site was observed for the 14-membered macrocycles, exemplified

by compounds **38b**, **40b**, **38f**, and **48a** with K_i values of 31, 6, 44, and 15 nM, respectively.

- Introducing a cyclopropylsulfonamide as a carboxylic acid bioisostere in P2 cyclopentane compounds **38b**, **40b**, and **38f** gave inhibitors **41**, **42**, and **44**, which showed even better activity in the enzyme assay and very promising effects in the cell-based assay, as indicated by their respective K_i values of 0.07, 0.19, and 0.41 nM, and EC_{50} values of 530, 33, and 9.1 nM.
- Interestingly, even though they lack the P4 substituent, compounds **42** and **44** are highly active HCV NS3 protease inhibitors.

Paper III:

- Several potent BACE-1 inhibitors were synthesized that comprise a statine-based central core containing phenyloxymethyl and benzyloxymethyl residues in the P1 position.
- These templates were obtained by employing an efficient synthesis route starting from the carbohydrate 3-deoxy-1,2-*O*-isopropylidene-α-D-glucose (**49**).
- Different substituents were evaluated to study the SAR of this class of inhibitors. Carboxylate functionalities in the P3´ position were found to be required to obtain highly potent inhibitors, such as **65** (13 nM), **70** (14 nM), **75** (37 nM), and **77** (12 nM).
- Compound **75** was co-crystallized with BACE-1, and the X-ray crystal structure revealed the key binding interactions with the active site. Modeling studies were also conducted and conclusions were drawn based on the information obtained from the crystal structure. An interaction with Lys75 was found, which may explain the increase in activity of the P3´-functionalized compounds.

Paper IV

- BACE-1 inhibitors with a hydroxyethylene central core, comprising a methoxy residue in the P1´ position, were synthesized.
- Extended P1 substituents were introduced with the aim to explore possible interactions with the S1-S3 pocket.
- Incorporation of the more advanced P1 substituents produced promising inhibitors in the low micromolar range.

5. Acknowledgments

Big thanks go to *all of you* that have been giving me love, support, guidance, comfort and happiness during the last 29 years of my life.

For help, support, guidance, fun times and good friendship during the years of my life as a graduate student at Linköping University I would like to thank the following people:

Ingemar Kvarnström, my supervisor, for trust, encouragement, guidance, and support, for fruitful discussions regarding chemistry in general and every day life in particular and for giving me the chance to see “the bigger picture” at various conference trips.

Bertil Samuelsson, the man in charge of the projects presented in this thesis, for your never-ending ideas and enthusiasm, for sharing your great knowledge regarding organic and medicinal chemistry, and for invaluable help with manuscript preparations.

Åsa Rosenquist, for being a very helpful and supportive contact person/supervisor at Medivir, for assistance with manuscript preparations and lots of other practical help.

Per-Ola Johansson, for excellent supervision during my diploma work, for being a great office-mate for more than two years, for being a good friend and for helping me to pick the best bottles among the broad selection of good Californian wines available at systembolaget.

Fredrik Thorstensson, for helping me out with my computer, ordering and database problems in the beginning, for being the persuasive force that resulted in lots of after work activities in the early days and for being an excellent map-reader in Miami and the southern parts of California.

Fredrik Wångsell, for being my closest colleague for more than a year, for all sorts of practical and technical help, for struggling together with me when writing our licentiate theses, and for being an excellent driver during our great conference trip in the states.

Veronica Sandgren, for being my closest colleague for the last two and a half years, for being the more talkative person in our group (which perhaps is not that difficult), for sharing the burden with me and for adding light to my office.

Jonas Nyhlén, for contributions to Paper III, and *Malek Mirzayan,* for the synthesis of the tertiary alcohol.

My diploma workers: *Johan Karlsson, Cecilia Tham, Kristina Bjurklo, Sofia Andersson, David Elmqvist, and Malin Sandgren* for contributions to different projects.

Susanne, for invaluable help with all the paperwork.

For company at lunches, coffee breaks, parties, and for creating a nice and familiar atmosphere at the chemistry department:
Former: *Markus H, Johan O, Patrik, Jussi, Johan R, Andreas C, Sofia H, Martin L, Jonas N, Martin K , Karin G, Bisse, Björn, Tobias…*
Present: *Timmy, Lan, Andreas, Roger, Alma, Roz, Jutta, Daniel, Robban, Leffe, Janosch, Patrik L, Fredrik, Anna-Lena, Linda, Karin, Peter N, Per, Peter K, Stefan, Sofia, Robin, colleagues "of the round lunch table", all teachers and other helpful staff…*

The staff at Medivir for good collaboration.

Patricia Ödman, for excellent linguistic improvements of this thesis.

My Parents, Birgitta och *Samuel,* and my *brother Fredrik.*
No specifications needed. Thanks for everything.

Linköping, April 2009

Marcus

6.References

1. Tyndall, J. D.; Nall, T.; Fairlie, D. P. *Chem. Rev.* **2005**, *105*, 973-99.
2. Leung, D.; Abbenante, G.; Fairlie, D. P. *J. Med. Chem.* **2000**, *43*, 305-41.
3. Hedstrom, L. *Chem. Rev.* **2002**, *102*, 4501-24.
4. Babine, R. E.; Bender, S. L. *Chemical Reviews* **1997**, *97*, 1359-1472.
5. Bursavich, M. G.; Rich, D. H. *J. Med. Chem.* **2002**, *45*, 541-58.
6. Aytac, U.; Dang, N. H. *Curr Drug Targets Immune Endocr Metabol Disord* **2004**, *4*, 11-8.
7. Schechter, I.; Berger, A. *Biochem. Biophys. Res. Commun.* **1967**, *27*, 157-62.
8. West, M. L.; Fairlie, D. P. *Trends Pharmacol. Sci.* **1995**, *16*, 67-75.
9. Pharmacodynamics explores what a drug does to the body.
10. Pharmacokinetics explores what the body does to the drug.
11. Patrick, L. G. *An Introduction to Medicinal Chemistry*; Oxford University Press, 2005; Vol. 3.
12. Lipinski, C. A.; Lombardo, F.; Dominy, B. W.; Feeney, P. J. *Adv. Drug Deliv. Rev.* **1997**, *23*, 3-25.
13. Veber, D. F.; Johnson, S. R.; Cheng, H. Y.; Smith, B. R.; Ward, K. W.; Kopple, K. D. *J. Med. Chem.* **2002**, *45*, 2615-2623.
14. Tan, S. L.; Pause, A.; Shi, Y. U.; Sonenberg, N. *Nat. Rev. Drug Discov.* **2002**, *1*, 867-881.
15. Di Bisceglie, A. M.; Bacon, B. R. *Sci. Am.* **1999**, *281*, 80-5.
16. Choo, Q. L.; Kuo, G.; Weiner, A. J.; Overby, L. R.; Bradley, D. W.; Houghton, M. *Science* **1989**, *244*, 359-362.
17. Di Bisceglie, A. M. *Lancet North Am. Ed.* **1998**, *351*, 351-355.
18. Shepard, C. W.; Finelli, L.; Alter, M. J. *Lancet Infect. Dis.* **2005**, *5*, 558-67.
19. De Francesco, R.; Migliaccio, G. *Nature* **2005**, *436*, 953-960.
20. Tsantrizos, Y. S. *Acc Chem Res* **2008**, *41*, 1252-63.
21. De Clercq, E. *Nat Rev Drug Discov* **2007**, *6*, 1001-18.
22. Chisari, F. V. *Nature* **2005**, *436*, 930-2.
23. Rehermann, B.; Nascimbeni, M. *Nat. Rev. Immunol.* **2005**, *5*, 215-229.
24. Ni, Z. J.; Wagman, A. S. *Curr. Opin. Drug Discov. Devel.* **2004**, *7*, 446-459.
25. Poynard, T.; Yuen, M. F.; Ratziu, V.; Lai, C. L. *Lancet* **2003**, *362*, 2095-100.
26. Gordon, C. P.; Keller, P. A. *J. Med. Chem.* **2005**, *48*, 1-20.
27. Goudreau, N.; Llinàs-Brunet, M. *Expert Opin. Investig. Drugs* **2005**, *14*, 1129-1144.
28. Thimme, R.; Lohmann, V.; Weber, F. *Antiviral Res* **2006**, *69*, 129-41.
29. Lindenbach, B. D.; Rice, C. M. *Nature* **2005**, *436*, 933-938.
30. Reprinted by permission from Macmillan Publishers Ltd: [Nature] *(Nature **2005,** 436, 933-938.*), © (2005).
31. Ago, H.; Adachi, T.; Yoshida, A.; Yamamoto, M.; Habuka, N.; Yatsunami, K.; Miyano, M. *Structure* **1999**, *7*, 1417-26.
32. Bressanelli, S.; Tomei, L.; Roussel, A.; Incitti, I.; Vitale, R. L.; Mathieu, M.; De Francesco, R.; Rey, F. A. *Proc. Natl. Acad. Sci. U.S.A.* **1999**, *96*, 13034-9.
33. Lesburg, C. A.; Cable, M. B.; Ferrari, E.; Hong, Z.; Mannarino, A. F.; Weber, P. C. *Nat Struct Biol* **1999**, *6*, 937-43.
34. Kwong, A. D.; McNair, L.; Jacobson, I.; George, S. *Curr Opin Pharmacol* **2008**, *8*, 522-31.
35. Liu-Young, G.; Kozal, M. J. *AIDS Patient Care STDS* **2008**, *22*, 449-57.

36. Paeshuyse, J.; Vliegen, I.; Coelmont, L.; Leyssen, P.; Tabarrini, O.; Herdewijn, P.; Mittendorfer, H.; Easmon, J.; Cecchetti, V.; Bartenschlager, R.; Puerstinger, G.; Neyts, J. *Antimicrob Agents Chemother* **2008**, *52*, 3433-7.
37. Ronn, R.; Sandstrom, A. *Curr Top Med Chem* **2008**, *8*, 533-62.
38. Tong, L. *Chem. Rev.* **2002**, *102*, 4609-26.
39. Beran, R. K.; Pyle, A. M. *J Biol Chem* **2008**, *283*, 29929-37.
40. De Francesco, R.; Tomei, L.; Altamura, S.; Summa, V.; Migliaccio, G. *Antiviral Res.* **2003**, *58*, 1-16.
41. Dymock, B. W.; Jones, P. S.; Wilson, F. X. *Antiviral Chem. Chemother.* **2000**, *11*, 79-96.
42. Lamarre, D.; Anderson, P. C.; Bailey, M.; Beaulieu, P.; Bolger, G.; Bonneau, P.; Bos, M.; Cameron, D. R.; Cartier, M.; Cordingley, M. G.; Faucher, A. M.; Goudreau, N.; Kawai, S. H.; Kukolj, G.; Lagace, L.; LaPlante, S. R.; Narjes, H.; Poupart, M. A.; Rancourt, J.; Sentjens, R. E.; St George, R.; Simoneau, B.; Steinmann, G.; Thibeault, D.; Tsantrizos, Y. S.; Weldon, S. M.; Yong, C. L.; Llinàs-Brunet, M. *Nature* **2003**, *426*, 186-189.
43. Steinkuhler, C.; Koch, U.; Narjes, F.; Matassa, V. G. *Curr. Med. Chem.* **2001**, *8*, 919-932.
44. Landro, J. A.; Raybuck, S. A.; Luong, Y. P.; O'Malley, E. T.; Harbeson, S. L.; Morgenstern, K. A.; Rao, G.; Livingston, D. J. *Biochemistry* **1997**, *36*, 9340-8.
45. Llinàs-Brunet, M.; Bailey, M.; Fazal, G.; Goulet, S.; Halmos, T.; Laplante, S.; Maurice, R.; Poirier, M.; Poupart, M. A.; Thibeault, D.; Wernic, D.; Lamarre, D. *Bioorg. Med. Chem. Lett.* **1998**, *8*, 1713-1718.
46. Steinkuhler, C.; Biasiol, G.; Brunetti, M.; Urbani, A.; Koch, U.; Cortese, R.; Pessi, A.; De Francesco, R. *Biochemistry* **1998**, *37*, 8899-905.
47. Ingallinella, P.; Altamura, S.; Bianchi, E.; Taliani, M.; Ingenito, R.; Cortese, R.; De Francesco, R.; Steinkuhler, C.; Pessi, A. *Biochemistry* **1998**, *37*, 8906-14.
48. Beaulieu, P. L.; Llinàs-Brunet, M. *Curr. Med. Chem. - Anti-Infective Agents* **2002**, *1*, 163-176.
49. Llinàs-Brunet, M.; Bailey, M. D.; Ghiro, E.; Gorys, V.; Halmos, T.; Poirier, M.; Rancourt, J.; Goudreau, N. *J. Med. Chem.* **2004**, *47*, 6584-94.
50. Goudreau, N.; Cameron, D. R.; Bonneau, P.; Gorys, V.; Plouffe, C.; Poirier, M.; Lamarre, D.; Llinàs-Brunet, M. *J. Med. Chem.* **2004**, *47*, 123-132.
51. Llinàs-Brunet, M.; Bailey, M.; Fazal, G.; Ghiro, E.; Gorys, V.; Goulet, S.; Halmos, T.; Maurice, R.; Poirier, M.; Poupart, M. A.; Rancourt, J.; Thibeault, D.; Wernic, D.; Lamarre, D. *Bioorg. Med. Chem. Lett.* **2000**, *10*, 2267-2270.
52. Poupart, M. A.; Cameron, D. R.; Chabot, C.; Ghiro, E.; Goudreau, N.; Goulet, S.; Poirier, M.; Tsantrizos, Y. S. *J. Org. Chem.* **2001**, *66*, 4743-51.
53. Rancourt, J.; Cameron, D. R.; Gorys, V.; Lamarre, D.; Poirier, M.; Thibeault, D.; Llinàs-Brunet, M. *J. Med. Chem.* **2004**, *47*, 2511-2522.
54. Narjes, F.; Koch, U.; Steinkuhler, C. *Expert Opin. Investig. Drugs* **2003**, *12*, 153-63.
55. Faucher, A. M.; Bailey, M. D.; Beaulieu, P. L.; Brochu, C.; Duceppe, J. S.; Ferland, J. M.; Ghiro, E.; Gorys, V.; Halmos, T.; Kawai, S. H.; Poirier, M.; Simoneau, B.; Tsantrizos, Y. S.; Llinàs-Brunet, M. *Org. Lett.* **2004**, *6*, 2901-2904.
56. Goudreau, N.; Brochu, C.; Cameron, D. R.; Duceppe, J. S.; Faucher, A. M.; Ferland, J. M.; Grand-Maitre, C.; Poirier, M.; Simoneau, B.; Tsantrizos, Y. S. *J. Org. Chem.* **2004**, *69*, 6185-6201.
57. Llinàs-Brunet, M.; Bailey, M. D.; Bolger, G.; Brochu, C.; Faucher, A. M.; Ferland, J. M.; Garneau, M.; Ghiro, E.; Gorys, V.; Grand-Maitre, C.; Halmos, T.; Lapeyre-Paquette, N.; Liard, F.; Poirier, M.; Rheaume, M.; Tsantrizos, Y. S.; Lamarre, D. *J. Med. Chem.* **2004**, *47*, 1605-1608.
58. Tsantrizos, Y. S.; Bolger, G.; Bonneau, P.; Cameron, D. R.; Goudreau, N.; Kukolj, G.; LaPlante, S. R.; Llinàs-Brunet, M.; Nar, H.; Lamarre, D. *Angew. Chem., Int. Ed.* **2003**, *42*, 1355-1360.
59. Reiser, M.; Hinrichsen, H.; Benhamou, Y.; Reesink, H. W.; Wedemeyer, H.; Avendano, C.; Riba, N.; Yong, C. L.; Nehmiz, G.; Steinmann, G. G. *Hepatology* **2005**, *41*, 832-5.
60. Chen, S. H.; Lamar, J.; Yip, Y.; Victor, F.; Johnson, R. B.; Wang, Q. M.; Glass, J. I.; Heinz, B.; Colacino, J.; Guo, D.; Tebbe, M.; Munroe, J. E. *Letters in Drug Design & Discovery* **2005**, *2*, 118-123.
61. Lin, K.; Perni, R. B.; Kwong, A. D.; Lin, C. *Antimicrob. Agents Chemother.* **2006**, *50*, 1813-22.
62. Yip, Y.; Victor, F.; Lamar, J.; Johnson, R.; Wang, Q. M.; Barket, D.; Glass, J.; Jin, L.; Liu, L. F.; Venable, D.; Wakulchik, M.; Xie, C. P.; Heinz, B.; Villarreal, E.; Colacino, J.; Yumibe, N.; Tebbe, M.; Munroe, J.; Chen, S. H. *Bioorg. Med. Chem. Lett.* **2004**, *14*, 251-256.

63. Malcolm, B. A.; Liu, R.; Lahser, F.; Agrawal, S.; Belanger, B.; Butkiewicz, N.; Chase, R.; Gheyas, F.; Hart, A.; Hesk, D.; Ingravallo, P.; Jiang, C.; Kong, R.; Lu, J.; Pichardo, J.; Prongay, A.; Skelton, A.; Tong, X.; Venkatraman, S.; Xia, E.; Girijavallabhan, V.; Njoroge, F. G. *Antimicrob. Agents Chemother.* **2006**, *50*, 1013-20.
64. Tong, X.; Chase, R.; Skelton, A.; Chen, T.; Wright-Minogue, J.; Malcolm, B. A. *Antiviral Res.* **2006**, *70*, 28-38.
65. Venkatraman, S.; Bogen, S. L.; Arasappan, A.; Bennett, F.; Chen, K.; Jao, E.; Liu, Y. T.; Lovey, R.; Hendrata, S.; Huang, Y.; Pan, W.; Parekh, T.; Pinto, P.; Popov, V.; Pike, R.; Ruan, S.; Santhanam, B.; Vibulbhan, B.; Wu, W.; Yang, W.; Kong, J.; Liang, X.; Wong, J.; Liu, R.; Butkiewicz, N.; Chase, R.; Hart, A.; Agrawal, S.; Ingravallo, P.; Pichardo, J.; Kong, R.; Baroudy, B.; Malcolm, B.; Guo, Z.; Prongay, A.; Madison, V.; Broske, L.; Cui, X.; Cheng, K. C.; Hsieh, Y.; Brisson, J. M.; Prelusky, D.; Korfmacher, W.; White, R.; Bogdanowich-Knipp, S.; Pavlovsky, A.; Bradley, P.; Saksena, A. K.; Ganguly, A.; Piwinski, J.; Girijavallabhan, V.; Njoroge, F. G. *J. Med. Chem.* **2006**, *49*, 6074-86.
66. Bogen, S. L.; Arasappan, A.; Bennett, F.; Chen, K.; Jao, E.; Liu, Y. T.; Lovey, R. G.; Venkatraman, S.; Pan, W.; Parekh, T.; Pike, R. E.; Ruan, S.; Liu, R.; Baroudy, B.; Agrawal, S.; Chase, R.; Ingravallo, P.; Pichardo, J.; Prongay, A.; Brisson, J. M.; Hsieh, T. Y.; Cheng, K. C.; Kemp, S. J.; Levy, O. E.; Lim-Wilby, M.; Tamura, S. Y.; Saksena, A. K.; Girijavallabhan, V.; Njoroge, F. G. *J. Med. Chem.* **2006**, *49*, 2750-7.
67. Njoroge, F. G.; Chen, K. X.; Shih, N. Y.; Piwinski, J. J. *Acc Chem Res* **2008**, *41*, 50-9.
68. Gentile, I.; Viola, C.; Borgia, F.; Castaldo, G.; Borgia, G. *Curr Med Chem* **2009**, *16*, 1115-21.
69. Mederacke, I.; Wedemeyer, H.; Manns, M. P. *Curr Opin Investig Drugs* **2009**, *10*, 181-9.
70. Lin, C.; Gates, C. A.; Rao, B. G.; Brennan, D. L.; Fulghum, J. R.; Luong, Y. P.; Frantz, J. D.; Lin, K.; Ma, S.; Wei, Y. Y.; Perni, R. B.; Kwong, A. D. *J. Biol. Chem.* **2005**, *280*, 36784-91.
71. Johansson, A.; Poliakov, A.; Åkerblom, E.; Wiklund, K.; Lindeberg, G.; Winiwarter, S.; Danielson, U. H.; Samuelsson, B.; Hallberg, A. *Bioorg. Med. Chem.* **2003**, *11*, 2551-2568.
72. Oscarsson, K.; Poliakov, A.; Oscarson, S.; Danielson, U. H.; Hallberg, A.; Samuelsson, B. *Bioorg. Med. Chem.* **2003**, *11*, 2955-63.
73. Poliakov, A.; Johansson, A.; Akerblom, E.; Oscarsson, K.; Samuelsson, B.; Hallberg, A.; Danielson, U. H. *Biochim. Biophys. Acta* **2004**, *1672*, 51-59.
74. Rönn, R.; Sabnis, Y. A.; Gossas, T.; Åkerblom, E.; Danielson, U. H.; Hallberg, A.; Johansson, A. *Bioorg. Med. Chem.* **2006**, *14*, 544-559.
75. Raboisson, P.; de Kock, H.; Rosenquist, A.; Nilsson, M.; Salvador-Oden, L.; Lin, T. I.; Roue, N.; Ivanov, V.; Wahling, H.; Wickstrom, K.; Hamelink, E.; Edlund, M.; Vrang, L.; Vendeville, S.; Van de Vreken, W.; McGowan, D.; Tahri, A.; Hu, L. L.; Boutton, C.; Lenz, O.; Delouvroy, F.; Pille, G.; Surleraux, D.; Wigerinck, P.; Samuelsson, B.; Simmen, K. *Bioorg. Med. Chem. Lett.* **2008**, *18*, 4853-4858.
76. Das, J.; Kimball, S. D. *Bioorg. Med. Chem.* **1995**, *3*, 999-1007.
77. Nöteberg, D.; Brånalt, J.; Kvarnström, I.; Classon, B.; Samuelsson, B.; Nillroth, U.; Danielson, H.; Karlen, A.; Hallberg, A. *Tetrahedron* **1997**, *53*, 7975-7984.
78. Turbanti, L.; Cerbai, G.; Dibugno, C.; Giorgi, R.; Garzelli, G.; Criscuoli, M.; Renzetti, A. R.; Subissi, A.; Bramanti, G. *J. Med. Chem.* **1993**, *36*, 699-707.
79. Nöteberg, D.; Brånalt, J.; Kvarnström, I.; Linschoten, M.; Musil, D.; Nystrom, J. E.; Zuccarello, G.; Samuelsson, B. *J. Med. Chem.* **2000**, *43*, 1705-13.
80. Thorstensson, F.; Kvarnström, I.; Musil, D.; Nilsson, I.; Samuelsson, B. *J. Med. Chem.* **2003**, *46*, 1165-79.
81. Beaulieu, P. L.; Gillard, J.; Bailey, M. D.; Boucher, C.; Duceppe, J. S.; Simoneau, B.; Wang, X. J.; Zhang, L.; Grozinger, K.; Houpis, I.; Farina, V.; Heimroth, H.; Krueger, T.; Schnaubelt, J. *J. Org. Chem.* **2005**, *70*, 5869-5879.
82. Giardina, G. A. M.; Sarau, H. M.; Farina, C.; Medhurst, A. D.; Grugni, M.; Raveglia, L. F.; Schmidt, D. B.; Rigolio, R.; Luttmann, M.; Vecchietti, V.; Hay, D. W. P. *J. Med. Chem.* **1997**, *40*, 1794-1807.
83. Freidinger, R. M.; Hinkle, S. J.; Perlow, D. S.; Arison, B. H. *J. Org. Chem.* **1983**, *48*, 77-81.
84. Bartlett, P. A.; Green III, F. R. *J. Am. Chem. Soc.* **1978**, *100*, 4858.
85. Suemune, H.; Tanaka, M.; Obaishi, H.; Sakai, K. *Chem. Pharm. Bull.* **1988**, *36*, 15-21.
86. Rosenquist, Å.; Kvarnsröm, I.; Svensson, S. C. T.; Classon, B.; Samuelsson, B. *Acta. Chem. Scand.* **1992**, *46*, 1127-1129.
87. Rosenquist, A.; Kvarnstrom, I.; Svensson, S. C. T.; Classon, B.; Samuelsson, B. *J. Org. Chem.* **1994**, *59*, 1779-1782.
88. Dhaon, M. K.; Olsen, R. K.; Ramasamy, K. *J. Org. Chem.* **1982**, *47*, 1962.

89. Oppenshaw, H. T.; Whittaker, N. *J. Chem. Soc* **1969** 89.
90. Mitsunobu, O. *Synthesis-Stuttgart* **1981** 1-28.
91. Barbato, G.; Cicero, D. O.; Cordier, F.; Narjes, F.; Gerlach, B.; Sambucini, S.; Grzesiek, S.; Matassa, V. G.; De Francesco, R.; Bazzo, R. *EMBO J.* **2000**, *19*, 1195-1206.
92. Johansson, A.; Hubatsch, I.; Åkerblom, E.; Lindeberg, G.; Winiwarter, S.; Danielson, U. H.; Hallberg, A. *Bioorg. Med. Chem. Lett.* **2001**, *11*, 203-206.
93. Johansson, A.; Poliakov, A.; Åkerblom, E.; Lindeberg, G.; Winwarter, S.; Samuelsson, B.; Danielson, U. H.; Hallberg, A. *Bioorg. Med. Chem.* **2002**, *10*, 3915-3922.
94. Yao, N. H.; Reichert, P.; Taremi, S. S.; Prosise, W. W.; Weber, P. C. *Structure* **1999**, *7*, 1353-1363.
95. Narjes, F.; Koehler, K. F.; Koch, U.; Gerlach, B.; Colarusso, S.; Steinkuhler, C.; Brunetti, M.; Altamura, S.; De Francesco, R.; Matassa, V. G. *Bioorg. Med. Chem. Lett.* **2002**, *12*, 701-4.
96. Thorstensson, F.; Wångsell, F.; Kvarnström, I.; Vrang, L.; Hamelink, E.; Jansson, K.; Hallberg, A.; Rosenquist, Å.; Samuelsson, B. *Bioorg. Med. Chem.* **2007**, *15*, 827-38.
97. Hansen, T. K. *Tetrahedron Lett.* **1999**, *40*, 9119-9120.
98. Farquhar, D.; Cherif, A.; Bakina, E.; Nelson, J. A. *J. Med. Chem.* **1998**, *41*, 965-972.
99. Callabretta, R.; Giordano, C.; Gallina, C.; Morea, V.; Scandurra, R. *Eur. J. Med. Chem.* **1995**, *30*, 931-941.
100. Weber, K.; Ohnmacht, U.; Gmeiner, P. *J. Org. Chem.* **2000**, *65*, 7406-16.
101. Dolby, L. J.; Esfandiari, S.; Ellinger, C. A.; Marshall, K. S. *J. Org. Chem.* **1971**, *36*, 1277-1285.
102. Molander, G. A.; Quirmbach, M. S.; Silva, L. F.; Spencer, K. C.; Balsells, J. *Org. Lett.* **2001**, *3*, 2257-2260.
103. Goedert, M.; Spillantini, M. G. *Science* **2006**, *314*, 777-81.
104. Barten, D. M.; Albright, C. F. *Molecular Neurobiology* **2008**, *37*, 171-186.
105. Citron, M. *Trends Pharmacol. Sci.* **2004**, *25*, 92-97.
106. Roberson, E. D.; Mucke, L. *Science* **2006**, *314*, 781-784.
107. Citron, M. *Nat. Rev. Neurosci.* **2004**, *5*, 677-685.
108. John, V.; Beck, J. P.; Bienkowski, M. J.; Sinha, S.; Heinrikson, R. L. *J. Med. Chem.* **2003**, *46*, 4625-30.
109. Reprinted by permission from Macmillan Publishers Ltd: [Nature] (*Nat. Rev. Neurosci*. **2004**, *5, 677-685*), © (2005)
110. Bertram, L.; Tanzi, R. E. *Nat. Rev. Neurosci.* **2008**, *9*, 768-778.
111. Hardy, J.; Selkoe, D. J. *Science* **2002**, *297*, 353-356.
112. Sisodia, S. S.; St George-Hyslop, P. H. *Nat. Rev. Neurosci.* **2002**, *3*, 281-90.
113. Skovronsky, D. M.; Lee, V. M. Y. *Trends Pharmacol. Sci.* **2000**, *21*, 161-163.
114. Vassar, R.; Bennett, B. D.; Babu-Khan, S.; Kahn, S.; Mendiaz, E. A.; Denis, P.; Teplow, D. B.; Ross, S.; Amarante, P.; Loeloff, R.; Luo, Y.; Fisher, S.; Fuller, L.; Edenson, S.; Lile, J.; Jarosinski, M. A.; Biere, A. L.; Curran, E.; Burgess, T.; Louis, J. C.; Collins, F.; Treanor, J.; Rogers, G.; Citron, M. *Science* **1999**, *286*, 735-741.
115. Baxter, W. E.; Reitz, B. A. *Annu. Rep. Med. Chem.* **2005**, *40*, 35-45.
116. Turner, R. T., 3rd; Loy, J. A.; Nguyen, C.; Devasamudram, T.; Ghosh, A. K.; Koelsch, G.; Tang, J. *Biochemistry* **2002**, *41*, 8742-6.
117. Ghosh, A. K.; Gemma, S.; Tang, J. *Neurotherapeutics* **2008**, *5*, 399-408.
118. Villaverde, M. C.; Gonzalez-Louro, L.; Sussman, F. *Curr Top Med Chem* **2007**, *7*, 980-90.
119. Ghosh, A. K.; Kumaragurubaran, N.; Hong, L.; Koelsh, G.; Tang, J. *Curr Alzheimer Res* **2008**, *5*, 121-31.
120. Luo, Y.; Bolon, B.; Kahn, S.; Bennett, B. D.; Babu-Khan, S.; Denis, P.; Fan, W.; Kha, H.; Zhang, J.; Gong, Y.; Martin, L.; Louis, J. C.; Yan, Q.; Richards, W. G.; Citron, M.; Vassar, R. *Nat. Neurosci.* **2001**, *4*, 231-2.
121. Roberds, S. L.; Anderson, J.; Basi, G.; Bienkowski, M. J.; Branstetter, D. G.; Chen, K. S.; Freedman, S. B.; Frigon, N. L.; Games, D.; Hu, K.; Johnson-Wood, K.; Kappenman, K. E.; Kawabe, T. T.; Kola, I.; Kuehn, R.; Lee, M.; Liu, W.; Motter, R.; Nichols, N. F.; Power, M.; Robertson, D. W.; Schenk, D.; Schoor, M.; Shopp, G. M.; Shuck, M. E.; Sinha, S.; Svensson, K. A.; Tatsuno, G.; Tintrup, H.; Wijsman, J.; Wright, S.; McConlogue, L. *Hum. Mol. Genet.* **2001**, *10*, 1317-24.
122. Senior, K. *Lancet* **2001**, *357*, 692-692.
123. Brik, A.; Wong, C. H. *Org. Biomol. Chem.* **2003**, *1*, 5-14.
124. Umezawa, H.; Aoyagi, T.; Morishima, H.; Matsuzaki, M.; Hamada, M. *J Antibiot (Tokyo)* **1970**, *23*, 259-62.

125. Silva, A. M.; Lee, A. Y.; Gulnik, S. V.; Maier, P.; Collins, J.; Bhat, T. N.; Collins, P. J.; Cachau, R. E.; Luker, K. E.; Gluzman, I. Y.; Francis, S. E.; Oksman, A.; Goldberg, D. E.; Erickson, J. W. *Proc. Natl. Acad. Sci. U.S.A.* **1996**, *93*, 10034-9.
126. John, V. *Curr Top Med Chem* **2006**, *6*, 569-78.
127. Tung, J. S.; Davis, D. L.; Anderson, J. P.; Walker, D. E.; Mamo, S.; Jewett, N.; Hom, R. K.; Sinha, S.; Thorsett, E. D.; John, V. *J. Med. Chem.* **2002**, *45*, 259-262.
128. Ghosh, A. K.; Bilcer, G.; Harwood, C.; Kawahama, R.; Shin, D.; Hussain, K. A.; Hong, L.; Loy, J. A.; Nguyen, C.; Koelsch, G.; Ermolieff, J.; Tang, J. *J. Med. Chem.* **2001**, *44*, 2865-2868.
129. Asai, M.; Hattori, C.; Iwata, N.; Saido, T. C.; Sasagawa, N.; Szabo, B.; Hashimoto, Y.; Maruyama, K.; Tanuma, S.; Kiso, Y.; Ishiura, S. *J Neurochem* **2006**, *96*, 533-40.
130. Kimura, T.; Shuto, D.; Hamada, Y.; Igawa, N.; Kasai, S.; Liu, P.; Hidaka, K.; Hamada, T.; Hayashi, Y.; Kiso, Y. *Bioorg. Med. Chem. Lett.* **2005**, *15*, 211-215.
131. Stachel, S. J.; Coburn, C. A.; Steele, T. G.; Jones, K. G.; Loutzenhiser, E. F.; Gregro, A. R.; Rajapakse, H. A.; Lai, M. T.; Crouthamel, M. C.; Xu, M.; Tugusheva, K.; Lineberger, J. E.; Pietrak, B. L.; Espeseth, A. S.; Shi, X. P.; Chen-Dodson, E.; Holloway, M. K.; Munshi, S.; Simon, A. J.; Kuo, L.; Vacca, J. P. *J. Med. Chem.* **2004**, *47*, 6447-50.
132. Rajapakse, H. A.; Nantermet, P. G.; Selnick, H. G.; Munshi, S.; McGaughey, G. B.; Lindsley, S. R.; Young, M. B.; Lai, M. T.; Espeseth, A. S.; Shi, X. P.; Colussi, D.; Pietrak, B.; Crouthamel, M. C.; Tugusheva, K.; Huang, Q.; Xu, M.; Simon, A. J.; Kuo, L.; Hazuda, D. J.; Graham, S.; Vacca, J. P. *J. Med. Chem.* **2006**, *49*, 7270-3.
133. Hills, I. D.; Vacca, J. P. *Curr. Opin. Drug Discov. Devel.* **2007**, *10*, 383-91.
134. Silvestri, R. *Med Res Rev* **2008**, *29*, 295-338.
135. Stachel, S. J.; Coburn, C. A.; Sankaranarayanan, S.; Price, E. A.; Wu, G.; Crouthamel, M.; Pietrak, B. L.; Huang, Q.; Lineberger, J.; Espeseth, A. S.; Jin, L.; Ellis, J.; Holloway, M. K.; Munshi, S.; Allison, T.; Hazuda, D.; Simon, A. J.; Graham, S. L.; Vacca, J. P. *J. Med. Chem.* **2006**, *49*, 6147-50.
136. Hom, R. K.; Fang, L. Y.; Mamo, S.; Tung, J. S.; Guinn, A. C.; Walker, D. E.; Davis, D. L.; Gailunas, A. F.; Thorsett, E. D.; Sinha, S.; Knops, J. E.; Jewett, N. E.; Anderson, J. P.; John, V. *J. Med. Chem.* **2003**, *46*, 1799-802.
137. Hu, B.; Fan, K. Y.; Bridges, K.; Chopra, R.; Lovering, F.; Cole, D.; Zhou, P.; Ellingboe, J.; Jin, G.; Cowling, R.; Bard, J. *Bioorg. Med. Chem. Lett.* **2004**, *14*, 3457-60.
138. Alterman, M.; Björsne, M.; Muhlman, A.; Classon, B.; Kvarnström, I.; Danielson, H.; Markgren, P. O.; Nillroth, U.; Unge, T.; Hallberg, A.; Samuelsson, B. *J. Med. Chem.* **1998**, *41*, 3782-92.
139. Johansson, P.-O.; Chen, Y. T.; Belfrage, A. K.; Blackman, M. J.; Kvarnström, I.; Jansson, K.; Vrang, L.; Hamelink, E.; Hallberg, A.; Rosenquist, Å.; Samuelsson, B. *J. Med. Chem.* **2004**, *47*, 3353-3366.
140. Johansson, P.-O.; Lindberg, J.; Blackman, M. J.; Kvarnström, I.; Vrang, L.; Hamelink, E.; Hallberg, A.; Rosenquist, Å.; Samuelsson, B. *J. Med. Chem.* **2005**, *48*, 4400-4409.
141. Pyring, D.; Lindberg, J.; Rosenquist, Å.; Zuccarello, G.; Kvarnström, I.; Zhang, H.; Vrang, L.; Unge, T.; Classon, B.; Hallberg, A.; Samuelsson, B. *J. Med. Chem.* **2001**, *44*, 3083-91.
142. Arslan, T.; Abraham, A. T.; Hecht, S. M. *Nucleosides Nucleotides* **1998**, *17*, 515-30.
143. Rasmussen, J. R.; Slinger, C. J.; Kordish, R. J.; Newman-Evans, D. D. *J. Org. Chem.* **1981**, *46*, 4843-4846.
144. Rondot, B.; Durand, T.; Girard, J. P.; Rossi, J. C.; Schio, L.; Khanapure, S. P.; Rokach, J. *Tetrahedron Lett.* **1993**, *34*, 8245-8248.
145. Rauter, A. P.; Figueiredo, J.; Ismael, M.; Canda, T.; Font, J.; Figueredo, M. *Tetrahedron Asymmetry* **2001**, *12*, 1131-1146.
146. Yanagisawa, H.; Kanazaki, T.; Nishi, T. *Chem. Lett.* **1989** 687-690.
147. Robinson, P. L.; Carey, N.; Barry, S.; Bass, W.; Jarvis, S. E.; Evans, S. A. *J. Org. Chem.* **1983**, *48*, 5396-5398.
148. Zuccarello, G.; Bouzide, A.; Kvarnström, I.; Niklasson, G.; Svensson, S. C. T.; Brisander, M.; Danielsson, H.; Nillroth, U.; Karlen, A.; Hallberg, A.; Classon, B.; Samuelsson, B. *J. Org. Chem.* **1998**, *63*, 4898-4906.
149. Muller, M.; Huchel, U.; Geyer, A.; Schmidt, R. R. *J. Org. Chem.* **1999**, *64*, 6190-6201.
150. Rich, D. H.; Sun, C. Q.; Vara Prasad, J. V.; Pathiasseril, A.; Toth, M. V.; Marshall, G. R.; Clare, M.; Mueller, R. A.; Houseman, K. *J. Med. Chem.* **1991**, *34*, 1222-1225.
151. Dess, D. B.; Martin, J. C. *J. Org. Chem.* **1983**, *48*, 4155-4156.

152. Baldwin, E. T.; Bhat, T. N.; Gulnik, S.; Hosur, M. V.; Sowder, R. C., 2nd; Cachau, R. E.; Collins, J.; Silva, A. M.; Erickson, J. W. *Proc. Natl. Acad. Sci. U.S.A.* **1993**, *90*, 6796-800.
153. Björklund, C.; Oscarson, S.; Benkestock, K.; Borkakoti, N.; Jansson, K.; Lindberg, J.; Hallberg, A.; Rosenquist, Å.; Samuelsson, B. *In manuscript*.
154. Rahuel, J.; Rasetti, V.; Maibaum, J.; Rueger, H.; Goschke, R.; Cohen, N. C.; Stutz, S.; Cumin, F.; Fuhrer, W.; Wood, J. M.; Grutter, M. G. *Chem Biol* **2000**, *7*, 493-504.
155. Simas, A. B. C.; Coelho, A. L.; Costa, P. R. R. *Synthesis-Stuttgart* **1999** 1017-1021.
156. Wångsell, F.; Gustafsson, K.; Kvarnström, I.; Borkakoti, N.; Edlund, M.; Jansson, K.; Lindberg, J.; Hallberg, A.; Rosenquist, Å.; Samuelsson, B. *Submitted to Bioorg. Med. Chem.*
157. Crich, D.; Vinogradova, O. *J. Org. Chem.* **2007**, *72*, 3581-3584.